HISTONE MODIFICATION AND THE EPIGENETICS OF X CHROMOSOME INACTIVATION

by

HUGH TIMOTHY SPOTSWOOD

A thesis submitted to
The University of Birmingham
for the degree of
DOCTOR OF PHILOSOPHY

Department of Anatomy
Medical School
The University of Birmingham
October 2002

ABSTRACT

Dosage compensation serves to equalise the levels of X-linked gene products between males and females. In mammals this occurs through the transcriptional silencing of the majority of the genes on one of the two female X chromosomes. The inactive X chromosome (Xi) differs from its active homologue in a number of ways, including the hypoacetylation of core histones, a common property of genetically inactive chromatin. This study has used Xi to explore the functional significance of hypoacetylation and patterns of histone methylation in silent chromatin. Xi was shown to be depleted for di- and tri-methylated lysine 4 of H3, but retained di-methylated lysine 9 of H3. I have examined the temporal order of these modifications as they become established using an *in vitro* model system for X inactivation; differentiating female embryonic stem cells. The results showed that the loss of tri-methylated lysine 4 of H3 preceded the loss of its di-methylated equivalent, which occurs during a time period of concurrent core histone deacetylation supporting a functional role to the level of lysine methylation. I have used cases of X;autosome translocation to examine how these modifications relate to late replication and transcriptional silencing. Results show that whilst the spread of X inactivation can occur in the absence of both of these properties, histone modifications are a more reliable indicator of the extent of spread of X inactivation than late replication. To explore mechanisms that drive changes in histone modification I have analysed the distribution of histone deacetylases across a region of defined histone deacetylation. The results showed a ubiquitous distribution that did not correlate with acetylated H3 or H4 suggesting that the global association of the Hdacs might serve to provide a rapid return the basal level of histone acetylation following specific targeting events.

DEDICATION

I would like to dedicate this thesis to the memory of Margaret Addison

ACKNOWLEDGEMENTS

I would like to thank Professor Bryan M. Turner for supervising this project and The Wellcome Trust for funding this work. Thanks also go to all members past and present of the Chromatin and Gene Expression Group for the lively lab discussions. I would also like to thank Professor F. C. Franklin for providing me with an appetite for chromatin research and Drs. A. Harel-Bellan and V. Orlando for visits to their respective groups. Finally I would like to thank my parents and my girlfriend Dr. Helen Travers for their emotional support during my time as a PhD student.

TABLE OF CONTENTS

TABLE OF FIGURES

LIST OF TABLES

1 INTRODUCTION – CHAPTER ONE

During the development of a multicellular organism cells take on properties that distinguish them functionally and morphologically. Cells adopt divergent roles during differentiation through the expression of specific genes and the silencing of others. For example during the development of *Drosophila* differences in the patterns of gene transcription in the developing fly embryo leads to a cascade of control, such that a gene switched on or off at one stage regulates expression of other genes at the next stage. Genes involved in regulating *Drosophila* development have been identified in the past based on mutations that are either lethal early in development or cause the development of abnormal structures, thus highlighting the importance of tightly regulated gene expression.

In addition to the appropriate *timing* of gene expression the *inactivation* of certain genes must occur in every cell. A useful example of this is the transcriptional silencing of the fetal haemoglobins following the switch to the production of adult haemoglobin after birth.

Early progress in the study of eukaryotic gene transcription was made *in vitro* using naked DNA. Studies demonstrated that virtually any eukaryotic gene promoter could be transcribed by a set of pure proteins consisting of components of the transcription machinery (Sayre *et al.*, 1992; Conaway and Conaway, 1993). The deficiency in the control of gene regulation and the poor response following the addition of activator proteins has subsequently been attributed to the absence of the proteins that associate ubiquitously with the DNA template. These proteins together with the DNA form chromatin, the template for gene regulation in eukaryotes. Chromatin and the

nucleosome repeat unit were once considered just an inconvenience to the process of gene transcription (Kornberg and Lorch, 1992). However, more recently chromatin has become regarded as an essential component of the machinery responsible for regulating gene transcription.

1.1 The nucleosome

The fundamental subunit of chromatin, the nucleosome, mediates the primary organisation of DNA in eukaryotes (Kornberg and Lorch, 1999). Two of each of the histones H2A, H2B, H3 and H4 form the nucleosome core. Each histone octamer consists of a tetramer of H3 and H4 and two dimers of H2A and H2B. The nucleosome core is surrounded by approximately 146bp of DNA, wrapped around each histone octamer 1.65 turns (Luger *et al.*, 1997). This generates the first level of DNA packaging which resembles a bead-like structure (figure 1a) (Lewin, 1997).

The histones are amongst the most invariant proteins known. Indeed histone H4 has a near perfect conservation across all species (Delange *et al.*, 1969). All four core histones contain an extended histone-fold domain at the carboxyl (C-) terminal end of the protein through which the histone-histone and histone-DNA interactions occur. Protruding away from the nucleosomal core particle are the highly charged histone amino (N-) terminal tails. The histone tails are responsible for interacting with structural components of chromatin (Moretti *et al.*, 1994; Edmonson *et al.*, 1996). They are also the sites of many enzyme catalysed post-translational modifications including acetylation, methylation, phosphorylation, ubiquitination and ADP-ribosylation (Wolffe, 1998; Wu and Grunstein, 2000; Zhang *et al.*, 2002). The sites of the histone N-terminal tail modifications are shown in figure 1b.

a

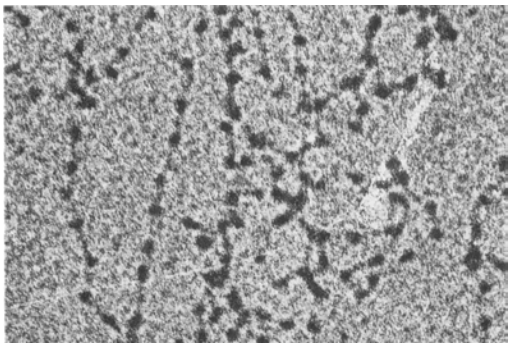

b

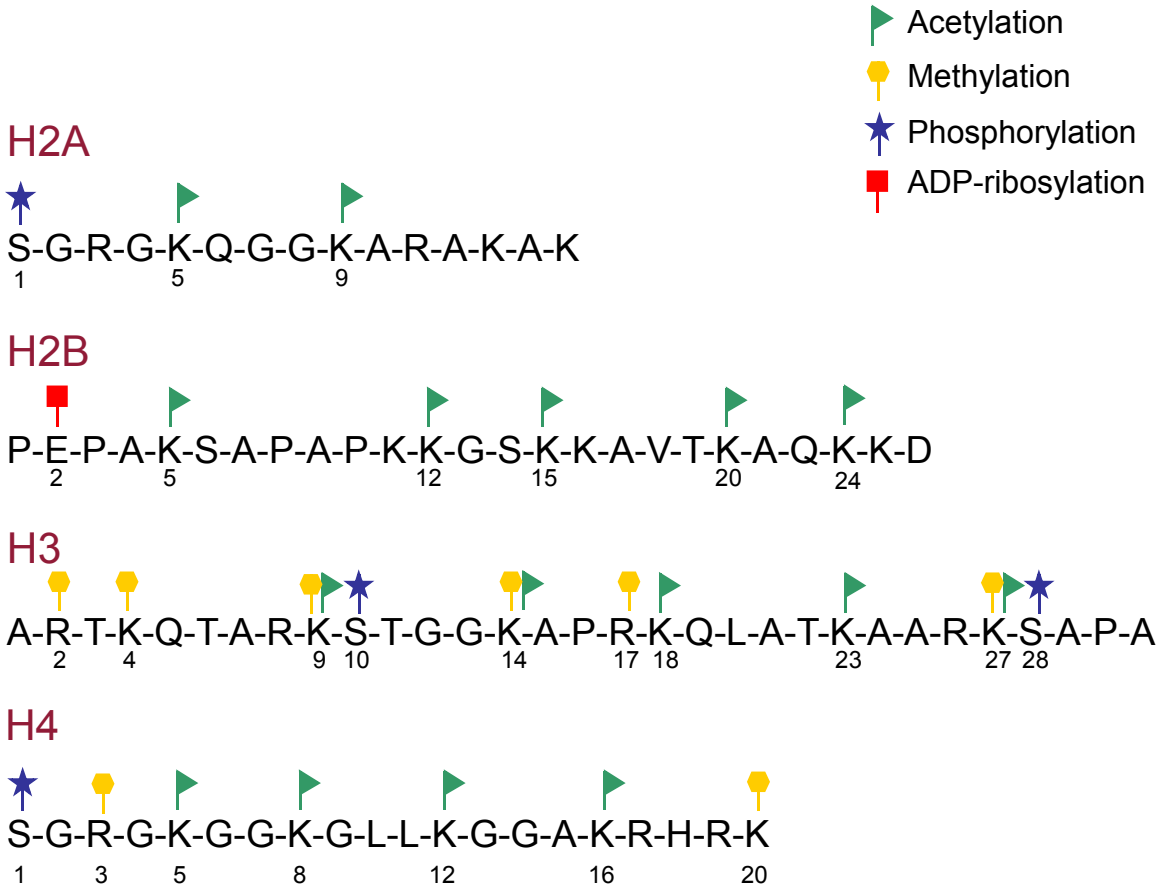

Figure 1. The chromatin fibre analysed using electron microscopy resembles a bead like structure (a). Adapted from Lewin (1997).

The sequences of the histone amino terminal tail regions are shown in single letter code in b. The sites of post-translational modification are indicated; acetylation (green), methylation (yellow), phosphorylation (blue) and ADP-ribosylation (red).

The most extensively studied histones modifications are acetylation, and more recently methylation of the ε-amino group of specific lysine residues. The acetylation of core histones occurs in all plant and animal species analysed (Csordas, 1990). Histone acetylation occurs in a reversible manner with the addition and removal of acetyl groups being catalysed by the histone acetyl-transferases (HATs) and the histone deacetylases (HDACs) respectively. The number of acetylated lysine residues per histone molecule is determined by an equilibrium between the HATs and the HDACs (figure 2a). Disruption of the equilibrium can be achieved through HDAC inhibitors such as Sodium Butyrate, Trichostatin A (TSA) and Trapoxin (Yoshida *et al.*, 1990).

The enzymes responsible for the deployment of specific methyl groups onto the histone tails, termed the histone methyl-transferases (HMTs), are less well characterised (Rea *et al.*, 2000; Kouzarides, 2002). As yet the enzymes responsible for the removal of methyl groups from the lysine residues (histone demethylases; HDMs) have not been identified. Given that the majority of the data suggests that the methyl modification is relatively irreversible (Shepherd *et al.*, 1971; Byvoet, 1972; Byvoet *et al.*, 1972), many speculate that the existence of an HDM is unlikely. However, enzymes with demethylase activity have been previously reported (Lee *et al.*, 1996), albeit with no activity towards a histone polypeptide.

Levels of histone acetylation are generally higher in transcriptionally active than in quiescent chromatin (Hebbes *et al.*, 1988; Braunstein *et al.*, 1993). Following this observation previously characterised transcriptional activators were show to carry histone acetyltransferase activity (Brownell *et al.*, 1996; Yang *et al.*, 1996) and some

a

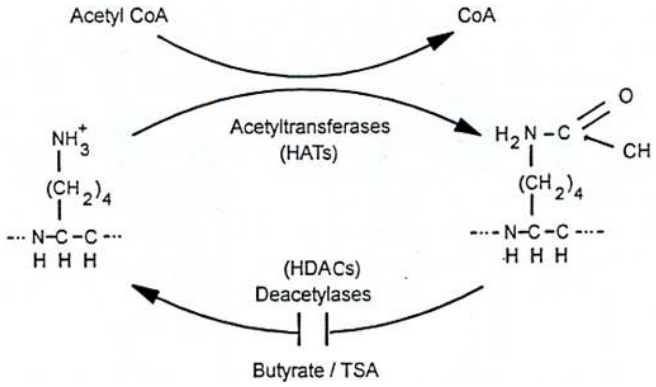

b

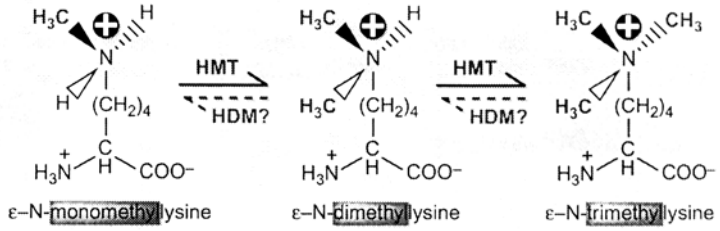

Figure 2. The acetylation of core histones is catalysed by the histone acetyl-transferases (HATs) and removed by the histone deacetylases (HDACs) (a). The number of acetylated lysine residues per histone molecule is determined by an equilibrium between the HATs and the HDACs. The equilibrium can be disrupted by the use of histone deacetylase inhibitors such as Sodium Butyrate or Trichostatin A (TSA), leading to chromatin with high levels of histone acetylation.

Core histone methylation is catalysed by the histone methyltransferases (HMTs) and may be removed by as yet unidentified histone demethylases (HDMs) (b). Histone methylation is more complex than histone acetylation in that lysines have the potential to be methylated at three levels; mono-, di- and tri-methyl lysine. Adapted from Rice and Allis (2001).

transcriptional repressors were found to be capable of histone deacetylation (Taunton *et al.*, 1996).

Histone methylation is more complicated than acetylation because individual lysine residues have the potential to be mono-, di-, or tri-methylated (figure 2b). Indeed it is unfortunate that the distinction is often not made. However, chromatin enriched in H3 di-methylated at lysine 4 has been shown to correlate with transcriptionally active genes (Strahl *et al.*, 1999; Noma *et al.*, 2001; Bernstein *et al.*, 2002). In contrast H3 di-methylated at lysine 9 has been shown to correspond to heterochromatic regions or transcriptionally inactive genes (Litt *et al.*, 2001; Xin *et al.*, 2001; Peters *et al.*, 2002).

The functional consequences of histone acetylation and methylation can be divided into two general but not mutually exclusive categories. Firstly the direct effects of acetylation and methylation on the structure of chromatin. The second mechanism is the generation of new sites on the surface of the nucleosome that specify a "code" read by non-histone proteins which dictate the transcriptional status of the chromatin. This implies that histone modifications can also act indirectly in the process of gene regulation.

1.1.1 Structural consequences of histone modification

Long standing models regarding the effects of histone acetylation on the structure of chromatin are relatively simplistic. They propose that the process of histone acetylation reduces the overall positive charge of the N-terminal tails by one. As these tails are basic, the effect is to reduce the affinity that the histones display for negatively charged DNA and thus influence the access by transcription factors (Turner, 1998; Wolffe and

Hayes, 1999). Support for this hypothesis comes from the finding that acetylation of the N-terminal tails does indeed weaken the association of histones with the DNA and thereby influences nucleosomal structure (Norton *et al.*, 1989). However, it appears that the most significant consequence of histone acetylation is in the weakening of protein-protein interactions with adjacent nucleosomes. This suggests that the acetylation of the histone tails "loosens" the chromatin conformation, which could enhance the access of transcription factors.

In contrast to acetylation the methylation of lysine residues does not influence the overall charge of the histone tails (Rice and Allis, 2001). Increasing the level of lysine methylation (mono-, di- and tri-) does increase the basicity and hydrophobicity of the N-terminal tails. Furthermore increased methylation of the histone tails increases their affinity for anionic molecules (i.e. DNA). This suggests that there is a tight association between the methylated histone tail and its associated DNA. Therefore, similar to acetylation the methylation of the histone tails may have the potential to influence the structure and function of the nucleosome.

However, if the acetylation and methylation of the lysine residues on the histone tails simply serves to disrupt or generate transcription factor accessibility it is perplexing why the enzymes responsible for depositing the histone modifications exhibit such specificity. For example the yeast histone acetyltransferase yGCN5 exhibits a preference for H3 lysine 14 *in vitro* and *in vivo* (Zhang *et al.*, 1998a). It is also puzzling how H3 di-methylated at lysine 4 correlates with regions of transcriptional activity whilst H3 di-methylated at lysine 9 correlates with transcriptionally silent domains if the determinant of transcriptional competence was purely based on the physical effects

of lysine methylation. Therefore it seems likely that the acetylation and methylation of specific sites impart different biological functions depending on the lysine residue modified.

1.1.2 Histone acetylation and methylation as epigenetic marks

Rather than the direct structural implications of acetylation and methylation the pattern of histone modification or "code" imposed on the histones by the various enzymes may be important in promoting the interaction of very specific non-histone proteins. This indirect mechanism requires that the amino terminal tails are bound by non-histone proteins that exert functional effects possibly through the formation of protein complexes required for transcription or gene silencing. This idea forms the basis of the "epigenetic code" (Turner, 1993, 2000), which has recently been revisited as the "histone code" (Strahl and Allis, 2000; Jenuwein and Allis, 2001).

Given the numerous sites for modification, shown in figure 1b, there is potentially an enormous amount of information that can be conveyed by the histone tails. Histones H2B, H3 and H4 each have 32 possible isoforms that differ purely in acetylation. The histone code is likely to extend to combinations of acetylation, methylation and ADP-ribosylation rather than the modification of a single site. Interestingly many modifications are close enough to each other on the histone tail to influence either positively or negatively the ability of enzymes to further modify these residues, suggesting some combinations may be rare *in vivo* (Strahl and Allis, 2000; Nishioka *et al.*, 2002). Evidence for this being the case of histone H3, where the phosphorylation of serine 10 is suppressed by an initial methylation at lysine 9 (Rea *et al.*, 2000).

1.1.2.1 Proteins that read the epigenetic code

Evidence that proteins are influenced by the modification state of the histone N-terminal tails was first provided by the Sir3/4 (Hecht *et al.*, 1995) and Tup1/Ssn6 (Edmonson *et al.*, 1996) proteins, which are involved in transcriptional silencing and repression in yeast. The binding of Tup1 was shown to be influenced by the acetylation state of the H3 and H4 N-terminal tails. Tup1 displays a clear preference for non- or mono-acetylated H3 and H4 compared with hyperacetylated (tri- or tetra-acetylated) H3 and H4. This supports the hypothesis that histone acetylation can modulate the binding of non-histone proteins. Interesting Tup1 has subsequently been shown to associate with a histone deacetylase suggesting that the retention of chromatin depleted in histone acetylation stably maintains the association of Tup1 at particular yeast loci (Watson *et al*., 2000).

The bromodomain of the histone acetyltransferase P/CAF (P300/CBP-associated factor) has been shown to specifically recognise acetylated lysine residues on histone N-termini (Dhalluin *et al*., 1999). The majority of the HATs share the bromodomain motif suggesting that it represents an essential component of chromatin targeting (Winston and Allis, 1999). Therefore the yeast Tup1 silencing complex and the HAT bromodomain display a preference for chromatin that is depleted or enriched in acetyl-lysine respectively. However, in these examples the level of histone acetylation rather than the specific lysines modified could be considered the determining factor for the recruitment of the proteins to specific loci.

Recent evidence has implicated the involvement site-specific methylation in the epigenetic code hypothesis. Human HP1 (Heterochromatin Protein 1) is localized at heterochromatin sites where it mediates gene silencing and has recently been shown to contain a motif referred to as the chromo (chromosome organization modifier) domain that preferentially binds to H3 methylated at lysine 9 *in vitro* (Bannister *et al.*, 2001; Lachner *et al.*, 2001). Interestingly, the correct localisation of HP1 depends on the activity of SUV39H1, the enzyme responsible for depositing methyl groups on lysine 9 of H3 (Lachner *et al.*, 2001). Whilst the chromodomain motif is shared by many heterochromatin proteins (Platero *et al.*, 1995) the H3 methylated at lysine 9 modification appears to be highly specific for HP1 as other chromodomain-containing proteins failed to bind an H3 peptide methylated at lysine 9. The binding of HP1 to H3 methylated at lysine 9 is now thought to be one of the final steps in the formation of heterochromatin.

1.1.2.2 Histone modifications as genomic marks

There are various examples where the specific pattern of histone modifications imposed on the N-terminal tails appears to serve as genomic markers for as yet unidentified non-histone proteins. For example in *S.cerevisiae* the majority of the genome is transcriptionally active and displays high levels of histone acetylation. However, there are transcriptionally silent domains such as the mating type loci which retain a unique pattern of histone acetylation. The chromatin of the mating type loci is depleted in H4 acetylated at all sites except for lysine 12 (Braunstein *et al.*, 1993; Ekwall *et al.*, 1997). This phenomenon is shared by *Drosophila* pericentric heterochromatin and suggests that this pattern of acetylation facilitates the recruitment of non-histone proteins involved in the formation of heterochromatin.

A further example where the site of acetylation distinguishes a genomic region comes from the immunolabelling of *Drosophila* salivary gland polytene chromosomes using antibodies that can distinguish H4 isoforms acetylated at lysines 5, 8, 12, or 16. H4 acetylated at lysine 16 was found predominantly on the X chromosome in male cells (Turner *et al.*, 1992). The significance of this stems from the fact that in *Drosophila*, the equalisation of X-linked gene products between males (XY) and females (XX) (dosage compensation) is achieved by increasing the transcriptional activity of the genes on the X chromosome in male cells (Meller and Kuroda, 2002). Therefore H4 acetylated at lysine 16 marks a chromosome required to be transcriptionally hyperactive. Subsequent to this study a *Drosophila* dosage compensation complex was identified containing a histone acetyltransferase subunit called MOF (Males Only on the First) with enzymatic specificity towards H4 lysine 16 (Smith *et al.*, 2000).

Histone methylation has been shown to serve as a genomic mark both globally (Strahl *et al.*, 1999; Heard *et al.*, 2001; Peters *et al.*, 2002) and locally (Litt *et al.*, 2001; Xin *et al.*, 2001). For example Litt *et al.*, (2001) showed an almost complete inverse correlation of H3 di-methylation at lysines 4 and 9 at the chicken β-globin locus using the technique of chromatin immunoprecipitation (ChIP). 10 day chicken embryo red blood cells, expressing β-globin were shown to display peaks of lysine 4 di-methylation across the β-globin locus that directly corresponded to regions of chromatin depleted in lysine 9 di-methylation. In contrast erythroid precursor cells, yet to express β-globin were shown to have regions significantly enriched for di-methylated lysine 9 but also depleted in di-methylated lysine 4.

A unique pattern of histone acetylation is also associated with mammalian dosage compensation. Mammals achieve equality of X-linked gene products between males and females by the genetic silencing of one of the two X chromosomes in female cells. The immunolabelling of metaphase spreads prepared from female somatic cells revealed that the female inactive X chromosome (Xi) is depleted in acetylated H2A, H3 and H4 and is clearly distinguishable from the autosomes and its active homologue (Belyaev *et al.*, 1996). The chromatin of the inactive X chromosome was subsequently confirmed to be depleted in acetylated H4 throughout its coding and promoter domains using chromatin immunoprecipitation (Keohane *et al.*, 1996; O'Neill *et al.*, 1999). Therefore in contrast to the specific epigenetic mark imposed on the *Drosophila* male X at H4 lysine 16, the mammalian Xi was confirmed as being depleted for acetyl-lysine at all sites, throughout its entire domain. However, recent experiments performed using human × hamster hybrid cell lines whose only human chromosome is either an active (Xa) or inactive (Xi) X chromosome have provided evidence that it is the promoter regions of silent genes that are specifically hypoacetylated (Gilbert and Sharp, 1999).

1.2 X chromosome inactivation

The process of mammalian X chromosome inactivation occurs early in embryonic development (figure 3a). During the earliest stages of female embryogenesis, both X chromosomes remain active. X inactivation is first observed in the trophectodermal tissue of the early blastocyst. The tissues of the trophectoderm and primitive endoderm (derived from the inner cell mass) undergoes imprinted X inactivation, whereby the paternally derived X chromosome is always inactivated (Takagi and Sasaki, 1975; Monk and Kathuria, 1977). The earliest sign of an inactive X chromosome in cells that

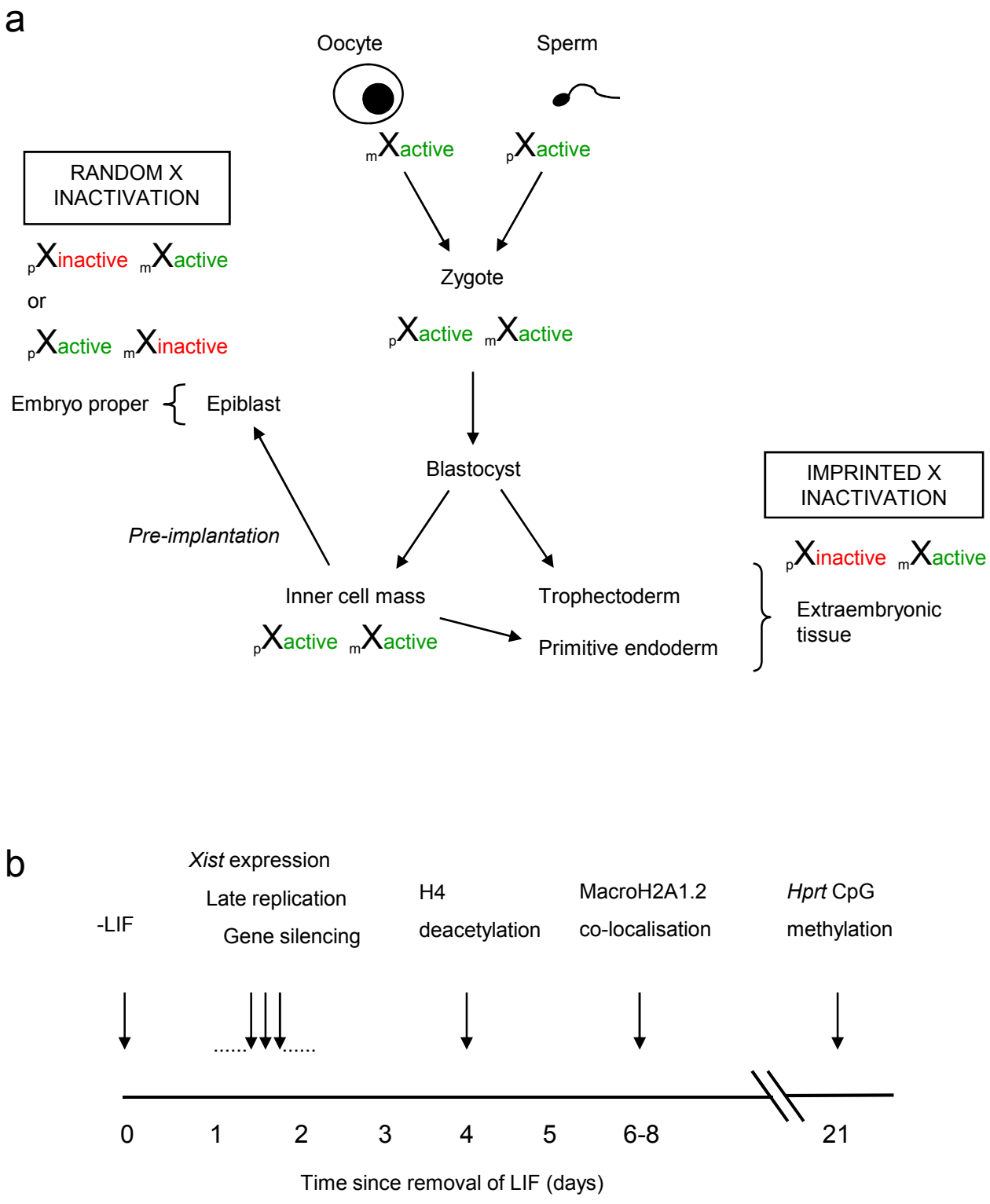

Figure 3. X inactivation in different cell lineages in the female mouse (a).

The timing of events associated with X inactivation in female embryonic stem cells (b). Vertical arrows represent the time at which each event was first detected following the induction to differentiate by the removal of LIF. Adapted from Keohane *et al.,* (1998). Experimental data defining macroH2A1.2 accumulation on the inactive X chromosome is taken from Mermoud *et al.,* (1999).

give rise to the embryo proper is during the pre-implantation blastocyst stage. In eutherian (placental) mammals the X chromosome to be inactivated is chosen at random between the paternally or maternally derived X chromosomes. The inactive X chromosome is stably inherited through successive cell generations in its transcriptionally silent state.

Following X chromosome inactivation Xi takes on properties that distinguish it as facultative heterochromatin. Facultative, as opposed to constitutive heterochromatin, can be defined as chromatin that harbours the potential to become either transcriptionally inactive or active, and is assembled and dismantled in a controlled, regulated manner. In addition to the epigenetic marks discussed above the facultative heterochromatin of the inactive X takes on properties that distinguish it from its active homologue. An early identifiable property was the densely staining Barr body or sex chromatin structure in female interphase cells (Barr and Bertram, 1949). The Barr body is often incorrectly referred to as "condensed" and morphological analysis of Xi has revealed differences in its shape rather than the degrees of compaction (Eils *et al.*, 1996).

Timing of replication was an early criterion used to identify Xi in metaphase cells (Takagi *et al.*, 1982). The inactive X chromosome replicates late in S phase and asynchronously with respect to its active homologue. Xi can be distinguished by pulsing with BrdU at the appropriate stage of the cell cycle followed by immunodetection using antibodies raised against the nucleotide analogue.

The inactive X chromosome has increased methylation of CpG dinucleotides (Norris *et al.*, 1991) and an enrichment for the histone variant macroH2A1.2 (Costanzi and Pehrson, 1998). However, it has been suggested that the enrichment of macroH2A1.2 is a consequence of a higher nucleosomal density on the inactive X chromosome rather than a specific function of this histone variant (Perche *et al.*, 2000).

1.2.1 The X inactivation centre (Xic)

Whilst the properties of Xi have been characterised extensively the molecular process that converts just one of the two female X chromosomes into a mature inactive X chromosome remains less clear. A region has been identified that is essential for the initiation of inactivation, called the X inactivation centre (*Xic*) (Rastan, 1983; Brown *et al.*, 1991). The *Xic*, a region of several hundred kilobases, contains several elements thought to have a role in X inactivation and at least six genes (figure 4) (Heard *et al*., 1997). One of these, the X (inactive)-specific transcript (*Xist*) gene has been shown to be an absolute requirement for the process of X inactivation *in vitro* (Penny *et al.*, 1996) and *in vivo* (Marahrens *et al.*, 1997) using mouse gene knock outs. The *Xist* gene is unique in that it is only expressed from Xi in female somatic cells (Brockdorff *et al.*, 1991; Brown *et al.*, 1991). The mouse *Xist* gene encodes a 17.4 kb nuclear RNA transcript that has no protein coding capacity (Brockdorff *et al.*, 1992; Hong *et al.*, 1999). The technique of RNA fluorescence *in situ* hybridisation (FISH) has shown that this transcript coats the inactive X chromosome of female somatic cells (Clemson *et al.*, 1998). However, the exact role played by *Xist* remains uncertain. The pattern of *Xist* expression as X inactivation progresses is best explained using data obtained from embryonic stem (ES) cells.

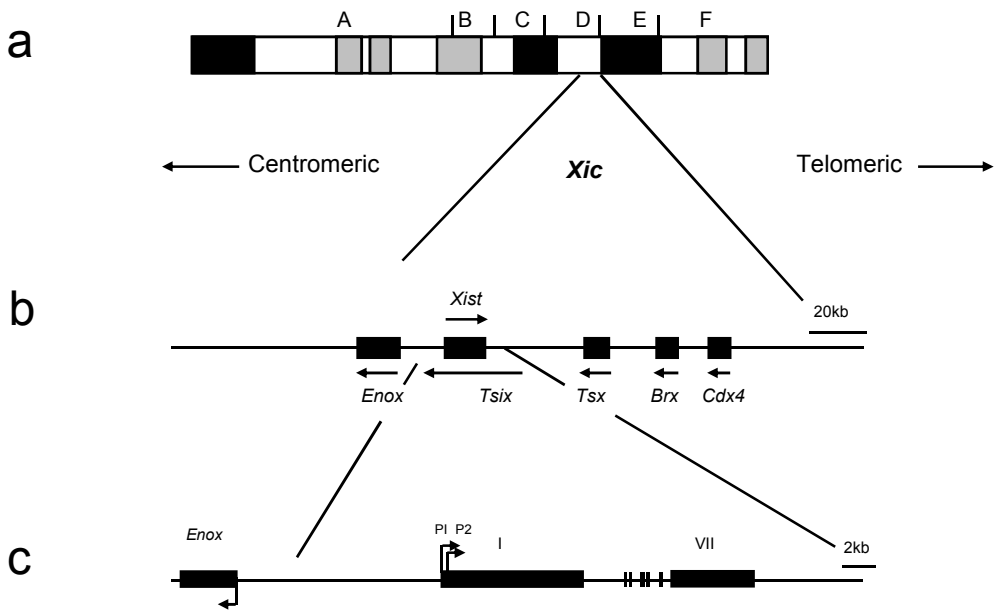

Figure 4. Chromosomal location and composition of the *Xic* region and the *Xist* gene. (a) The mouse X chromosome showing the major G-bands; regions A-F. (b) The mouse *Xic* with the orientation of the genes shown using horizontal arrows. (c) The mouse *Xist* gene showing the exons (dark boxes) and the two promoters, P1 and P2. Adapted from O'Neill *et al.,* (1999).

1.2.2 X inactivation using murine embryonic stem cells

Female embryonic stem cells can recapitulate the process of X inactivation *in vitro*. ES cells are derived from the inner cell mass of mouse blastocysts and can be maintained as undifferentiated cells with two active X chromosomes in medium containing the growth factor leukaemia inhibitory factor (LIF) (Williams *et al.*, 1988). ES cells can be induced to differentiate by the removal of LIF, whereby they form embryoid bodies and have the potential to differentiate into many different cell types (Martin and Evans, 1975; Keller, 1995). Within one week of differentiation ES cells inactivate one of their X chromosomes at random. Embryonic stem cells have provided an excellent model system for studying the sequential events that are necessary for the formation of an inactive X chromosome (Keohane *et al.*, 1996). In undifferentiated female cells *Xist* is expressed at low levels from both X chromosomes and can be visualised by RNA-FISH as two small punctate signals. Following the induction of differentiation the *Xist* transcript accumulates on and coats the future inactive X chromosome, spreading out from the *Xic*, whilst the *Xist* gene on the future active X chromosome becomes silenced (Sheardown *et al.*, 1997). The process of *Xist* gene silencing on the future Xa is not fully understood, although a putative control element must be the *Tsix* gene, transcribed antisense to *Xist* (figure 4b) (Lee *et al.*, 1999). Targeted deletions of *Tsix* leads to non-random X inactivation of the deleted X chromosome, suggesting that *Tsix* has an antagonistic role in the suppression of transcripts accumulating from *Xist* (Lee and Lu, 1999).

The timing of *Xist* RNA accumulation on Xi can be compared with the accumulation of the epigenetic characteristics discussed previously using female ES cells (figure 3b). A study performed by Keohane *et al*., (1996) reported that the earliest detectable change

was the appearance of a late replicating (X) chromosome and increased levels of *Xist* RNA, both detected after two days of differentiation. Transcriptional silencing of four X-linked genes was detectable by day's two to four, but an X chromosome distinguishable on account of its low levels of H4 acetylation was only detected after four days of differentiation. Interestingly, methylation of the CpG residues in the promoter region of the *Hprt* gene was not observed until at least 21 days of differentiation. Additionally in an independent study the co-localisation of macroH2A1.2 with Xi was not observed until six to eight days of differentiation (Mermoud *et al.*, 1999). CpG island methylation and the accumulation of macroH2A1.2 on the inactive X both appear to occur earlier *in vivo* (Grant *et al.*, 1992; Costanzi *et al.*, 2000). These studies clearly showed a sequential order of events in the process of X inactivation. Together the *in vivo* and *in vitro* studies suggest that H4 hypoacetylation, CpG methylation and macroH2A1.2 each serve to stabilise and maintain the transcriptional silencing that was initiated by the *Xist* gene.

1.2.3 Chromatin of the Xist gene

The *Xist* transcript is derived from two promoters denoted P1 and P2 (figure 4c). Both promoters generate the stable *Xist* transcript that accumulates on the inactive X chromosome. The *Xist* gene is flanked by two genes encoded in the antisense orientation. Downstream of *Xist* is the *Tsix* gene transcribed through the entire *Xist* coding domain. *Tsix* has been shown to have an antagonistic role during X inactivation by preventing the accumulation of *Xist* transcripts on the future active X chromosome (Lee and Lu, 1999). Approximately 10kb upstream from the *Xist* promoter region is the recently identified *Enox* (Expressed Neighbour Of *Xist*) gene

shown to display partial escape from X inactivation but with no identifiable role in the process of X inactivation (Johnston *et al.*, 2002).

The *Xist* minimal promoter region has previously been defined using reporter gene constructs as extending from -81 to +1 relative to the main transcription start site (P1) (Pillet *et al.*, 1995). The *Xist* promoter region contains binding sequences for the ubiquitous transcription factors TBP (TATA box binding protein), Sp1 (Pillet *et al.*, 1995) and has a near consensus YY1 site (Hendrich *et al.*, 1993; Goto and Monk, 1998). Interesting a 100kDa protein has also been identified that binds (-44 to -36) to the *Xist* promoter in a DNA methylation dependent and sequence-specific manner (Huntriss *et al.*, 1997).

Given the critical role of the *Xist* gene during the initiation of X chromosome inactivation it was of interest to determine the active chromatin domain of *Xist*. A study performed by McCabe *et al*., (1999) showed a deoxyribonuclease 1 (*DNaseI*) sensitive domain that extended 10kb upstream of the main *Xist* promoter P1. Chromatin within this domain was found to be acetylated at H4 in female (XX) somatic cells but also in male (XY) cells where *Xist* is never expressed. An exception to this was the *Xist* minimal promoter region, which was acetylated only in female cells. This supports the idea that local promoter acetylation is of primary functional significance when related to transcriptional competence (Kuo *et al.*, 2000).

The H4 acetylation of the *Xist* gene has also been investigated at a higher resolution using embryonic stem cells. This is of particular interest given the behaviour of *Xist* expression during female ES cell differentiation. O'Neill *et al*., (1999) identified a

region of H4 hyperacetylation that extended 120kb upstream of the P1 promoter. Interestingly the hyperacetylated region was not observed in male cells and was lost in female cells following differentiation.

A subsequent study by Heard *et al.,* (2001) showed that this 120kb domain was also enriched for H3 di-methylated at lysine 9. This is somewhat paradoxical given the general trend of these histone modifications. However, a particular combination of modifications may mark this domain for a particular function during X chromosome inactivation. The next step must be to focus on how the enzymes capable of histone modification (i.e. HMTs, HATs and HDACs) are targeted to this domain.

1.2.4 Epigenetic mechanisms are synergistic in the maintenance of X chromosome inactivation

X inactivation is a very stable process of gene silencing in mammals. Following inactivation Xi is clonally inherited from one cell generation to another as transcriptionally silent chromatin. The silencing mechanisms employed by *Xist* RNA, methylation of CpG islands and H4 hypoacetylation have been shown to act synergistically in maintaining the inactive state (Csankovszki *et al.*, 2001). Attempts to reactivate silent genes on Xi have centred on interfering with CpG island methylation through the inhibition of DNA methyltransferase 1 (Dnmt1) by 5-azacytidine. Reports have documented the derepression of several genes using this inhibitor and provided evidence for the role of DNA methylation in the maintenance of X inactivation (Mohandas *et al.*, 1981; Graves, 1982). An *in vivo* demonstration of the importance of CpG methylation is the instability of silencing on Xi in ICF (Immunodeficiency Centromeric instability Facial abnormalities) patients. The inactive X in patients

suffering from this syndrome is hypomethylated at all CpG islands analysed on account of mutations in the DNA methyltransferase DNMT3B (Hansen *et al.*, 2000). ICF cases have been shown to display abnormal escape from X inactivation with the genes subject to reactivation replicating early in the same time period as their active homologue.

Reactivation of X-linked genes by altering histone acetylation levels has not yet been reported. Indeed, the hypoacetylated Xi is remarkably resistant to histone deacetylase inhibitors such as Trichostatin A (Csankovszki *et al.*, 2001). *Xist* RNA is essential for the initiation of X inactivation (Penny *et al.*, 1996; Marahrens *et al.*, 1997). However, evidence suggests that after X inactivation has been established *Xist* is no longer required for maintenance of the silent state (Brown and Willard, 1994; Rack *et al.*, 1994). This is despite its continued association with Xi throughout the lifetime of the female mammal (Clemson *et al.*, 1996).

Despite the synergism displayed by CpG island methylation and histone hypoacetylation on Xi these properties, as well as the characteristic of late replication are in fact separable and not dependent on one another. DNA methylation and late replication were shown to be independent in patients suffering from ICF syndrome. Whilst all of the CpG islands analysed on Xi displayed DNA hypomethylation, a proportion of the genes were transcriptionally silent and replicated as normal in the late S phase of the cell cycle (Hansen *et al.*, 2000). Studies using the Dnmt1 inhibitor 5-azacytidine support this data, and suggest that late replication can operate independently of CpG island methylation (Hansen *et al.*, 1996).

Keohane *et al*., (1998) demonstrated that late replication and H4 hypoacetylation are separable using the histone deacetylase inhibitor Trichostatin A (TSA). Whilst Xi in female somatic cells exhibits remarkable resistance to this inhibitor, the appearance of a hypoacetylated Xi can be prevented by differentiating embryonic stem cells in medium supplemented with the inhibitor. However, a late replicating Xi was detected within its usual time frame following three days of differentiation. This demonstrates that the hypoacetylated Xi is not simply a consequence of late replication.

Immunolabelling of marsupial metaphase chromosomes has shown that histone hypoacetylation occurs in the absence of CpG island methylation on Xi (Wakefield *et al.*, 1997). Female marsupials are subject to imprinted X chromosome inactivation in much the same manner as the extraembryonic tissues of the mouse. However, the only molecular aspect shared between marsupial and eutherian mammals is that of histone hypoacetylation. This suggests that histone hypoacetylation was a feature of dosage compensation in a common mammalian ancestor. The lack of CpG methylation and the synergism generated by the epigenetic features mentioned previously may explain why the marsupial Xi appears to be less stable, with gene reactivation occurring *in vitro* (Kaslow and Migeon, 1987).

1.2.5 The epigenetics of Xi can spread into autosomal chromatin in X;autosome translocations

The spread of the X inactivation signal into autosomal DNA was first observed in mice carrying X;autosome translocations by Russell (1963). Using coat colour variegation as a genetic marker it was shown that gene silencing was capable of spreading in a limited fashion into the autosomal segment (Russell, 1963). This has been confirmed by

numerous subsequent studies and extended to show that the epigenetic features associated with the inactive X can accompany the spread of gene silencing (Keitges and Palmer, 1986; Jones *et al.*, 1997). The spread of late replication has been the most widely used tool for studying the extent of spread of X inactivation into autosomal DNA. This has often been shown to correlate well with the severity of the clinical phenotype displayed by carrier individuals (Mohandas *et al.*, 1982; Canun *et al.*, 1998). Individuals carrying unbalanced X;autosome translocations are trisomic for the genes on the autosomal segment of the translocated chromosome. These cases often exhibit a clinical phenotype less severe than expected, assumed to be on account of the spreading of the X inactivation signal into the autosomal portion of the translocated chromosome thereby creating functional disomy.

Too often the extent of spread of X inactivation has been purely based on late replication analysis, assessment of the severity of the clinical phenotype or the transcriptional analysis of a single autosomal gene. This is important in view of the fact that the characteristics of Xi do not always correlate with one another (section 1.2.4) or the transcriptional competence of a particular region (Sharp *et al.*, 2001). Indeed recently it has become clear that the study of X;autosome translocations must incorporate gene expression analysis of the autosomal segment on the translocated chromosome in conjunction with late replication or histone hypoacetylation (White *et al.*, 1998; Sharp *et al.*, 2001).

The process of spread of the X inactivation signal from the *Xic* occurs in *cis* and was proposed to be facilitated by DNA elements that served to amplify and spread the signal along the entire length of the chromosome (Gartler and Riggs, 1983). This model

has been expanded upon to propose that the DNA sequences responsible were LINE-1 (L1) elements (Lyon, 1998). L1 elements are mammalian-specific retrotransposons that are specifically enriched on the mouse and human X chromosomes (Korenberg and Rykowski, 1988; Boyle *et al.*, 1990). Subsequent to this report sequence data showed that the human X chromosome was enriched by two fold relative to autosomal DNA for the L1 repeat element, with the greatest enrichment at the *Xic* (Bailey *et al.*, 2000). Given the variable degrees of spread of the X inactivation signal in cases of X;autosome translocation, it was speculated that autosomal chromatin lacks certain features associated with the spread of X inactivation making it resistant to the acquisition of properties associated with Xi. Lyon's L1 repeat hypothesis is supported by data suggesting that the failure of the inactivation signal to spread into the autosomal chromatin often correlates with translocation breakpoints deficient in L1 elements (Lyon, 1998).

1.3 The enzymology of chromatin – the establishment of an epigenetic code

The steady state level of histone acetylation at a particular chromatin domain is established and maintained by multiple histone acetyltransferases (HATs) and deacetylases (HDACs). In different species an increasing number of HATs and HDACs are being identified suggesting that they might be involved in specialised functions.

1.3.1 Mammalian histone deacetylases

The identification of the first histone deacetylase revealed the existence of a family of proteins related to the yeast transcriptional regulator Rpd3. These proteins share a common catalytic domain and are referred to as the class I histone deacetylases (HDACs 1, 2, 3, 8) (Khochbin *et al.*, 2001). HDAC1 and 2 have been identified as

members of two multiprotein complexes known as Sin3/HDAC and NuRD/Mi2/NRD (Knoepfler and Eisenman, 1999). In addition to HDAC1 and 2, these independently identified complexes share common components such as RbAp46/48, capable of binding directly to histone H4 and suggested to mediate core histone binding for the Sin3/HDAC complex (Verreault *et al.*, 1998). However, aside from these multisubunit complexes, an increasing number of individual transcription factors have been shown to associate with the deacetylases. For example HDAC1 or HDAC2 were found associated with Rb, YY1, and Sp1 (Ng and Bird, 2000). HDAC3 is not found in either the Sin3/HDAC or NuRD/Mi2/NRD complexes and its function appears integrally linked with the activity of nuclear receptor corepressors such as SMRT or N-CoR (Li *et al.*, 2000).

Class II histone deacetylases (HDACs 4, 5, 6, 7, 9, 10) (Grozinger *et al.*, 1999; Verdel and Khochbin, 1999; Zhou *et al.*, 2001; Kao *et al.*, 2002) were classified based on their homology to the yeast histone deacetylase HDA1. They possess several features that distinguish them from class I deacetylases; they are larger and the catalytic domain is located at the C-terminus rather than the N-terminus as in the class I HDACs. Whilst our understanding of the process of transcriptional control by the class II HDACs remains in its infancy progress has been made through the study of their subcellular distribution (Lemercier *et al.*, 2002). Class II HDACs have been shown to form distinctive "MAD" (matrix associated deacetylase) bodies in the nucleus composed of corepressors N-CoR and SMRT together with class I HDACs (1, 2 and 3) (Downes *et al.*, 2000), suggesting that class I and II HDACs can be found in the same complex. Class II HDACs have also been shown to be subject to nucleocytoplasmic shuttling,

their function being dependent on cellular localisation (Miska *et al.*, 1999; Grozinger and Schreiber, 2000).

The most recently identified class of histone deacetylases; the class III or Sir2 class was identified based on homology to the yeast transcriptional repressor Sir2 (Imai *et al.*, 2000). The Sir2 enzyme possesses nicotinamide adenine dinucleotide (NAD^+)-dependent histone deacetylase and ADP-ribosylation activity. Although no complexes containing this enzyme have been identified, it is generally assumed that the class III members are involved in functions not shared by the class I and II HDACs. This idea is based on the putative control of Sir2 by cellular pathways involving NAD. However, mammalian Sir2α has recently been shown to have involvement in modulating the p53-dependent apoptotic response (Luo *et al*., 2001) suggesting that histones may not be its only substrate *in vivo*.

1.3.2 Mammalian histone methyltransferases

Histone methylation is catalysed by the recently discovered histone methyltransferases (HMTs) that are specific to either lysine or arginine (Khan and Hampsey, 2002; Kouzarides, 2002). The Su(var)3-9 gene was originally identified as a suppressor of position effect variegation in *Drosophila*, but was subsequently shown to possess lysine methyltransferases activity (Rea *et al.*, 2000). This identification revealed a class of HMTs related to Su(var)3-9 capable of catalysing the addition of methyl groups onto lysine 9 of H3. The lysine methyltransferase catalytic domain resides within a highly conserved structure referred to as the SET (Su(var)3-9, Enhancer of zeste, Trithorax) domain. Based on the similarity between the SET domains of the HMTs and their relationship with SET domain proteins in yeast, it has been proposed that there are at

least four classes of lysine methyltransferases in humans; SUV39, SET1, SET2 and RIZ families (Kouzarides, 2002; Schneider *et al.*, 2002). The SET1 family in yeast has the potential to methylate lysine 4 of H3, a modification linked with transcriptionally active regions (Briggs *et al.*, 2001; Roguev *et al.*, 2001). The SET2 family have the potential to methylate histone H3, whilst the RIZ family have an as yet undefined substrate specificity (Kouzarides, 2002).

1.3.3 Enzyme-mediated repression of gene transcription

The involvement of both histone deacetylases and methyltransferases in gene transcriptional repression can be best explained using the example of cell proliferation and differentiation control by the retinoblastoma (Rb) protein (Brehm and Kouzarides, 1999). The target proteins of Rb include the E2F group of transcription factors, which activate genes essential for the progression of the cell cycle into S phase. Binding of Rb inhibits the ability of E2F to activate transcription. In differentiating cells the E2F target genes are transcriptionally silent because of the repression mediated by Rb and its associated histone deacetylase (HDAC1) (Magnaghi-Jaulin *et al.*, 1998; Ferreira *et al.*, 2001) and methyltransferase (SUV39) (Nielsen *et al.*, 2001). Evidence suggests that HDAC1 and SUV39, both with no DNA binding capacity, are "delivered" by Rb to E2F causing deacetylation and methylation of H3 lysine 9 at the promoter regions of E2F regulated genes (figure 5). Subsequent binding of heterochromatin protein HP1 to di-methylated lysine 9 of H3 stabilises the E2F target genes in a transcriptionally silent state (Nielsen *et al.*, 2001). In proliferating cells the E2F target genes are expressed in a cell cycle dependent manner; silent during early G1 owing to the association of Rb with E2F and the associated HDAC/HMT complex, but expressed following the restriction

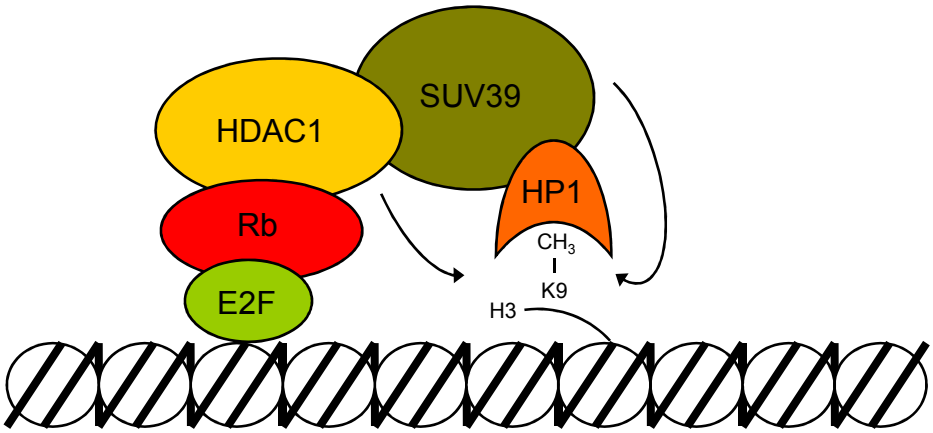

Figure 5. The histone deacetylase HDAC1 and the histone methyltransferase SUV39 are “delivered” to the E2F target genes by the retinoblastoma protein (Rb). Recruitment of HDAC1 and SUV39 results in histone deacetylation and H3 lysine 9 methylation. The inactive state is stabilised by the subsequent binding of heterochromatin protein HP1 to methylated lysine 9 of H3. Adapted from Kouzarides (2002).

point between the G1 and S phases of the cell cycle. The activation of the E2F target genes occurs due to the dissociation of Rb/HDAC/HMT from E2F, alleviating the transcriptional repression. Aside from a few specific examples such as this the recruitment and distribution of the mammalian histone deacetylases and methyltransferases remains poorly characterised across the genome.

Rpd3, a yeast histone deacetylase homologue of the mammalian class I HDACs has also been shown to exert gene-specific transcriptional repression through recruitment by DNA binding proteins such as Ume6 (Kadosh and Struhl, 1997; Rundlett *et al.,* 1998). However, despite this targeted recruitment, Rpd3 has also been shown to function over large chromosomal domains in a process referred to as "global deacetylation" (Vogelauer *et al.,* 2000). It was proposed by Vogelauer *et al.,* (2000) that targeted histone modifications occur in a background of global acetylation and deacetylation that serves to allow a rapid return to the initial state of acetylation when targeting is removed. Furthermore in contrast to targeted loci "global" deacetylation may occur through the binding of Rpd3 in a sequence-independent manner to histones or histone binding proteins. This was reiterated by a subsequent study, Kurdistani *et al.,* (2002) which showed that Rpd3 was found specifically enriched at the *INO1* gene but also in a 10kb chromatin domain surrounding the gene. Interestingly, the global Rpd3 binding was not dependent on the presence of Ume6 or Ume1, both shown to direct Rpd3 during gene-specific transcriptional repression (Kurdistani *et al.*, 2002).

1.3.4 Reactivation of silenced genes by histone deacetylase inhibitors

Aberrant histone acetylation of genes important in cell cycle regulation has been linked to malignant diseases in some cases. Inhibitors of histone deacetylases have

become important owing to their ability to modulate transcription and induce differentiation and apoptosis (Johnstone, 2002). HDAC inhibitors can be classified on the basis of structure and mode of inhibition. Reversible inhibitors include *n*-butyric acid and other related short chain fatty acids (Candido *et al.*, 1978; Sealy and Chalkley, 1978), the microbial antibiotic Trichostatin A (TSA) (Yoshida *et al.*, 1990), and hybrid polar compounds such as Suberoylanilide Hydroxamic Acid (SAHA) (Richon *et al.*, 1998). The mode of inhibition by these inhibitors is likely to be through the binding of the of a catalytic zinc ion at the active site of HDAC (Hassig *et al.*, 1998). Irreversible inhibitors including Trapoxin and related natural products such as HC toxin are thought to bind irreversibly to the enzymes active site (Johnson, 2000).

TSA and SAHA have both been shown to markedly induce differentiation and apoptosis in transformed cell lines (Richon *et al.*, 1998; Kosugi *et al.*, 1999) giving hope for use of HDAC inhibitors in cancer chemotherapy.

However, interfering with histone deacetylases through the use of inhibitors or by gene knock outs has often produced no detectable increase in the transcription of genes known to be controlled by histone deacetylases (Ferreira *et al.*, 2001; Kurdistani *et al.*, 2002). Indeed a recent study suggested SAHA induced the expression of less than 2% of genes in cultured cells (Butler *et al.*, 2002).

Therefore it can be concluded that the control of gene expression involves many synergistic and perhaps partially redundant epigenetic features that cannot always be disrupted by targeting one aspect alone. The following study has used the female inactive X chromosome to analyse the histone modifications that accompany gene silencing. This seems appropriate given the parallels that can be drawn between

silencing at the single gene level and at the global chromosomal level. Furthermore many features of the inactive X chromosome such as H4 hypoacetylation, late replication and DNA methylation are shared by other gene silencing pathways. The aims of this project were to examine the patterns of histone methylation and hypoacetylation that characterise the silent chromatin of Xi and define their temporal order as they become established *in vitro* using differentiating mouse embryonic stem cells. It was also my intention to examine how these histone modifications relate to actual transcriptional silencing using cases of X;autosome translocation. These cases allow the spread of X inactivation as defined by gene silencing to be directly compared to the replication timing of the DNA and the epigenetics of the chromatin. Finally I have examined a potential mechanism that might serve to drive changes in patterns of histone modification. I have analysed the distribution of the class I histone deacetylases across a region of defined histone deacetylation upstream of the *Xist* gene (O'Neill *et al.*, 1999).

2 MATERIALS AND METHODS – CHAPTER TWO

2.1 Cells and cell culture

The female mouse embryonic stem (ES) cell line Pgk12.1 has been described previously (Norris *et al.,* 1994). The male ES cell line CCE/R was derived from a 129 mouse and was provided by Dr. G. Anderson, University of Birmingham, Birmingham. The ES cell lines were maintained as undifferentiated monolayers in Dulbecco's Modified Eagle Medium (DMEM) supplemented with penicillin/streptomycin, L-glutamine, non-essential amino acids, 20% fetal calf serum and 10^3 U/ml murine Leukaemia Inhibitory Factor (LIF: all reagents Gibco-BRL) (Williams *et al.,* 1988; Nichols *et al.,* 1990). All cells were cultured at 37^{o}C in 5% CO_2 in air. Flasks (Falcon) were coated in 0.1% gelatine prior to plating of cells and cultures were split 1:4 every 2-3 days. Cells were induced to differentiate into non-attached embryoid bodies by trypsinisation (trypsin-EDTA, Gibco-BRL) and transfer to petri dishes (Sterilin) in medium lacking LIF. ES cells were not harvested later than passage 25. In some experiments the culture medium was supplemented with the histone deacetylase inhibitor Trichostatin A (TSA, Sigma) at a final concentration of 5ngml^{-1} in order to study its long-term effects.

Primary mouse embryonic fibroblasts (PMEFs) were isolated by following standard procedures (Robertson, 1987). 12-13d old pregnant females were sacrificed by cervical dislocation and the embryos removed. Following decapitation and the removal of all internal organs the embryos were washed three times in sterile PBS. Five to eight carcasses were then placed in the barrel of a sterile 3ml syringe and passed through an 18-gauge needle four or five times or until all the clumps of cells had been dispersed into a sterile petri dish. DMEM/10%FCS/penicillin/streptomycin

was then added to the resulting cell suspension and incubated at 37^{o}C overnight. After 48hrs the old medium was replaced with fresh and the fibroblasts were allowed to establish over the next three days without splitting. Primary fibroblasts were maintained in culture for a maximum of 8 passages.

The human-hamster somatic cell hybrid line X8-6T2S1 contains a human inactive X chromosome in a male hamster background. The cell line was provided by Dr. S. M. Gartler, University of Washington, Seattle, USA and was grown as an attached monolayer in RPMI (Gibco-BRL) medium containing 8% fetal calf serum, L-glutamine and penicillin/streptomycin. HeLa cells were maintained under identical culture conditions.

EBV-transformed human lymphoblastoid cell lines AH, SP, SR, AL0044, BO0566 and GM12616, were all provided by A. J. Sharp, Wessex Regional Genetics Laboratory, Salisbury and were maintained as suspension cultures in RPMI medium supplemented with penicillin/streptomycin, 8% fetal calf serum, and L-glutamine. The HL60 cell line was derived from a human promyeloid leukaemia and was grown under identical culture conditions.

2.2 Antibodies

The preparation of polyclonal antisera against the acetylated and methylated histone isoforms has been described previously (Turner and Fellows, 1989; Turner *et al.*, 1989). Antibodies were raised in rabbits against synthetic peptides conjugated to ovalbumin, unless otherwise stated. All histone antibodies were raised in Birmingham unless otherwise indicated and specificities confirmed using peptide inhibition ELISA

(Enzyme Linked Immunosorbant Assay) and SDS-PAGE/Western blot. For chromatin immunoprecipitation experiments histone antibodies were affinity purified on peptide-Sepharose columns prior to use (White *et al.,* 1999). Antisera were prepared against components of human deacetylase complexes using the following synthetic peptides, HDAC1, EEKPEAKGVKEEVKLA; HDAC2, GEKTDTKGTKSEQLSNP; HDAC3, APNEFTDGDHDNDKESDVEI; RbAp48, ENIYNDEDPEGSVDPEGQGS. Histone deacetylase antisera were column-purified for total IgG using protein A-Sepharose as described by the manufacturer (Amersham Biosciences, Inc.). All histone deacetylase antibodies were shown to recognize a single protein band of appropriate size using SDS-PAGE and Western blotting. The antibodies used in this study are displayed in Table 1.

2.3 Indirect immunofluorescence

The immunolabelling of metaphase chromosomes was performed as described previously (Keohane *et al.*, 1996; O'Neill *et al.*, 1999) unless otherwise stated. Mitotic cells were collected following growth for 2-3h in medium containing Colcemid (Gibco-BRL, 2ngml^{-1} except ES cells 0.5ngml^{-1}). For immunolabelling experiments using antibodies to acetylated H2A, H2B and H3, Trichostatin A (25ngml^{-1}) was added concurrently to the Colcemid. Cells were harvested by mitotic shake-off for undifferentiated ES cells, X8-6TS1 and PMEFs or by dissociating embryoid bodies using a Pasteur pipette for differentiated ES cell samples. Cells were washed twice in ice-cold PBS (140mM NaCl, 2mM KCl, 5mM Na_2HPO4, 2mM NaH_2PO_4) and counted. Cells were centrifuged following each wash at 1000rpm in a MSE chillspin for 7 minutes at 4^{o}C. The cells were resuspended in 75mM KCl for human and 100mM KCl for mouse cells, both at a density of 3×10^5 cells ml^{-1} for 10 minutes.

Table 1. Antibodies and their specificities (Ac – Acetylated, Me – Methylated)

Antibody	Epitope	Notes
R41	H4 AcK5	
R232	H4 AcK8	
R101	H4 AcK12	
R252	H4 AcK16	
R243	H4 Ac	No lysine specificity. Recognises all acetylated lysine sites of histone H4.
R224	H3 AcK14	
R123	H2A AcK5	
R209	H2B AcK12/15	
R148	$H3Me_2K4$	
	$H3Me_3K4/9$	Provided by Dr. A. J. Bannister and Dr. T. Kouzarides / Abcam, Cambridge, UK
R183	$H3Me_3K4$	
R151	$H3Me_2K9$	
	$H3Me_2K9$	Obtained from Upstate - Derived using a linear peptide.
	$H3Me_2K9_{BCH}$	Provided by Dr. T. Jenuwein - Derived using a "branched" hexameric peptide
	$H3Me_3K9/27$	Provided by Dr. A. J. Bannister and Dr. T. Kouzarides / Abcam, Cambridge, UK
R153	$H4Me_2K20$	
R238	Hdac1	
R272	Hdac2	
R274	Hdac3	
	Hdac3	Obtained from BD Transduction Laboratories – Mouse monoclonal antibody shown to recognize Hdacs 1, 2 and 3
	Hdac4	Provided by Dr. A. Wang, McGill University, Montreal, Quebec, Canada
	Sir2α	Obtained from Upstate – Mouse monoclonal antibody
R63	RbAp48	

Approximately 6×10^4 cells were cytospun (Shandon Cytospin 3) onto each ethanol washed glass slide (Gold Star) at 1800rpm for 10 minutes. The slides were incubated in KCM buffer (120mM KCl, 20mM NaCl, 10mM Tris-HCl, ph8, 0.5mM EDTA, 0.1% (v/v) Triton X-100) for 10 minutes. Slides were incubated with the primary antibody at the appropriate dilution for one hour in a humid chamber at 4^oC. All antibodies were applied in 1% (w/v) BSA (Sigma)/KCM. For peptide inhibition experiments the antisera were incubated with the synthetic peptide ($0.5mgml^{-1}$) for 30 minutes on a rotating turntable prior to immunolabelling. Slides were washed for 10

minutes in KCM buffer before incubation with the secondary antibody. A FITC (Fluorescein Isothiocyanate) conjugated goat anti-rabbit secondary antibody (Sigma), diluted ×50 was applied for one hour before a final KCM wash and fixation in 4% (v/v) formaldehyde (Sigma USP)/KCM. Slides were counterstained using 4', 6-diamidino-2-phenylindole dihydrochloride (DAPI; 1μgml^{-1}; Sigma) in Vectorshield (Vector labs). Images were visualized with a Photometrics SenSys KAF 1400-G2 CCD fitted to a Zeiss Axioplan fluorescence microscope and captured by using Quips M-FISH software (Vysis) running on a Macintosh G3 computer.

2.4 Indirect immunofluorescence detection using H3Me$_2$K9$_{BCH}$

Immunofluorescence detection of H3Me$_2$K9$_{BCH}$ was performed using unfixed and fixed conditions. Unfixed chromosomes were prepared and labelled using the method described above and fixed conditions were based on the method in Mermoud *et al*., (2002). Metaphase spreads were generated as above and fixed using ice-cold 2% (v/v) formaldehyde (Sigma, USP)/PBS/0.1% (v/v) Tween 20 (Sigma) for 25 minutes. Cells were blocked in 3% BSA/PBS/0.1% Tween 20 for 10 minutes and incubated at 37^{o}C for two hours with the primary antibody prepared at a dilution of 1:1000 in PBS/0.1% Tween 20. Slides were washed using PBS/0.1% Tween 20 followed by detection using the secondary antibody described above diluted in PBS/0.1% Tween 20 and applied for 30 minutes at 37^{o}C. After a final wash the slides were mounted and the images were recorded as described above.

2.5 Combined immuno-FISH (fluorescence in situ hybridisation) using a human X chromosome DNA probe

For combined immunofluorescence and fluorescence *in situ* hybridisation (FISH) cells were immunolabelled and captured as above. The England Finder positions of the appropriate metaphase spreads were recorded. The coverslip was removed carefully and slides were washed in 4×SSC/0.1% Tween 20 for two minutes. Slides were incubated in ice-cold methanol: acetic acid (3:1) for 10 minutes and dehydrated in an ice-cold ethanol series (70%, 90%, 100%) for two minutes each. Slides were air-dried and RNase/Pepsin (Oncor) was applied under a coverslip for two minutes at room temperature. Slides were dehydrated using an ethanol series as above and air-dried. Digoxigenin labelled DNA probe DXZ2 (Oncor), hybridising to human X chromosome α-satellite DNA was applied to the cells, a coverslip was added and the edges sealed with rubber cement. The slides together with the probe were co-denatured on a hotplate at 72^{o}C for three minutes. The probe was incubated for a minimum of one hour at 37^{o}C. The coverslip was removed and the slides were incubated twice in a stringent wash (0.1×SSC/0.1% Tween 20) for five minutes each at 65^{o}C. The blocking reagent (Roche) was applied under a coverslip and incubated for 30 minutes at room temperature. The TRITC (Tetramethylrhodamine Isothiocyanate) conjugated anti-digoxigenin antibody (Vector labs) was applied to the slide in the dark at 37^{o}C for 30 minutes. The coverslip was removed and the slide was washed in 4×SSC/0.1% Tween 20. Finally the slide was mounted with DAPI as before. Metaphases were relocated and the FISH/immunolabelling was superimposed using Adobe Photoshop 7.

2.6 Combined immuno-FISH using a mouse whole X chromosome paint

Slides were captured and treated as above. A whole X chromosome paint (Oncor) was directly labelled with FITC and applied as defined by the manufacturer with minor modifications. Briefly slides were denatured at 75^{o}C for one minute in 70% deionised formamide/2xSSC, passed through an alcohol series of ice-cold 75%, 95%, 100% methanol and dried on a hot plate. The probe was denatured at 75^{o}C for five minutes snap chilled on ice for 30 seconds and warmed at 37^{o}C for five minutes. The probe mixture was placed on the denatured slide, and sealed under a coverslip. Slides were hybridised at 37^{o}C overnight. Post hybridisation washes were performed in 2×SSC at 75^{o}C for five minutes, washed in PN buffer (4l of 0.1M sodium phosphate (dibasic solution) titrated with 0.1M sodium phosphate (monobasic solution) to pH8, 0.1125% (v/v) NP40) for 10 minutes. The slides were mounted and captured as defined above.

2.7 Isolation of histones

Cells were harvested as usual and washed twice in ice-cold PBS with 5mM Sodium Butyrate. Cells were resuspended in Triton Extraction Buffer (TEB: PBS containing 0.5% Triton X 100, 2mM phenylmethylsulfonyl fluoride (PMSF), 0.02% (v/v) NaN_3) at a cell density of 10^7 cells ml^{-1}. Cells were kept on ice for 10 minutes, and centrifuged at 2000rpm for 10 minutes at 4^{o}C. Cells were washed in half the volume of TEB and centrifuged at 2000rpm. Pellets were resuspended in 0.2N HCl at a cell density of 4×10^7cells ml^{-1}. Histones were acid extracted over night at 4^{o}C. Samples were centrifuged at 2000rpm for 10 minutes at 4^{o}C. The supernatant was removed and kept at –20^{o}C. The protein content of the histone extract was assayed using Pierce^{TM} reagent, used as directed by the manufacturer.

2.8 Sodium dodecyl sulphate (SDS), acid urea triton (AUT) polyacrylamide gel electrophoresis and Western blotting

Polyacrylamide gels containing SDS were prepared and run as in Sambrook *et al.,* (1989). Histones were separated using 15% gels and the deacetylases using 7.5%. Low molecular weight markers (Bio Rad) were run adjacent to the deacetylases. AUT gels were prepared and run as described previously (Turner *et al.,* 1989). Gels were either stained with Coomassie Blue or transferred to nitrocellulose membranes (Hybond C+, Amersham) as previously described (Sambrook *et al.,* 1989). Western blots used standard blocking buffer (50mM Tris-HCl, pH 7.5, 150mM NaCl, 0.05% Tween 20 containing 5% (w/v) non fat powdered dry milk (Marvel^{TM})). Hybond C membranes were blocked for one hour on a rotating turntable before labelling with the antibody for a further hour. Saturated ammonium sulphate (SAS) cuts of antisera were used for immunolabelling with dilutions between 400 and 1000 in blocking buffer. Membranes were washed in blocking buffer without the dry milk three times for 15 minutes each before immunodetection with a peroxidase conjugated secondary antibody (Sigma) diluted ×1000. Following labelling with the secondary antibody for one hour and washing as described detection was performed using enhanced chemiluminescence (ECL) as defined by the manufacturer.

2.9 Native chromatin immunoprecipitation (NChIP)

The immunoprecipitation of native chromatin (NChIP) was performed as described previously (O'Neill and Turner, 1995). ES cells were grown overnight in medium supplemented with ^{3}H-Thymidine (2mCi/mmol) at 0.25μCi/ml. Undifferentiated cells were harvested by trypsinisation (trypsin-EDTA, Gibco-BRL). Embryoid bodies were harvested by treatment of collagenase/dispase/PBS (5μgml^{-1}, Sigma). Cells were

washed twice in ice-cold PBS/5mM sodium butyrate. The cell pellet was resuspended in TBS (10mM Tris-HCl pH 7.5, 3mM $CaCl_2$, 2mM $MgCl_2$, 5mM Na Butyrate) at a density of 2×10^7cellsml^{-1}. An equal volume of TBS/1% (v/v) Tween 40 (Sigma) was added in addition to PMSF at a final concentration of 0.1mM. The cell suspensions were left stirring on ice for one hour. Cell lysates were homogenised using a Dounce homogeniser (tight seal) to generate nuclei. The nuclei were pelleted by centrifugation at 3000rpm at 4^{o}C for 20 minutes and resuspended in 25% (w/v) Sucrose (Sigma)/TBS at a density of 10^6cellsml^{-1}. This was underlayed with half the volume of 50% Sucrose (Sigma)/TBS. The sucrose gradient was centrifuged at 3000rpm for 10 minutes at 4^{o}C. The nuclei pellet was resuspended in 5ml digestion buffer (0.32M Sucrose, 50mM Tris-HCl pH 7.5, 1mM $CaCl_2$, 4mM $MgCl_2$, 5mM Na Butyrate, 0.1mM PMSF). The mass of chromatin was calculated by taking A260 readings. An aliquot of nuclei was diluted 25× in 0.1% SDS and readings taken using an Ultrospec 2100 pro spectrophotometer. The nuclei were centrifuged at 2000rpm for 10 minutes and resuspended in digestion buffer at a concentration of 0.5mgml^{-1}. Resuspended nuclei were separated into 1ml aliquots in 1.6ml eppendorfs. A 1ml aliquot of chromatin was digested using 50U Micrococcal nuclease (MNase) for five minutes at 37^{o}C. The digestion reaction was terminated by the addition of EDTA to a final volume of 15mM. Samples were chilled on ice for five minutes before centrifuging at 13000rpm for 10 minutes. The supernatant was removed and kept at 4^{o}C and designated SN1. The supernatant contains the chromatin most accessible to the MNase and consists largely of mono- and di-nucleosome fragments. The pellet was resuspended in 1ml lysis buffer (1mM Tris-HCl pH 7.4, 0.2mM EDTA, 5mM Na Butyrate, 0.2mM PMSF) and dialysed overnight against 2 litres of the same buffer. Following overnight dialysis the samples were centrifuged at 2000rpm at 4^{o}C for 10

minutes. The supernatant was removed and designated SN2. The pellet was resuspended in 200µl lysis buffer. The chromatin was analysed by A260 (as before), scintillation counting (dpm), and electrophoresed using 1.2% Agarose gels (Sigma) in 0.5×TBE (45mM Tris-Borate, 1mM EDTA) as directed in Sambrook *et al.,* (1989). Prior to electrophoresis 2µg of each of the chromatin fractions were added to 3µl 0.1% SDS and 2µl DNA loading buffer (0.25% (w/v) Bromophenol blue (Sigma), 0.25% (w/v) Xylene cyanol FF (Sigma), 15% (v/v) Ficoll (Pharmacia) in water) and made up to 30µl using dH_20. The DNA was visualised by staining with Ethidium Bromide ($0.5\mu gml^{-1}$) and capturing using a Syngene biomaging system.

Chromatin fractions SN1 and SN2 were pooled into siliconised 1.6ml eppendorfs and A260 readings taken. In a typical experiment 150µg of chromatin was made up to 1ml using incubation buffer (50mM NaCl, 20mM Tris-HCl pH 7.5, 5mM EDTA, 5mM Na Butyrate, 0.1mM PMSF) and incubated with affinity purified histone antibodies together with a no-antibody control overnight on a rotating turntable at 4^oC. A 100µl aliquot of a 50% (v/v) slurry of protein A-Sepharose (PAS, Pharmacia) was added for two hours on a rotating turntable at room temperature. The PAS was pre-swollen overnight in wash buffer A (see below). The PAS was pelleted by pulse centrifuging at 13000rpm. The supernatant was removed and kept as the UNBOUND fraction. The PAS was transferred to 15ml Falcon tubes using 1ml of wash buffer A (50mM NaCl, 50mM Tris-HCl pH 7.5, 10mM EDTA, 5mM Na Butyrate). The PAS pellets were washed using 10mls of wash buffer A before being pelleted and washed using buffers B and C (same as A except 100mM and 175mM NaCl respectively). The PAS pellets were transferred back to siliconised eppendorfs using wash buffer C, pelleted and resuspended in 250µl 1% SDS/incubation buffer. Immunocomplexes were eluted

from the PAS by vortexing and rotating on a turntable at room temperature. Following pulse centrifugation the supernatant was kept as the BOUND fraction. This was repeated to give 500µl. This fraction contained chromatin enriched for the targeted histone modification. 500µl of incubation buffer was added to each of the bound samples.

The protein and DNA were recovered by adding 330µl of phenol (Q.BIOgene): chloroform (BDH) (both prepared as outlined in Sambrook *et al.,* (1989)), vortexing and centrifuging for five minutes at 2000rpm. The supernatant was removed each time and transferred into fresh tubes. This was repeated, followed by chloroform purification. To the final supernatant 100µl 4M LiCl, 4ml Absolute Ethanol, and 20µg Glycogen (Roche) was added. The DNA was precipitated overnight at –20^{o}C. The DNA was centrifuged at 2000rpm for 30 minutes and the supernatant removed. The DNA pellet was left to air dry before being resuspended in 250µl dH_2O. To the first phenol: chloroform phase 10µl 10M H_2SO_4, 4ml Acetone and 10µg BSA (Sigma) was added. The protein was precipitated at –20^{o}C overnight and pelleted the following morning by centrifuging at 2000rpm for 30 minutes. Protein pellets were washed twice in dry acetone, centrifuging at 2000rpm each time before vacuum drying for 30 minutes. For the analysis of protein the pellet was resuspended in 1×standard dissociating buffer (SDB, 100mM Tris-HCl pH 7.2, 1mM EDTA, 1% SDS, 143mM Mercaptoethanol) and electrophoresed using 15% SDS-PAGE (see above), followed by western blotting using the same antibody. The DNA was analysed by electrophoresis using a 1.2% Agarose gel to assay the degree of precipitation relative to the no-antibody control. 10µl of UNBOUND and 20µl of BOUND material were electrophoresed using the conditions mentioned above. ^{3}H-thymidine content was

assayed by taking scintillation counts (Optiphase High Safe 3) from each of the samples. Samples were adjusted using 0.6M NaCl to give equal dpm counts for BOUND and UNBOUND fractions. Following heat denaturating at 94^{o}C for 10 minutes the samples were chilled on ice. The DNA was serially diluted using 2M Ammonium Acetate and applied to nylon filters (Hybond N^{+}, Amersham) by slot blotting using a BioRad slot blot manifold.

Specific DNA sequences were detected by hybridisation with ^{32}P-labelled DNA probes. For the analysis of X-linked genes, probes were prepared by PCR using the primers and conditions explained below. DNA was extracted using a Qiagen PCR purification kit, as defined by the manufacturer. The *Tuba1* (*α-Tubulin*) probe used for slot blotting was a 1.5 kb *Pst* fragment of the coding region (Promega). Probes were ^{32}P-labelled by random priming with an oligolabelling kit (Pharmacia) used according to the manufacturer's instructions. The Het947 probe corresponded to mouse α-satellite DNA and was labelled using end labelling as described in Sambrook *et al*., (1989). Following overnight incubation with the probe and extensive washing, the filters were exposed to Phosphor screens (Molecular Dynamics) and quantified on a PhosphorImager (Molecular Dynamics). The relative histone acetylation levels of a DNA sequence were expressed as the intensity of the BOUND fraction divided by the UNBOUND fraction (B/UB).

2.10 Preparation of whole cell extracts

Cells were harvested and washed twice in ice-cold PBS. Cell pellets were resuspended in lysis buffer (10mM Tris pH 8, 150mM NaCl, 5mM EDTA, 5mM EGTA, 1mM β-Mercaptoethanol, 0.02% NaN_3, 1% Nonidet P40, and 1×protease inhibitor cocktail

(Roche)) at a cell density of 6×10^7cells ml^{-1}. Samples were on left ice for 30 minutes with gentle stirring. The cell suspension was sonicated using a Sanyo Soniprep 150 fitted with a parabolic probe. Sonication was performed on a mixture of ice, salt and water four times at setting 6. The cell extract was centrifuged at 13000rpm at 4°C for 10 minutes. The supernatant was removed and kept as a whole cell extract, with mass of protein assayed by Pierce™ reagent.

2.11 Immunoprecipitation of Hdac complexes using whole cell extracts

Whole cell extracts prepared from Pgk12.1 ES or HeLa cells were prepared as above. In a typical experiment 100µl of WCE (containing 100µg of soluble protein) was diluted with 850µl incubation buffer (identical to lysis buffer except the omission of Nonidet P40) and incubated with 20µg of IgG over night on a rotating turntable at 4°C. Control immunoprecipitations omitted antisera. All immunoprecipitations were performed in siliconised 1.6ml eppendorfs tubes. A 50µl aliquot of a 50% (v/v) slurry of low leaching protein A-Agarose (PAA, Sigma), washed previously in lysis buffer was added to the immunocomplexes and incubated at room temperature for three hours. The PAA was pelleted in a microcentrifuge (8000 rpm, 2 minutes) and washed 3 times in wash buffer (identical to lysis buffer except Nonidet P40 was at 0.1%). Immunocomplexes were eluted in 1% SDS and resolved using 7.5% SDS-PAGE under standard conditions (Sambrook *et al.,* 1989).

2.12 Formaldehyde cross-linking chromatin immunoprecipitation (XChIP)

XChIP was performed essentially as described previously (Orlando *et al.*, 1997; Orlando, 2000; Ferreira *et al.*, 2001). Approximately 2×10^8cells embryonic stem cells undifferentiated or differentiated for the appropriate number of days were cross-linked

directly using a final concentration of 1% formaldehyde (Sigma USP). Undifferentiated cells were trypsinised off the bed of the flask and resuspended in trypsin free medium. All cells were fixed as cell suspensions using fixation buffer (100mM NaCl, 1mM EDTA, 1mM EGTA, 50mM HEPES pH 8, 11% formaldehyde) at 37^{o}C for 8 minutes. Cross-linking was terminated by the addition of Glycine to a final concentration of 125mM. Fixed cells were washed twice in ice-cold PBS containing 1mM PMSF and 5mM Na Butyrate. Cells were resuspended in cell lysis buffer (5mM PIPES, 85mM KCl, 0.5% Nonidet P40, 1mM PMSF, 5mM Na But, 1×protease inhibitor cocktail) for 10 minutes on ice at a density of 4×10^{7}cells ml^{-1}. Cells were homogenised using a Dounce homogeniser. Nuclei were pelleted at 4000rpm for 20 minutes and lysed by resuspending in nuclear lysis buffer (50mM Tris-HCl pH8.1, 10mM EDTA, 1% SDS, 1mM PMSF, 5mM Na But, 1×protease inhibitor cocktail) at a density of 1×10^{8}cells ml^{-1}. Nuclei extracts were stirred on ice for 10 minutes.

Extracts were sonicated in 1.6ml eppendorfs tubes on a mixture of ice, salt and water using a Sanyo Soniprep 150 with a parabolic probe. Glass beads (400nm, BDH) were added prior to sonication. Samples were sonicated for 6 × 20 second bursts at setting 15 at a depth that prevented foaming. A 10µl aliquot of sonicated sample was removed and the cross-links were reversed overnight (see cross-linking reversal details) before recovery of the DNA using phenol: chloroform purification. Half the DNA from the samples was electrophoresed using a 0.8% Agarose gel. It was required that the majority of the chromatin fragments were below 2kb with an average of 500bp. Further sonications were necessary if the chromatin was of insufficient resolution. Chromatin of appropriate size was centrifuged at 13000rpm for 30 minutes

at 4°C. Soluble chromatin supernatants were removed and A260 readings taken. The samples were equalised for total DNA content using nuclear lysis buffer and diluted ten fold using ChIP dilution buffer (0.01% SDS, 1.1% Triton X 100, 1.2mM EDTA, 16.7mM Tris HCl pH 8.1, 167mM NaCl, 1mM PMSF, 5mM Na But, 1×protease inhibitor cocktail). Samples were pre-cleared using 200µl of a 50% slurry of pre-hybridised protein A-Sepharose (Pharmacia) on a rotating platform for 30 minutes at 4°C. Pre-swollen protein A-Sepharose was pre-hybridised over night using sonicated salmon sperm DNA (100µgml^{-1}, Sigma) and BSA (250µgml^{-1}, Sigma). Samples were centrifuged and the pre-cleared material was split into the appropriate number of 15ml-siliconised tubes. An input control (100µl) was retained to assay the efficiency of PCR on the sonicated material. In a typical experiment 30µl of IgG purified deacetylase antisera was added. A no-antibody sample served as a control for immunoprecipitation. The antibodies were incubated over night on a rotating turntable at 4°C.

A 50µl aliquot of a 50% (v/v) slurry of pre-hybridised Protein-A Sepharose (PAS) was added for two hours on a rotating turntable at room temperature. The PAS was pelleted by pulse spinning in a microcentrifuge at 8000rpm. The PAS was transferred to 1.6ml-siliconised eppendorfs by using 1.4ml dialysis buffer (2mM EDTA, 50mM Tris-HCl pH 8.0, 0.2% Sarkosyl, 1mM PMSF, 5mM Na But, 1×protease inhibitor cocktail). The tubes were inverted and the samples were washed twice using 1ml of dialysis buffer. The PAS pellet was washed a further four times using wash buffer (100mM Tris-HCl pH 9.0, 500mM LiCl, 1% Nonidet P40, 1% deoxycholic acid, 1mM PMSF, 5mM Na But, 1×protease inhibitor cocktail). The PAS was pelleted and the immunocomplexes were eluted twice at 65°C for 15 minutes using 150µl elution

buffer (50mM $NaHCO_3$, 1% SDS in filtered dH_2O). For the analysis of precipitated protein, complexes were eluted at room temperature using 1×SDB, boiled for one hour, chilled on ice and loaded onto a 7.5% SDS PAGE (see above).

To reverse the cross-links and prepare for the analysis of DNA, the two 150µl elutions were pooled and 10µg RNase I was added together with 18µl 5M NaCl. The samples were incubated in a water bath at 65°C over night. Proteinase K buffer (20µg Proteinase K (Roche), 10mM EDTA, 40mM Tris-HCl pH 6.5) was added before making the final volume up to 500µl. The samples were vortexed and transferred to a water bath at 45°C for two hours. The DNA was recovered using two phenol: chloroform and one chloroform purification. The DNA was precipitated over night at –70°C using a carrier (20µg Glycogen, 90µl 5M NaCl, 1ml Absolute Ethanol). The DNA was pelleted by centrifuging at 13000rpm for 30 minutes and washed using chilled 70% ethanol. The pellets were left to air dry before being resuspended in 30µl filtered DNA free dH_2O (Sigma).

2.13 Polymerase chain reaction (PCR) analysis of XChIP DNA

The precipitated DNA was amplified using PCR primers from Invitrogen resuspended in DNA/RNase free H_2O (Sigma) and a PCR master mix from AB Gene (Reddymix) used as defined by the manufacturer. In a typical experiment 1µl of each primer (10µM) were added to 45µl of Reddymix (prepared as a stock mix). Into each sample 1µl of template DNA and 1µCi α^{32}P dCTP (Amersham) were added. All primers were at a final concentration of 0.2µM except Mxp (0.4µM) and X141 (1.0µM) and amplified using an annealing temperature of 60°C except *Tuba6* (58°C). Primers were designed with an annealing temperature as close to 60°C as possible using the web-

based design programme http://alces.med.umn.edu/rawtm.html (Breslauer *et al.*, 1986). For the analysis of the *Xist* and *Pgk-1* genes, promoter and coding regions were co-amplified in a multiplex reaction. Each of the primer pairs were tested extensively and determined not to influence each other during amplification. Pilot experiments determined the cycle number when 75ng of input DNA was in the linear range. This guaranteed that the experimental DNA was being amplified in a linear fashion, as the input sample was invariably a more intense product. Input samples also served as controls for the potential bias of a given product during multiplex PCR. Samples were amplified using a MJ Research PTC-200 thermal cycler using cycles of: 94^{o}C for 40 seconds, 60^{o}C/58^{o}C for 60 seconds, and 72^{o}C for 60 seconds. A 20µl aliquot of the PCR product was electrophoresed using non-denaturing DNA polyacrylamide gels as described in Sambrook *et al*., (1989). All products were run on 7.5% polyacrylamide gels against 1×TBE (see above) except following PCR of *Xist* when 13.5% gels were used. Gels were dried using a BioRad Slab dryer and exposed to Phosphor screens (Molecular Dynamics) for 48 hours.

2.14 Reverse transcription PCR

To analyse the histone deacetylase expression profiles in undifferentiated and differentiated female ES cells, reverse transcription PCR was performed. Undifferentiated and cells differentiated for 8 days were harvested and washed twice in ice-cold PBS. Cells were resuspended in PBS at a density of 1×10^{6}cellsml^{-1} and aliquoted into autoclaved 1.6ml eppendorfs. Cells were pelleted and the residual PBS was removed. RNA was extracted from 1×10^{6}cells using the RNeasy MINI Kit (Qiagen) as directed by the manufacturer. Samples were homogenised by centrifuging through a QIAshredder spin column (Qiagen) and DNase I treated using an RNase-

free DNase set (Qiagen) both performed as directed by the manufacturer. Total RNA was washed using buffer RPE (Qiagen) and eluted using 30µl filtered DNA free dH_2O. The RNA extracts were electrophoresed using a 1% Agarose gel (see above) in a peroxidase treated gel tank. Reservoir tanks were peroxidase treated for 30 minutes using a 1:100 dilution of H_2O_2 (Sigma). The RNA was confirmed to be suitable for reverse transcription based on appropriately migrating tRNA and rRNA bands.

For reverse transcription 10µl of the RNA extract from each of the day points was aliquoted into two autoclaved eppendorfs. Both RNA extracts were treated identically except with the omission of the reverse transcriptase enzyme in one. This controlled for possible DNA contamination. Samples were denoted +/- RT before the addition of 3.5µl of oligo dT ($150\mu gml^{-1}$, Pharmacia). The RNA was denatured at 60^oC for five minutes and cooled on ice for three minutes. A master mix for (n+1) samples was prepared on ice using (n+1) × (0.5µl RNase inhibitor (Roche), 5µl Ultra pure dNTP (10mM, Pharmacia), 10µl first strand buffer (Gibco-BRL), 5µl DTT (Gibco-BRL)). An aliquot of 35.5µl was added to each of the samples before incubating on a water bath at 37^oC for 40 minutes. Tubes were transferred to ice and 2µl Superscript II reverse transcriptase (Gibco-BRL) was added to the samples designated +RT. Samples were incubated for a further 40 minutes at 37^oC. The cDNA samples were stored at -20^oC until PCR.

PCR of cDNA was performed as described above. In a given reaction 2µl of cDNA template was amplified using the PCR Reddymix (AB Gene). Aliquots of 5µl were taken from each of the samples at cycles 28, 31, 34, 37, 40 and 43. Samples were

electrophoresed using 1.5% Agarose gels and visualised and captured as described above.

2.15 PCR primers

The primer pairs used in this study are listed in Table 2.

Table 2. PCR Primer pairs, accession numbers and product sizes

Gene *Primer name*	Primer sequence (5' to 3')	Position	Accession N°	Product size
G6pdx *G6pdx*	F ACTCGCCCCATTTTTCAAGGC R AGCTGCTAGTTTGGCTTCGG	-1215 to -1065	X53617	150bp
Pgk-1 *Pgk-1*	F TAGTGGCTGAGATGTGGCACAG R GCTCACTTCCTTTCTCAGGCAG	+1341 to +1507	NM_008828	166bp
Rps4x *Rps4x*	F AGGGTCGCTTTGCTGGTTCA R GCTCACTTCCTTTCTCAGGCAG	+315 to +475	NM_009094	160bp
Hprt *Hprt*	F CGAGGAGTCCTGTTGATGTTGC R TGGCCTATAGGCTCATAGTGC	+684 to +856	J00423.1	172bp
Tuba6 *α-Tubulin*	F CCTGCTGGGAGCTCTACT R GGGTTCCAGGTCTACGAA	+56 to +217	NM_009448	161bp
Xist *X8u*	F CATGTTGGAAAGTTGCCGAAG R CTGGCTACAGCTGAGGAGAGC	-9053 to -8826	AJ010350	227bp
X4u	F GGACTTCAGTCCATGCCCC R CCTCTCAGCTCATACTCCGG	-4888 to -4651	AJ010350	237bp
Hx4	F GGGATTCACAGGCATAAGCTAC R AGGCATCCAGTCTCTCCAGG	-2677 to -2431	AJ010350	248bp
Mxp	F GTCACTGAGCTTACGTACCTCC R AGAGAAACCACGGAAGAACC	-173 to +47	AJ010350/ L04961	220bp
Hx1	F GTCCTACCTTGTGCCACTCG R CACAGTCTAATTCCATCCTGGC	+1573 to +1778	L04961	205bp
X141 *X141*	F CATACTGACACTTGACGTCA R CACTACCTCTTTTGGTGGT	Microsatellite DNA rich in L1	X58239	178bp
Pgk-1 *Pgk100*	F TAGGTGGTGGAGACACTGCC R GGAGCACAGGAACCAAAGG	+1199 to +1299	NM_008828	100bp
Pgp	F GGGAGCTGAGAAAGCAGAGG R GGTGGATGTGGAATGTGTGC	-597 to -408	M18735	189bp
Rpo1-2 *Rpo1-2*	F CATCCTGGCCAAATCTAAGG R GCAACACTGTGACAATCATCC	+384 to +760	NM_009089	376bp
Hdac5 *mHdac5*	F CTCCAGGAATTCCTGTTGTCC R GGCTACCTTCTGTTTAAGCCTC	+616 to +879	NM_010414	263bp
Hdac6 *mHdac6*	F GCCAGTTGGTACTGGATTGG R CCCCTTCATTCATGTACTGG	+713 to +514	NM_010413	241bp
Hdac7 *mHdac7*	F GCGTAAAACAGTGTCTGAACCC R GGCCTAAAGTTGAATGGGTCC	+519 to +784	AF207749	265bp
Sirt1 *mSirt1*	F GGGTTTCTGTCTCCTCTGGG R GGCCTAAAGTTGAATGGGTCC	+811 to +1097	NM_019812	286bp
Sirt2 *mSirt2*	F GCAGAACATGAGCACGCTGG R GGAGAAGTCTGACAGCATGC	+583 to +841	NM_022432	258bp

3 RESULTS - CHAPTER THREE

3.1 HISTONE ACETYLATION AND X CHROMOSOME INACTIVATION

Female embryonic stem (ES) cells, derived from the inner cell mass of a mouse blastocyst provide an excellent model system for the study of X chromosome inactivation. These cells can be maintained in culture as an undifferentiated monolayer with two active X chromosomes. When induced to differentiate they form embryoid bodies and inactivate one of their two X chromosomes at random. Thus, ES cells allow the study of the steps involved in the establishment of silent chromatin along the inactive X chromosome (Xi). Allowing cells to differentiate to a specific time point we can analyse the characteristics of Xi as they become detectable. This allows events characterising X inactivation to be ordered and provides evidence to their role, whether they are intrinsic to the initiation of X chromosome inactivation or involved in the maintenance of the silent chromatin state. In addition the process of X chromosome inactivation is in itself a more general model for the study of chromatin silencing, given that we can study the characteristics of the chromatin state at the chromosome level by immunofluorescence or on a nucleosomal scale by chromatin immunoprecipitation. Xi is characterised by its low level of histone acetylation of H2A, H3 and H4 (Jeppesen and Turner, 1993; Belyaev *et al.*, 1996) and can be identified as a pale staining chromosome by preparing metaphase spreads from female somatic cells and immunolabelling using antisera to acetylated histones. Using antiserum to acetylated H4 a pale staining chromosome, undetectable in undifferentiated ES cells was detected with increasing frequency as the cells differentiated (Keohane *et al.*, 1996; O'Neill *et al.*, 1999). More specifically, the earliest time at which the inactive X chromosome was shown to be hypoacetylated and differentially staining was after four days of differentiation. These findings were supported by O'Neill *et al.,* (1999) who

demonstrated that the coding regions of four X-linked genes were deacetylated for histone H4 following female ES cell differentiation using chromatin immunoprecipitation (NChIP). In contrast Gilbert and Sharp, (1999) have recently reported a promoter-specific hypoacetylation on the inactive X chromosome following ChIP experiments performed on somatic cell hybrid cell lines containing either the human active or inactive X chromosome. In light of this discrepancy I have investigated the epigenetics of a human hamster hybrid line by immunolabelling metaphase chromosomes and have analysed the level of acetylation for all of the core histones in both promoter and coding regions of Xi by performing ChIP on embryonic stem cells.

O'Neill *et al.,* (1999) additionally showed that a pale staining chromosome was undetectable when ES cells were differentiated in low concentrations of the histone deacetylase inhibitor Trichostatin A (TSA), even after 12 days of differentiation. However, supplementing culture medium with TSA following the establishment of a pale staining Xi did not result in a reversal to an acetylated Xi. Given that the histone acetylation status of chromatin is the sum of the effects of the histone acetyltransferases and the deacetylases, we can propose that there are TSA sensitive and resistant steps during ES cell differentiation. Indeed we can speculate that there is a differentiation step following which Xi becomes TSA resistant.

Therefore the specific timing of core histone deacetylation and the stage of differentiation when Xi becomes unresponsive to TSA was of significant interest.

3.1.1 All four core histones are deacetylated concurrently between 3 and 5 days of ES cell differentiation

Metaphase spreads from undifferentiated embryonic stem cells and cells differentiated for 3, 4, 5 and 7 days were prepared and immunostained using antibodies to acetylated H2A (H2A AcK5), H2B (H2B AcK12/15), H3 (H3 AcK14) and H4 (H4 AcK8). Metaphases were counted for the presence of a pale staining chromosome. Only metaphases of sufficient quality were scored i.e. that had a full karyotype and possessed good morphology. All four antisera revealed a pale staining chromosome in a proportion of the cells. Immunolabelled metaphase spreads from a typical experiment are shown in figure 6 with their DAPI counterstain (pseudo-coloured as white) on the right of each image. Several characteristics were shared between all four of the core histones. Firstly in undifferentiated cells (figure 6: a, e, i and m) there was ubiquitous histone acetylation across all of the chromosomes including the centromeric heterochromatin as indicated by the arrowheads. Metaphase spreads with a pale staining chromosome were observed very infrequently (1-2%; figure 7a). The frequency of spreads with a pale staining chromosome and unlabelled centromeric heterochromatin increased as the cells differentiated, as shown with arrows in figure 6; c, g, k and o. Unlabelled centromeric heterochromatin is particularly prominent in figure 6c (arrowhead).

As shown in figure 7a, between days three and five of differentiation the frequency of metaphase spreads displaying a pale staining chromosome increased at least four fold for all of the acetylated histone antibodies. The frequency continued to increase, at a slower rate up to day 7 of differentiation, the last time point analysed. The increase in

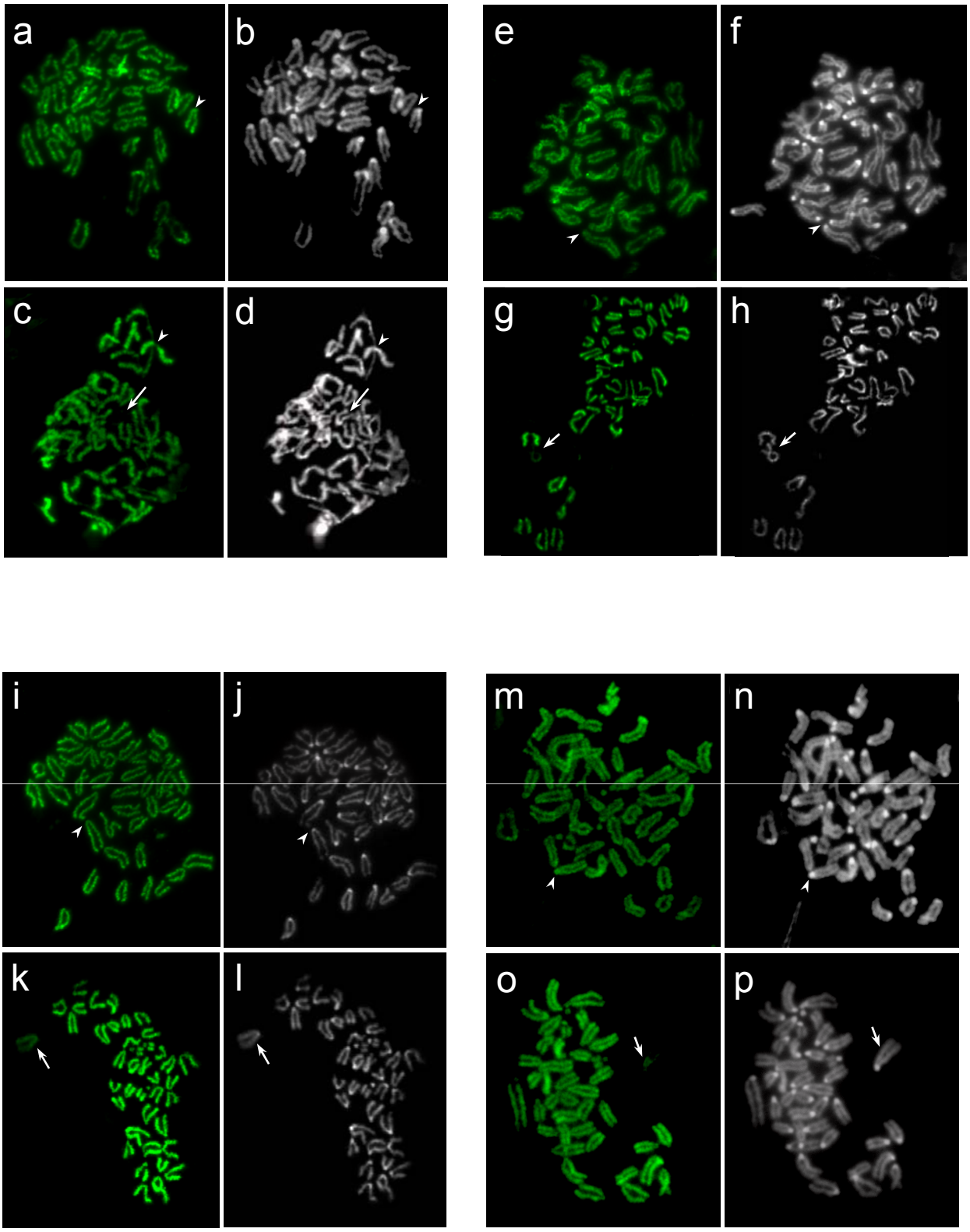

Figure 6. Metaphase spreads prepared from undifferentiated (a, e, i, m) and differentiated (c, g, k, o) female ES cells were immunolabelled using antisera to αH2A AcK5 (a, c), αH2B AcK12/15 (e, g), αH3 AcK14 (i, k), and αH4 AcK8 (m, o). The DAPI counterstain of each immunolabelling is shown pseudocoloured as white on the right of each image (b, d, f, h, j, l, n, p). Centric heterochromatin remained acetylated for all of the core histones in undifferentiated cells (arrowheads) but was underacetylated in differentiated cells (arrowhead in c). A pale staining chromosome was rarely observed in spreads derived from undifferentiated cells whereas cells differentiated for 7 days provided metaphase spreads with a pale staining chromosome at high frequencies (arrows in c, g, k, o).

the frequency of a pale staining chromosome as differentiation progresses is remarkably similar for each of the four core histones.

The pale chromosome previously identified as Xi (Jeppesen and Turner, 1993) was clearly distinguishable from the rest of the chromosomes and was usually uniformly pale. Xi was pale throughout its entire length except for detectable histone acetylation proximal to the centromere in the pseudo-autosomal region (PAR) as demonstrated in figure 6g. There were notable exceptions when Xi was pale over a fraction of its length and labelled distal to the centromere as shown by the arrows in figures 7b and d. These spreads would support the hypothesis that there is a spreading of hypoacetylation along Xi from the centromere to the telomere. However, given that these were observed at low frequency (<1%), it is likely that the deacetylation of Xi takes place relatively quickly, i.e. during a single cell cycle. An alternative explanation for these metaphase spreads is that they are rare X;autosome translocations. This is supported by the fact that the pale chromosomes in figures 7b and d are both unusually large.

3.1.2 TSA prevents deacetylation of Xi only if present during the first three days of differentiation

It has been shown previously that embryonic stem cells can be cultured and differentiated in low concentrations of TSA that induce histone hyperacetylation but do not prevent cell growth (Keohane *et al.*, 1998; O'Neill *et al.*, 1999). The differentiation of female ES cells in medium supplemented with TSA ($5ngml^{-1}$) was shown to prevent the appearance of a pale staining chromosome. However, the

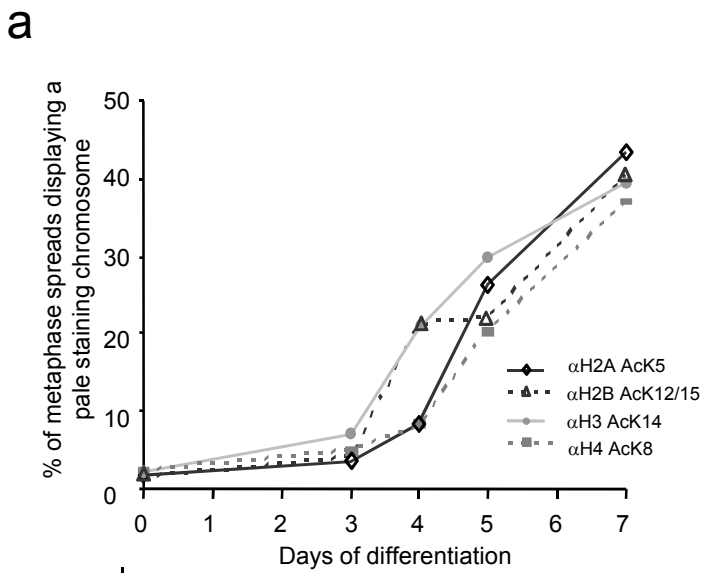

	n							
αH2A AcK5	113	ND	ND	28	36	68	ND	46
αH2B AcK12/15	83	ND	ND	25	19	32	ND	47
αH3 AcK14	45	ND	ND	102	29	20	ND	28
αH4 AcK8	55	ND	ND	40	50	41	ND	60

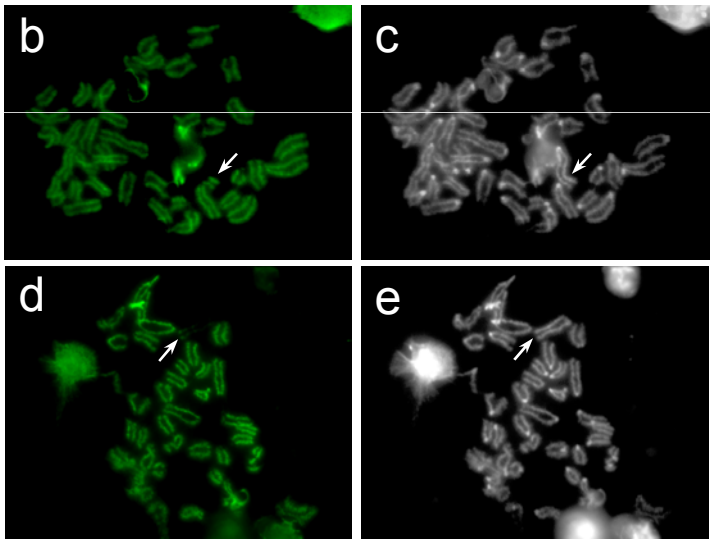

Figure 7. The timing of core histone deacetylation in female ES cells was analysed by differentiating cells for the appropriate number of days and immunostaining metaphase spreads using antisera to acetylated H2A (αH2A AcK5), H2B (αH2B AcK12/15), H3 (αH3 AcK14) and H4 (αH4 AcK8). The frequency of metaphase spreads displaying a pale staining chromosome was calculated (a).

The deacetylation of core histones occurs during a single cell cycle. Spreads containing a pale staining chromosome labelled over a fraction of its length (b and d) were observed only at low frequency. The DAPI counterstain is shown pseudocoloured as white on the right of each image.

addition of TSA failed to interfere with the maintenance of the underacetylated state following X chromosome inactivation. To determine the stage of differentiation at which TSA exerts an effect the inhibitor was added after 0, 1, 2, and 3 days of differentiation and the frequency of pale staining chromosomes were determined at day 8 using immunostaining. For each experiment a no TSA sample was included as a control. However, control experiments were performed initially to confirm that TSA does indeed induce histone hyperacetylation in the day 8 embryoid bodies. This was particularly important in view of publications documenting the degradation of the inhibitor in culture (Yoshida *et al.*, 1990). It was also therefore important to replace the culture medium with fresh medium every day of the experiment.

Whilst the cells were clearly cycling, given that metaphase chromosomes were always successfully generated, the size of the embryoid bodies derived from cells differentiated in TSA (shown in figure 8a) were consistently smaller than those derived from control cells without the inhibitor (figure 8b).

The growth of undifferentiated ES cells for up to six hours in the presence of TSA ($100ngml^{-1}$) has been shown to lead to a dramatic increase in H4 acetylation by electrophoresis on acid/urea/Triton (AUT) gels such that the di-, tri- and tetra-acetylated isoforms become the most prominent (O'Neill *et al.*, 1999). It has also been demonstrated that that rate of acetate turnover falls after the first few days of differentiation (Keohane *et al.*, 1998) such that cells appear less responsive to a six hour pulse of the inhibitor. Therefore given that day 8 embryoid bodies were to be analysed that had been cultured in concentrations of TSA significantly less that in the aforementioned study, it was crucial that the levels of H4 acetylation were analysed.

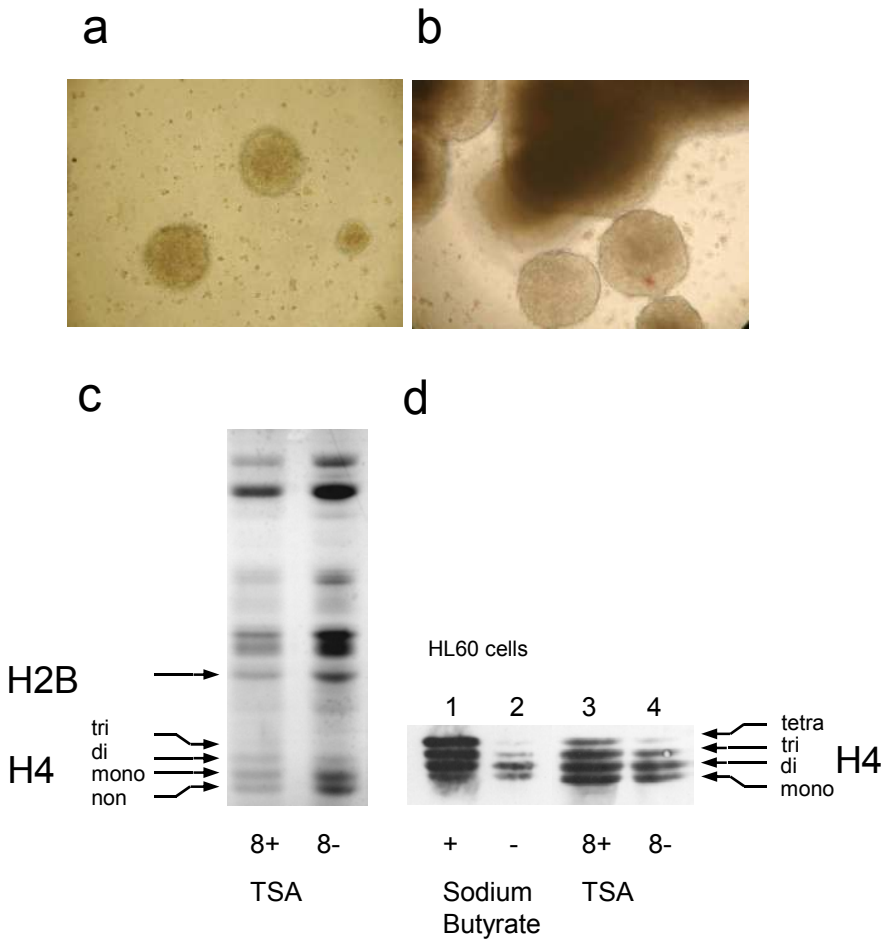

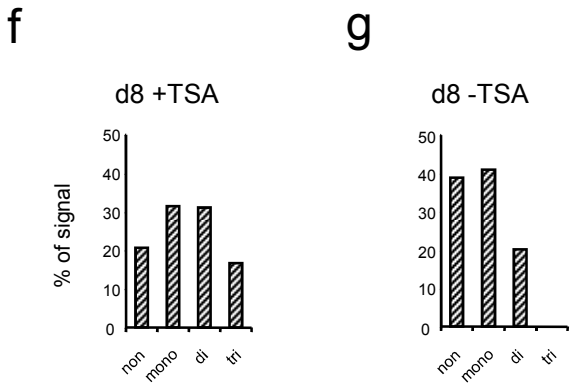

Figure 8. Female ES cells were differentiated for 8 days in medium supplemented with or without the histone deacetylase inhibitor Trichostatin A (TSA). Histones were acid extracted and AUT electrophoresis was performed together with western blotting. Photographs of cells cultured in TSA or TSA free medium are shown in (a) and (b) respectively.

Following AUT electrophoresis the gel was stained with Coomassie Blue (c) and the relative levels of non-, mono-, di- and tri- acetylated H4 were quantified using laser densitometry. These levels are illustrated in f and g, collectively expressed as 100%. Western blotting was performed using an antibody that has the capacity to recognise all 4 levels of H4 acetylation, shown using HL60 histones induced to hyperacetylate (d lane 1). A western blot of histones extracted from ES cells cultured for 8 days with or without TSA is shown in d, lanes 3 and 4 respectively.

Histones were acid extracted from female ES cells cultured for 8 days with or without TSA and resolved using AUT gel electrophoresis. The resulting Coomassie Blue stained gel is shown in figure 8c. Using laser densitometry the relative levels of non-, mono-, di- and tri-acetylated H4 were quantified (tetra-acetylated H4 was undetectable using Coomassie Blue stain). As shown in figure 8f and g when these levels are collectively expressed as 100% there is more di- and tri-acetylated H4 in the sample extracted from cells grown in TSA than in the untreated cells.

The level of H4 acetylation was investigated further using the more sensitive technique of western blotting. An antibody recognising acetylated H4 but exhibiting no lysine specificity was used (R243). It was initially characterised using histones extracted from cells cultured under conditions known to induce histone hyperacetylation (10mM Sodium Butyrate for six hours). As shown in figure 8d, lane 1, the antibody displays the potential to recognise all four levels of H4 acetylation in the Butyrate treated (+) cells. Control cells cultured without Butyrate (-) are included in lane 2. This antibody was used to immunolabel histones extracted from ES cells cultured with or without TSA for 8 days. The histones derived from the cells grown in TSA showed higher levels of tri- and tetra-acetylated histone H4 than the untreated cells. So TSA was confirmed as inducing increased levels of H4 acetylation.

Therefore, in order to determine the differentiation time point at which an underacetylated Xi becomes unresponsive to TSA, the inhibitor was added after 0, 1, 2, and 3 days of differentiation and the frequency of pale staining chromosomes determined at day 8 using immunostaining. The immunolabelling was performed using four different antisera recognising H4 acetylated at lysines 5, 8, 12 or 16. All

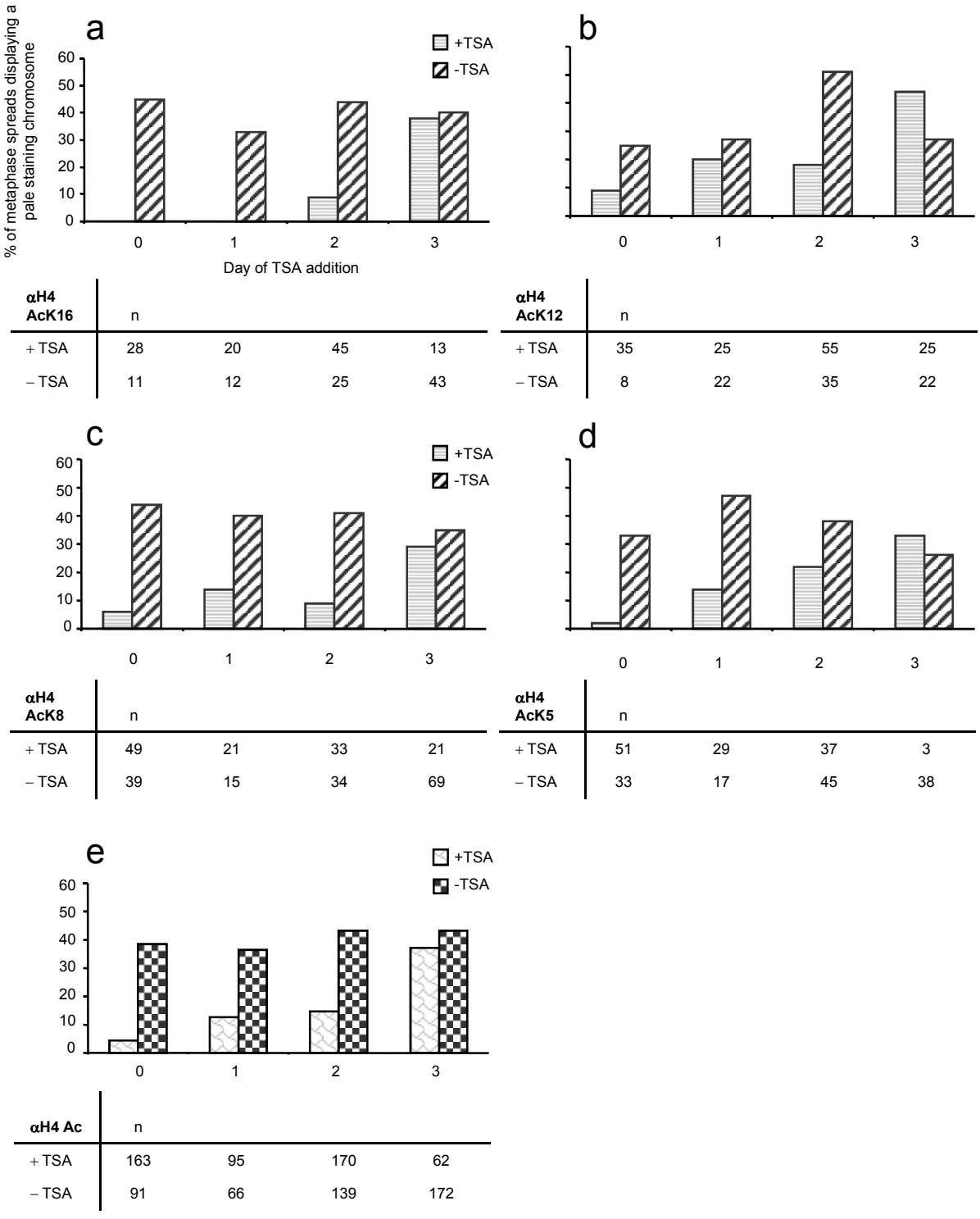

Figure 9. Immunofluorescence was performed on female ES cells differentiated for 8 days in the presence or absence of low concentrations of TSA. The TSA was supplemented into the culture medium from the day indicated. Immunolabelling was performed using antisera to H4 AcK16 (a), H4 AcK12 (b), H4 AcK8 (c), H4 AcK5 (d), and the frequency of metaphase spreads with a pale staining chromosome was monitored. All four antisera gave similar results and are shown collectively in e. Total numbers of cells counted (n) are indicated beneath each histogram.

four antisera gave similar results. These are shown individually in figures 9a, b, c and d and collectively in figure 9e. TSA present from day 0 caused a ten fold reduction overall in the percentage of cells with a pale staining chromosome at day 8. TSA present from day 1 or 2 caused a lesser effect; although still a significant reduction (about three fold overall). In contrast TSA added at day 3 had little or no effect on the frequency of cells with a pale staining chromosome at day 8. Importantly in section 3.1.1 the global deacetylation of Xi was shown to occur between days 3 and 5. Therefore the deacetylation of Xi can proceed despite the presence of TSA. However, this is conditional on the addition of TSA being preceded by a time window of two days when the cells are free of the inhibitor.

Whilst all of the H4 isoforms behaved similarly the data suggests that H4 AcK16 was the most sensitive to the TSA treatment during the first two days of differentiation as there was a complete absence of a pale staining chromosome at day 8.

3.1.3 Deacetylation of all four core histones occurs on both coding and promoter regions of X-linked genes in female cells

The data presented in section 3.1.1 demonstrates that all four core histones are deacetylated across Xi in a large proportion of female metaphase cells following 7 days of differentiation. To analyse interphase cells and to quantify differences in histone acetylation that occur at the single gene level during ES cell differentiation the technique of native chromatin immunoprecipitation (NChIP) was employed.

Chromatin fragments were prepared from unfixed nuclei using a mild micrococcal nuclease digestion. The chromatin was immunoprecipitated using affinity purified

antiserum against acetylated H3 (H3 AcK14) The precipitated DNA was analysed using DNA electrophoresis and ^{3}H-thymidine content to assay the degree of precipitation relative to the no-antibody control. The precipitated protein was recovered and analysed by western blotting using the same antibody to examine the specificity during the immunoprecipitation. The raw data from a typical experiment performed on undifferentiated ES cells and cells differentiated for 7 days is shown in figure 10. Whilst the antibody clearly precipitated DNA (figure 10a; BOUND fraction) there was undetectable amounts recovered in the no-antibody control (NAC). This demonstrates that the recovery of chromatin was dependent on the presence of the antibody. In figure 10b the protein recovered from the BOUND and UNBOUND fractions was initially equalised using laser densitometry of a Coomassie Blue stained SDS polyacrylamide gel (data not shown) and western blotted using the same antibody. Whilst H3 AcK14 is present in both the BOUND and UNBOUND fractions the chromatin in the BOUND fraction was significantly enriched for this histone modification.

Equal amounts of DNA from the BOUND and UNBOUND fractions, based on ^{3}H-thymidine content were slot blotted onto nylon membranes. The DNA was blotted on duplicate slots using three serial dilutions. To assay a DNA region for the level of H3 AcK14, ^{32}P labelled DNA probes were hybridised to the membrane and the relative intensity of the BOUND (B) divided by UNBOUND (UB) fraction was calculated. A DNA region with high levels of histone acetylation will be enriched in the BOUND fraction and depleted in the UNBOUND fraction following immunoprecipitation, giving a ratio greater than one. Figures 10c (undifferentiated) and d (differentiated)

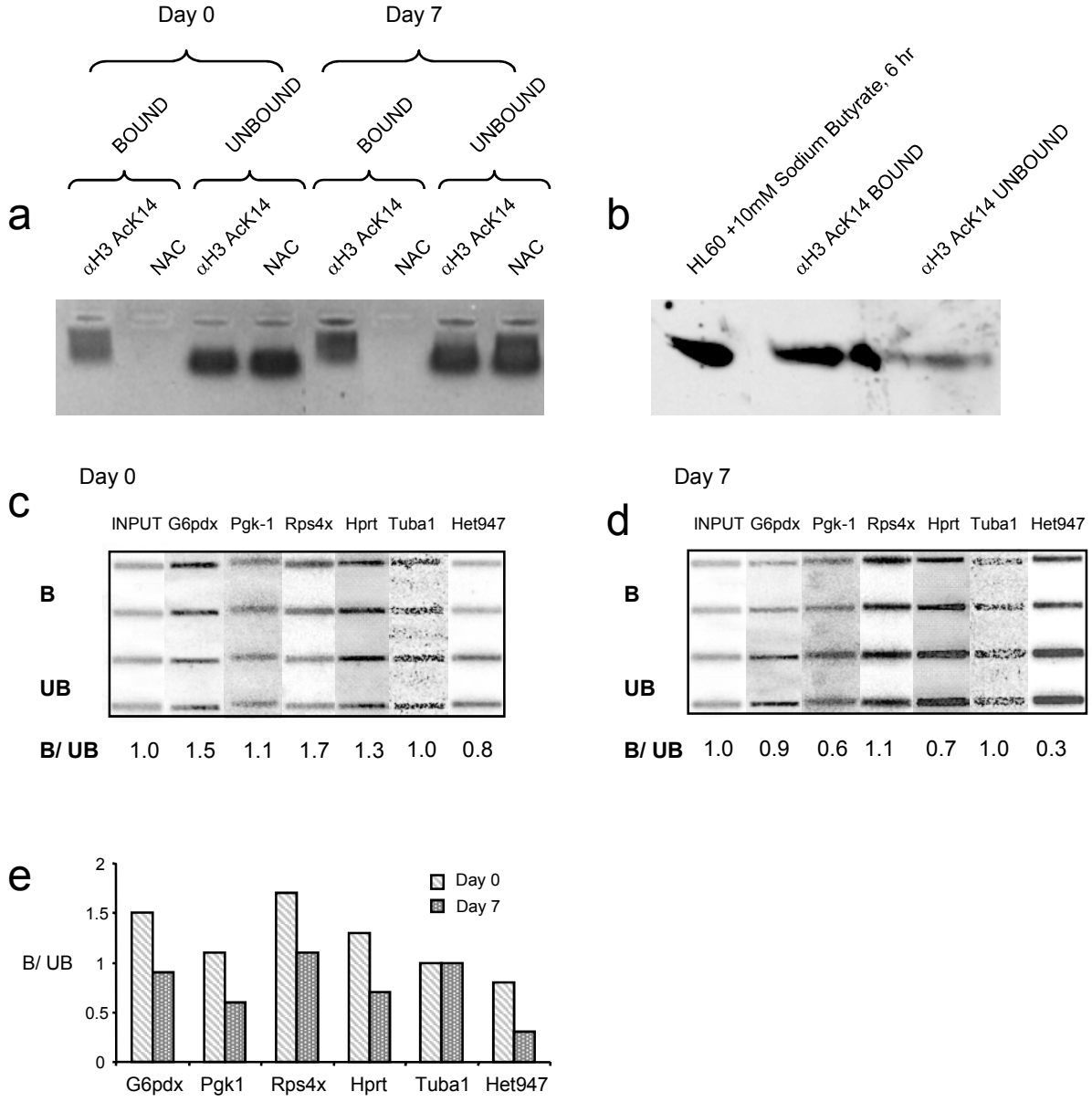

Figure 10. Native chromatin immunoprecipitation (NChIP) was performed on undifferentiated ES cells and cells differentiated for 7 days using antisera to H3 AcK14. Chromatin fragments were prepared using a mild micrococcal nuclease digestion and immunoprecipitated an affinity purified antibody. The DNA and protein were analysed. 5% of the DNA from the UNBOUND fraction (depleted for H3 AcK14) and 10% of the BOUND fraction (enriched for H3 AcK14) were analysed using agarose gel electrophoresis. A negative image of an ethidium bromide stained gel is shown in a. The protein was analysed using SDS-PAGE followed by western blotting (b). Equal amounts of protein from the BOUND and UNBOUND fractions, based on a Coomassie Blue stained pilot gel (data not shown) were electrophoresed, transferred and immunolabelled using αH3 AcK14. A positive control of HL60 histones was included that had been induced to hyperacetylate following a six hour incubation in Sodium Butyrate.

Equal amounts of DNA from the BOUND and UNBOUND fractions was applied to nylon membranes and hybridised with ^{32}P labelled DNA probes. Figure c and d show the result of hybridisation using the following probes; INPUT DNA, the promoter region of the X-linked gene *G6pdx*, the coding regions of X-linked *Pgk-1*, *Rps4x* and *Hprt*, the coding region of the housekeeping gene *Tuba1* and the centromeric α-satellite repeat region (Het947). The levels of H3 acetylation are expressed as a BOUND to UNBOUND ratio (e).

show the results of hybridising the precipitated DNA with the following probes; INPUT DNA, the promoter region of the X-linked gene *G6pdx*, the coding regions of X-linked *Pgk-1*, *Rps4x* and *Hprt*, the coding region of the housekeeping gene *Tuba1* and the centromeric □satellite repeat region (Het947).

The level of H3 acetylation of all X-linked genes was always lower in differentiated (day 7) compared to undifferentiated cells (figure 10e). This is consistent with the immunofluorescence data in section 3.1.1, and previous reports that have analysed H4 acetylation along the X chromosome using NChIP (Keohane *et al.*, 1996; O'Neill *et al.*, 1999). In contrast there were no observed changes in the level of H3 acetylation of the autosomal gene *Tuba1*. However, the level of H3 acetylation at the centric heterochromatin fell dramatically following 7 days of differentiation, consistent with the observations made in section 3.1.1. These results were of sufficient interest to warrant further investigation by Dr. L. P. O'Neill.

NChIP experiments performed by Dr. L. P. O'Neill using antisera against acetylated H4 (H4 AcK16), H3 (H3 AcK14), H2A (H2A AcK5) and H2B (H2B AcK12/15) showed that the four X-linked genes analysed above were subject to a drop in core histone acetylation. There was no significant difference between individual core histones or the extent of deacetylation from one X-linked gene to another. Furthermore there were no observed changes in the histone acetylation of the autosomal gene *Tuba1*, and a dramatic fall in the level of histone acetylation of centric heterochromatin following 7 days of differentiation.

3.2 HISTONE METHYLATION AND X CHROMOSOME INACTIVATION

According to the histone code hypothesis the activity of a given gene is dependent on the pattern of different histone N-terminal tail modifications in the chromatin surrounding the gene. The methylation of selective lysine residues on H3, H4 and H2B is one such modification. The □-amino group of these lysine residues have the potential to be mono-, di-, or tri-methylated (Me). All three methylation levels occur *in vivo* but their functional significance remains to be determined.

Using the facultative heterochromatin of the inactive X chromosome as an example, I wanted to establish the significance of methylation at particular lysine residues and explore the possibility that different levels of methylation may provide a new complexity to the histone code.

3.2.1 Derivation of antibodies that can distinguish between di- and tri-methylated H3 isoforms

New antisera were raised as described previously (White *et al.,* 1999) using the synthetic peptides shown, incorporating di-methyl lysine at positions 4 or 9.

H3Me_2K4: A.R.T.Me_2K.Q.T.A.R.K.S.C

H3Me_2K9: Q.T.A.R.Me_2K.S.T.G.G.K.C

These sites were chosen based on published data reporting their presence *in vivo* (Strahl *et al.*, 1999). In addition an antibody was obtained from Drs. T. Kouzarides and A. J. Bannister, University of Cambridge, Cambridge that was raised using a mixture of H3 peptides containing tri-methyl lysine incorporated at positions 4 and/or 9. All of the antisera were tested by Dr. L. P. O'Neill for their epitope specificity using inhibition ELISA (Enzyme Linked Immunosorbant Assay). Using immobilised

histones as the antibody substrate the antisera were tested for the inhibition of binding using the appropriate di-methylated peptides and their tri-methylated equivalents. The results are summarised in figure 11. The antiserum raised against H3Me$_2$K4 (figure 11a) was inhibited with increasing concentrations of the immunising peptide but not by the equivalent peptide tri-methylated at lysine 4 or an unrelated non-histone peptide. The antiserum is therefore specific for H3 di-methylated at lysine 4. As shown in figure 11b there was a similar specificity by the antiserum to H3Me$_2$K9 for its immunising peptide but not for its tri-methylated isoform or an irrelevant peptide. Figure 11c demonstrates that the antiserum raised using a mixture of tri-methylated lysine peptides at position 4 and/or 9 was shown to recognise H3 tri-methylated at lysines 4 and 9 but not a peptide that was di-methylated at lysines 4 or 9. Given these specificities the antisera were denoted □H3Me$_2$K4, □H3Me$_2$K9 and □H3Me$_3$K4/9.

3.2.2 The facultative heterochromatin of Xi is differentially methylated at lysines 4 and 9

To determine the significance of H3 methylation immunocytochemistry was performed on a human female somatic cell line. Metaphase chromosome spreads were prepared from lymphoblastoid cell line GM12616 and immunostained using □H4 AcK8, □H3 AcK14, □H2B AcK12/15, □H3Me$_2$K4, □H3Me$_2$K9, and □H3Me$_3$K4/9. Representative spreads are shown in figures 11 and 12. As expected and previously reported (Jeppesen and Turner, 1993; Belyaev *et al*., 1996; see section 3.1.1), the inactive X chromosome was clearly distinguishable from the rest of the chromosomes on account of its low levels of acetylation on H4 (figure 11d), H3 (figure 11f) and H2B (figure 11h). Xi is indicated using arrows.

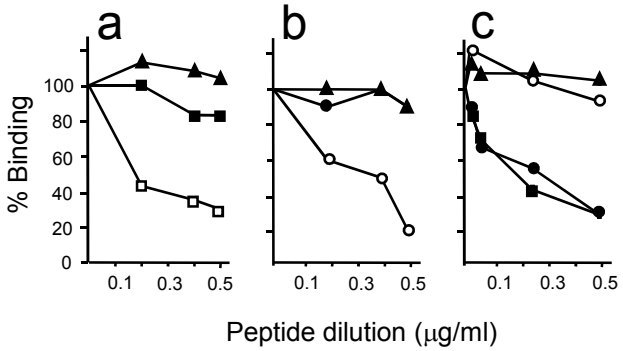

Figure 11. ELISA shows that antibodies can distinguish between di-methylated and tri-methylated H3 isoforms (a-c) and immunofluorescence microscopy reveals differences in the distribution of these isoforms across metaphase chromosomes of a female lymphoblastoid cell line (d-l). ELISA analysis was performed using histones immobilised on microtitre plates. Antisera to $H3Me_2K4$ (a) was tested using increasing concentrations of the immunising peptide (□), the equivalent peptide tri-methylated at lysine 4 (■) and an unrelated non-histone peptide (▲). Antisera against $H3Me_2K9$ (b) was tested using the immunising peptide (○), its tri-methylated isoform (●) or an irrelevant peptide (▲). Antisera to $H3Me_3K4/9$ (c) was tested using the tri-methylated peptides mentioned above (■ and ●) and a peptide that was di-methylated at lysines 4 or 9 (○)

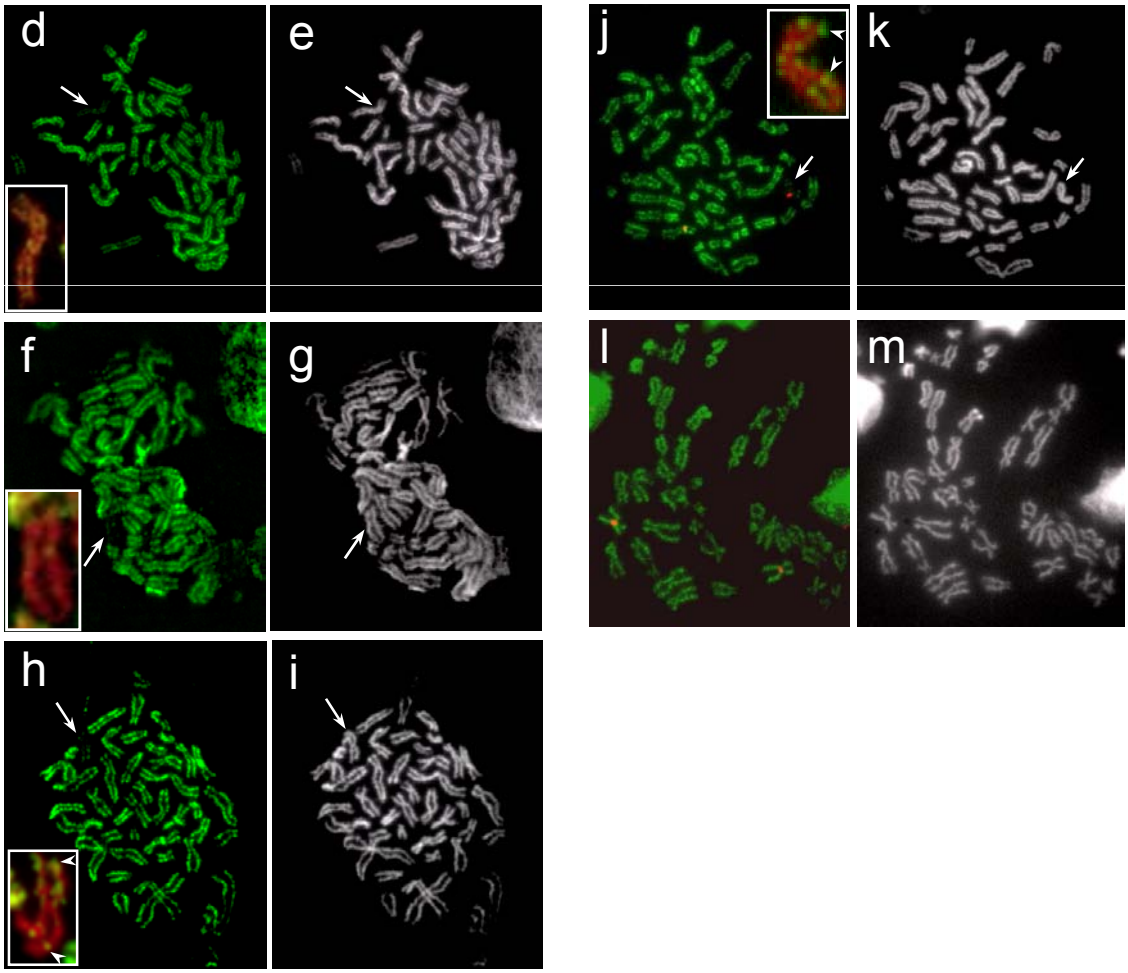

Metaphase spreads from female lymphoblastoid cell line GM12616 were immunostained using antisera to H4 AcK8 (d), H3 AcK14 (f), H2B AcK12/15 (h), $H3Me_2K4$ (j), and $H3Me_2K9$ (l). In j and l the X chromosomes were identified using centromeric FISH (red). The DAPI counterstain is shown pseudocoloured as white on the right of each image. An enlargement of the pale staining chromosome is shown with DAPI pseudocoloured as red for contrast against the antibody (green).

Immunostaining using antiserum to $H3Me_2K4$ resulted in the appearance of chromosome that was pale staining (figure 11j). This was shown to be one of the human X chromosomes by performing fluorescence *in situ* hybridisation (FISH) using an X centromeric DNA probe. They are shown as red punctate signals.

In order to demonstrate that the pale staining chromosome was the inactive X chromosome, immuno-FISH was performed on a somatic cell hybrid line containing the human Xi as the only human chromosome (see below). This was shown to be differentially staining and confirms that the chromosome was indeed Xi.

Immunolabelling with an antibody to $H3Me_2K9$ (figure 11l) resulted in ubiquitous staining that was evenly distributed across all of the chromosomes in the majority of metaphase spreads. The X chromosomes were detected using X centromeric FISH as before. The inactive X chromosome was found to retain di-methylation at lysine 9 of H3 and is entirely consistent with publications subsequent to this work (Heard *et al.*, 2001; Boggs *et al.*, 2002; Peters *et al.*, 2002). Similar staining was obtained using a commercial antibody from Upstate. However, in a small fraction (~10%) of metaphase spreads this antibody detected a brightly stained chromosome, distinguishable on account of higher levels of $H3Me_2K9$ and shown to be an X chromosome using immuno-FISH (see section 3.2.5). However, in general (~90% of metaphase spreads) and contrary to the aforementioned reports Xi was not specifically enriched for lysine 9 di-methylation using either of the antibodies, nor was the immunolabelling largely confined to the centromeric heterochromatin (see section 3.2.5) as published by Mermoud *et al.,* (2002).

In contrast a pale staining chromosome was observed following immunostaining using antiserum to H3Me$_3$K4/9 (figure 12a). The pale staining chromosome was once again demonstrated to be Xi by performing immuno-FISH on a somatic cell hybrid line containing Xi as the only human chromosome (see section 3.2.4). The finding of a depletion of tri-methylated lysine 9 on Xi is in direct contrast to Cowell *et al.,* (2002) who reported a specific enrichment on the inactive X chromosome. However, the results here suggest that Xi is depleted in H3Me$_2$K4, H3Me$_3$K4 and H3Me$_3$K9 but specifically retains H3Me$_2$K9. Given the cross-reaction of the antiserum used to investigate the significance of the tri-methyl lysine isoforms I wanted to confirm my data using independent antisera specific for both the individual lysine and the tri-methyl level of methylation.

Antiserum to H3 tri-methylated at lysine 4 was raised in Birmingham and an antibody against H3 tri-methylated at lysine 9 was raised in Cambridge by Drs. T. Kouzarides and A. J. Bannister. The Birmingham antiserum was shown by ELISA (L. P. O'Neill; data not shown) to be inhibited by its immunising peptide but not by its di-methylated equivalent or peptides methylated at lysine 9 of H3. The Cambridge antiserum has been shown by western blot experiments to be inhibited by its immunising peptide in addition to a peptide tri-methylated at lysine 27 (A. J. Bannister; data not shown). Lysine 27 of H3 is subject to methylation *in vivo* (Cao *et al.*, 2002) and is flanked by a similar sequence to that of lysine 9; -A-R-K-S (see Figure 1). The antiserum will thus be referred to as H3Me$_3$K9/27. It should be noted that the antiserum against H3Me$_3$K4/9 displayed no apparent cross-reaction against methylation at lysine 27 (A. J. Bannister; data not shown).

Immunostaining was performed as before using the Birmingham antiserum against $H3Me_3K4$. A pale chromosome was detectable (figure 12c) and confirms the previous observations using the antiserum against $H3Me_3K4/9$. Immuno-FISH using antiserum from Cambridge against $H3Me_3K9/27$ revealed an altogether different staining pattern (figure 12e). Perhaps the most prominent observation was the particularly brightly stained centric heterochromatin (arrowhead). Using a DNA-FISH probe specific for the centromere of the X chromosomes it can be seen that both the active and inactive X chromosomes (arrows) retain similar levels of tri-methylation at lysines 9 and 27 as one another and the rest of the autosomes. This labelling was highly analogous to the immunostaining observed using the Upstate antiserum against $H3Me_2K9$. Furthermore in a fraction (~10%) of metaphase spreads a chromosome was identified as particularly brightly stained on account of its degree of tri-methylation. This chromosome was shown to be one of the two X chromosomes using centromeric FISH as before. This result suggests that Xi retains H3 lysine 9 and/or 27 tri-methylation at a level at or above those found elsewhere in the genome.

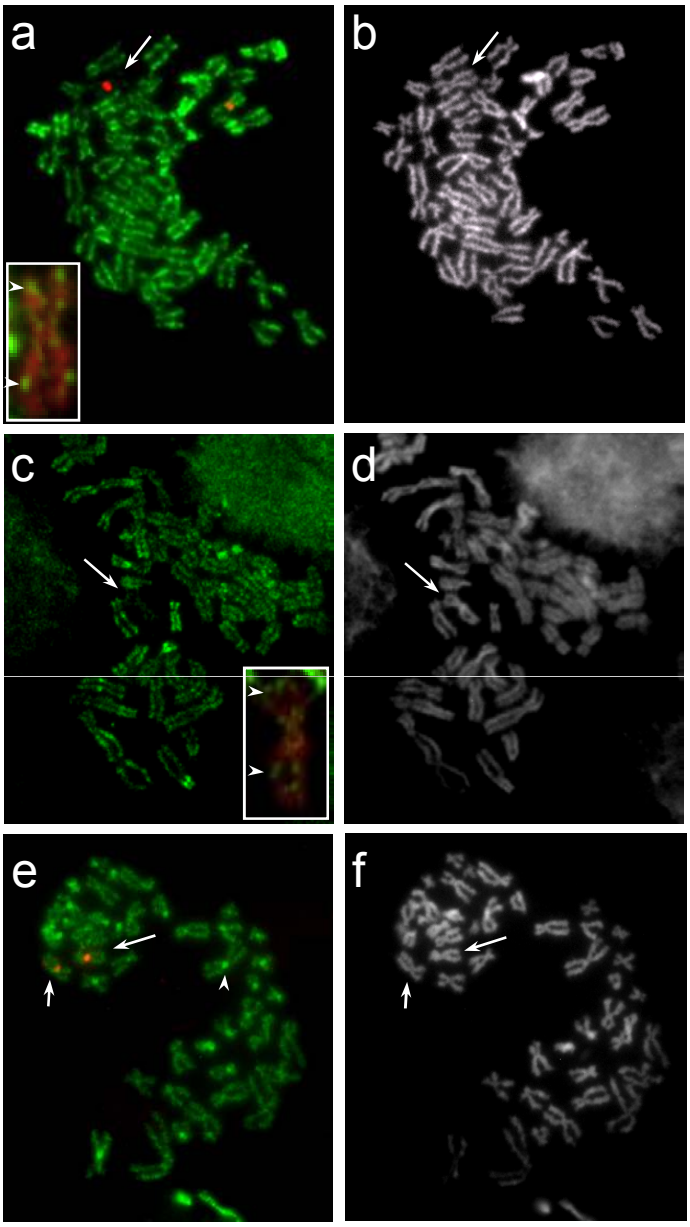

Figure 12. Metaphase spreads from female lymphoblastoid cell line GM12616 were immunostained using antisera to $H3Me_3K4/9$ (a), $H3Me_3K4$ (c) and $H3Me_3K9/27$ (e). In a and e the X chromosomes were identified by centromeric FISH (red). The DAPI counterstain is shown pseudocoloured as white on the right of each image. An enlargement of the pale staining chromosome in a and c is shown with DAPI pseudocoloured as red for contrast against the antibody (green).

3.2.3 Histone methylation hot spots on the human inactive X chromosome

Whilst Xi is clearly distinguishable from the rest of the chromosomes on account of the absence of staining using antisera against $H3Me_2K4$, $H3Me_3K4/9$ and $H3Me_3K4$ there are localised regions on Xi that are labelled as brightly as the rest of the chromosomes. An enlarged Xi is shown in the corner of each of the images with the DAPI counterstain pseudocoloured as red to give contrast against any label (green) that may be retained. Xi was hypoacetylated for H3 and H4 along its entire length in the majority of spreads, as shown in figures 11d and f. Xi was occasionally labelled at the end of Xp as previously reported (Jeppesen and Turner, 1993; Belyaev *et al.*, 1996), corresponding to the pseudoautosomal region (PAR), known to escape X chromosome inactivation. In the majority of spreads Xi was found to be highly acetylated for H2B (figure 11h) at the PAR and additionally on the long arm of the X at approximately Xq22-25. Identical staining to H2B was observed following immunolabelling using antisera to $H3Me_2K4$, $H3Me_3K4/9$ and $H3Me_3K4$ (figures 11j, 12a and 12c respectively). This localised labelling was reproducible in the cell line GM12616 and in an additional five X;autosome translocated lymphoblastoid cell lines (see section 4.1). Interestingly in translocated cell line SP, Xi displayed H3 and H4 acetylation at the region estimated here as Xq22-25. This was never seen in the wild type cell line GM12616 or in the remaining four translocated cell lines but demonstrates the potential for H3 and H4 acetylation at this region as reported previously (Jeppesen and Turner, 1993). Therefore we can conclude that there are two specific regions of the inactive X chromosome in wild type cells that are highly enriched for acetylated H2B, H3 di- and tri-methylated at lysine 4 and H3 tri-methylated at lysine 9. These areas may relate to the hot spots identified by Boggs *et al.,* (2002) following the immunolabelling of Xi with antiserum to $H3Me_2K4$. One of

them has recently been estimated to correspond to the DXZ4 locus at Xq24 (Chadwick and Willard, 2002).

3.2.4 The epigenetics properties of Xi persists in somatic cell hybrid lines

Somatic cell hybrid lines containing a human X chromosome in a foreign rodent background have been used extensively in the area of X chromosome inactivation. They have been employed to study genes that escape X chromosome inactivation (Mohandas *et al.*, 1980; Miller and Willard, 1998; Carrel and Willard, 1999), the effect on the *XIST* gene resulting from transferring the human Xi into a hamster background (Hansen *et al.,* 1998), the requirement of *XIST* for sustained gene silencing (Brown and Willard, 1994) and the epigenetics of Xi and Xa using cross-linking chromatin immunoprecipitation (Gilbert and Sharp, 1999; Boggs *et al.*, 2002). Despite the foreign background the cell lines have been reliable, although they have occasionally exhibited variability in expression that might be more attributable to the cell line than the gene in question (Carrel and Willard, 1999). Using a male hamster hybrid line containing a human inactive X chromosome (X8-6TS1) Hansen *et al.,* (1998) demonstrated that the transcript from the human *XIST* gene fails to associate correctly with Xi. This raised the possibility that the human *XIST* gene functions incorrectly in a rodent background. Given the integral role *XIST* plays during X chromosome inactivation I wanted to investigate whether the new epigenetic modifications characterised in section 3.2.2 were retained in this cell line.

Metaphase chromosomes were prepared from the hybrid line X8-6TS1 and immunolabelled using antisera against H4 AcK8 (figure 13a), H3Me$_2$K4 (figure 13c), H3Me$_2$K9 (figure 13e), H3Me$_3$K4/9 (figure 13g), and H4Me$_2$K20 (figure 13i). FISH

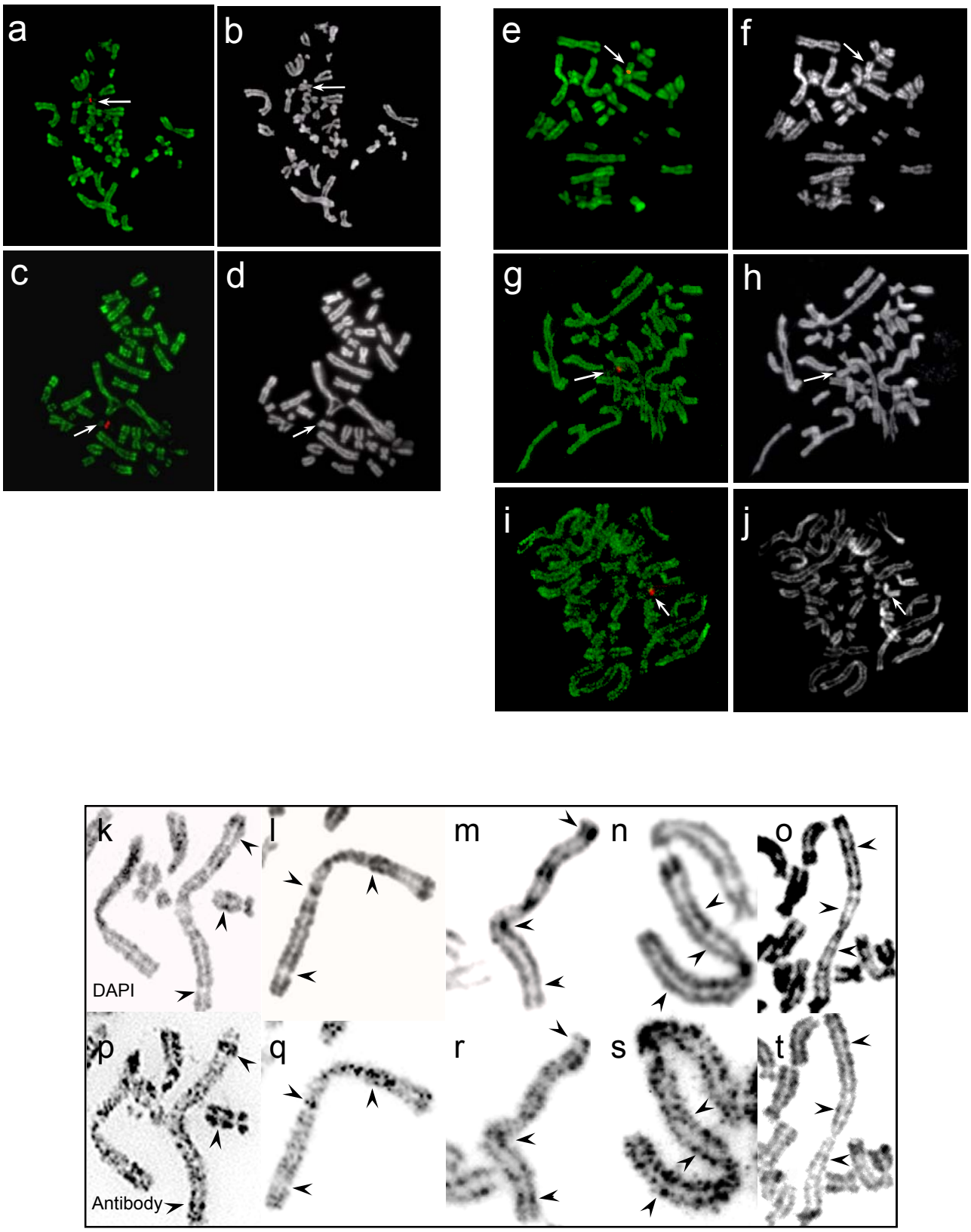

Figure 13. Combined immuno-DNA FISH of somatic cell hybrid line X8-6TS1.The hybrid line contains a human inactive X chromosome (arrow) in a male hamster background. A human specific X centromeric DNA probe (red punctate signal) was used together with antisera against H4 AcK8 (a and t), H3 Me_2K4 (c and p), H3 Me_2K9 (e and q), H3 Me_3K4/9 (g and r) and H4 Me_2K20 (i and s). The DAPI counterstain is pseudocoloured as white on the right of each image.

Following immunolabelling the same hamster chromosome was enlarged and a negative black and white image recorded in order to determine the relationship between the antibody (p, q, r, s, t) banding and conventional G banding from the DAPI (k, l, m, n, o) counterstain. Corresponding regions are shown using arrowheads.

was performed to identify the human Xi, which can be seen as a red punctate signal. Remarkably the human Xi was pale staining along its entire length using antibodies to H4 AcK8, H3Me_2K4, H3Me_3K4/9 and H4Me_2K20 but retained levels of H3Me_2K9 that was comparable to the rest of the genome. This is consistent with the data shown in section 3.2.2, but also a represents a novel finding demonstrating the depletion of H4Me_2K20 on the inactive X chromosome. The antiserum against H4Me_2K20 has been shown by ELISA to be specific for H4 di-methylated at lysine 20 and have no cross-reaction against di-methylated lysines 4 or 9 (L. P. O'Neill; data not shown). Using this antibody numerous attempts were made to immunolabel human lymphoblastoid cells and mouse ES cells under unfixed and cross-linked conditions. However, the antiserum failed to label human or mouse metaphase chromosomes using either of these techniques. This may have been on account of the position of the antigen recognised by the antibody, given that lysine 20 is close to the globular core of the nucleosome and may display restricted accessibility to antibodies. This is supported by a relatively high titre of the antiserum in western blot experiments using denatured histones.

Collectively these results suggest that the human inactive X chromosome is retained in a hamster background with the appropriate histone modifications, as found in human and mouse cells. They also suggest that the continued coating by *XIST* RNA is not necessary for the global underacetylation of Xi. However, the human Xi failed to retain the localised methylation hot spots reported above. It is possible that the hamster background may compromise the epigenetics at a more local level, perhaps casting concern on studies using XChIP to study Xi in somatic cell hybrid lines (Gilbert and Sharp, 1999; Gilbert *et al.*, 2000).

Interestingly methylated H3 was not uniformly distributed across the hamster metaphase chromosome arms, but in an alternating pattern of bright and dim regions giving some of the chromosomes a banded appearance (see figure 13c). To establish how these bands relate to the G bands seen in conventional metaphase spreads, I used the large, well extended Chinese Hamster chromosomes to compare the antibody bands to the bands revealed by the DNA-binding counterstain DAPI. Using the same chromosome in each case $H3Me_2K4$ was shown to locate preferentially to DAPI weak (R band, gene rich) regions (see arrowheads in figures 13k and p) and $H3Me_2K9$ co-localised with DAPI strong (G band, gene poor) regions (figures 13l and q). The antibodies to $H3Me_3K4/9$ (figures 13m and r), $H4Me_2K20$ (figures 13n and s) and acetylated H4 (H4 AcK8) gave a different staining pattern. Whilst there were frequent examples of strongly stained interband regions, and weakly labelled DAPI bands, some DAPI strong regions were also labelled. This data suggests that the distribution of the tri-methylated isoforms of H3 differ from that of their di-methylated equivalents and is consistent with a recent report (Santos-Rosa *et al.*, 2002) suggesting that different levels of lysine methylation have functional significance *in vivo*. It also suggests that acetylated H4 and di-methylated lysine 20 of H4 do not display a clear relationship with regions defined by DAPI as gene rich, R bands. This is in contrast to Jeppesen and Turner, (1993) who reported significant correlation between R bands and regions enriched in acetylated H4. However, this was the result of immunolabelling metaphase chromosomes prepared from cells cultured in the presence of the histone deacetylase inhibitor sodium butyrate.

3.2.5 Apparent enrichment of constitutive and facultative heterochromatin for H3Me$_2$K9 and H3Me$_3$K9

Whilst the data in section 3.2.2 was consistent with subsequent reports (Heard *et al.*, 2001; Boggs *et al.*, 2002; Cowell *et al.*, 2002; Mermoud *et al.*, 2002; Peters *et al.*, 2002), it was a concern that the immunostaining only detected a enrichment on Xi for di- or tri-methylated lysine 9 of H3 in a fraction of spreads and only when using the commercial Upstate antibody against H3Me$_2$K9 or the antibody obtained from Cambridge against H3Me$_3$K9/27. The published data documenting an enrichment for histone methylation at lysine 9 of H3 has involved the use of three different antisera. Heard *et al.,* (2001) and Boggs *et al.,* (2002) each used antiserum from Upstate specific for H3Me$_2$K9, whilst Peters *et al.,* (2002) and Mermoud *et al.,* (2002) each used antiserum raised using a branched hexameric immunising peptide. Cowell *et al.,* (2002) used antiserum raised against a tri-methylated lysine 9 peptide. Using the available antisera from Upstate and Dr. T. Jenuwein (branched hexameric immunising peptide) I wanted to examine the discrepancies between the study here and the published data.

3.2.5.1 Immunodetection using antisera against H3Me$_2$K9 (Upstate) and H3Me$_3$K9/27

The antiserum specific for H3Me$_2$K9 from Upstate identified a chromosome that displayed higher levels of methylation in a fraction of spreads (~10%) prepared from human lymphoblastoids (figure 14a) and mouse primary embryonic fibroblasts (figure 14d). However, one could have argued that the enrichment occurred in a background of ubiquitous H3Me$_2$K9 immunolabelling across all of the other chromosomes; something not reported by Boggs *et al.,* (2002) or Peters *et al.,* (2002). However, a

specific enrichment on Xi became more prominent by changing the threshold level of the imaging software (figures 14b, e, g), giving an altogether unrealistic impression of $H3Me_2K9$ distribution. Similar observations were made following the immunolabelling of metaphase spreads prepared from human lymphoblastoid cells using antiserum specific for $H3Me_3K9/27$ (figure 14i). In each case the brightly stained chromosome was confirmed as one of the X chromosomes by performing X-specific centromeric FISH (figures 14h, j). This suggests that in selective spreads the inactive X chromosome does indeed display elevated levels of di-methylation at lysine 9 and tri-methylation at lysine 9 and/or 27, consistent with the published data (Boggs *et al.*, 2002; Cowell *et al.*, 2002; Peters *et al.*, 2002). Note that elevated levels of tri-methylation specific to lysine 9 cannot be concluded using this antiserum due to its recognition of lysine 27.

However, the observations made here suggest that the genome wide distribution of $H3Me_2K9$ and $H3Me_3K9/27$ as determined by the immunolabelling of metaphase chromosomes is somewhat more ubiquitous than previously suggested.

Given that the $H3Me_2K9$ antiserum raised in Birmingham never detected a specific enrichment of a single chromosome it was interesting to compare the behaviour of the Upstate antisera using inhibition ELISA. Therefore, in an extension of the antibody specificity experiments Dr. L. P. O'Neill analysed the Upstate and Birmingham antisera in parallel using peptides containing various combinations of modifications. In the past antibodies have been shown to have certain restrictions in that modifications adjacent to the epitope of interest have been shown to potentially

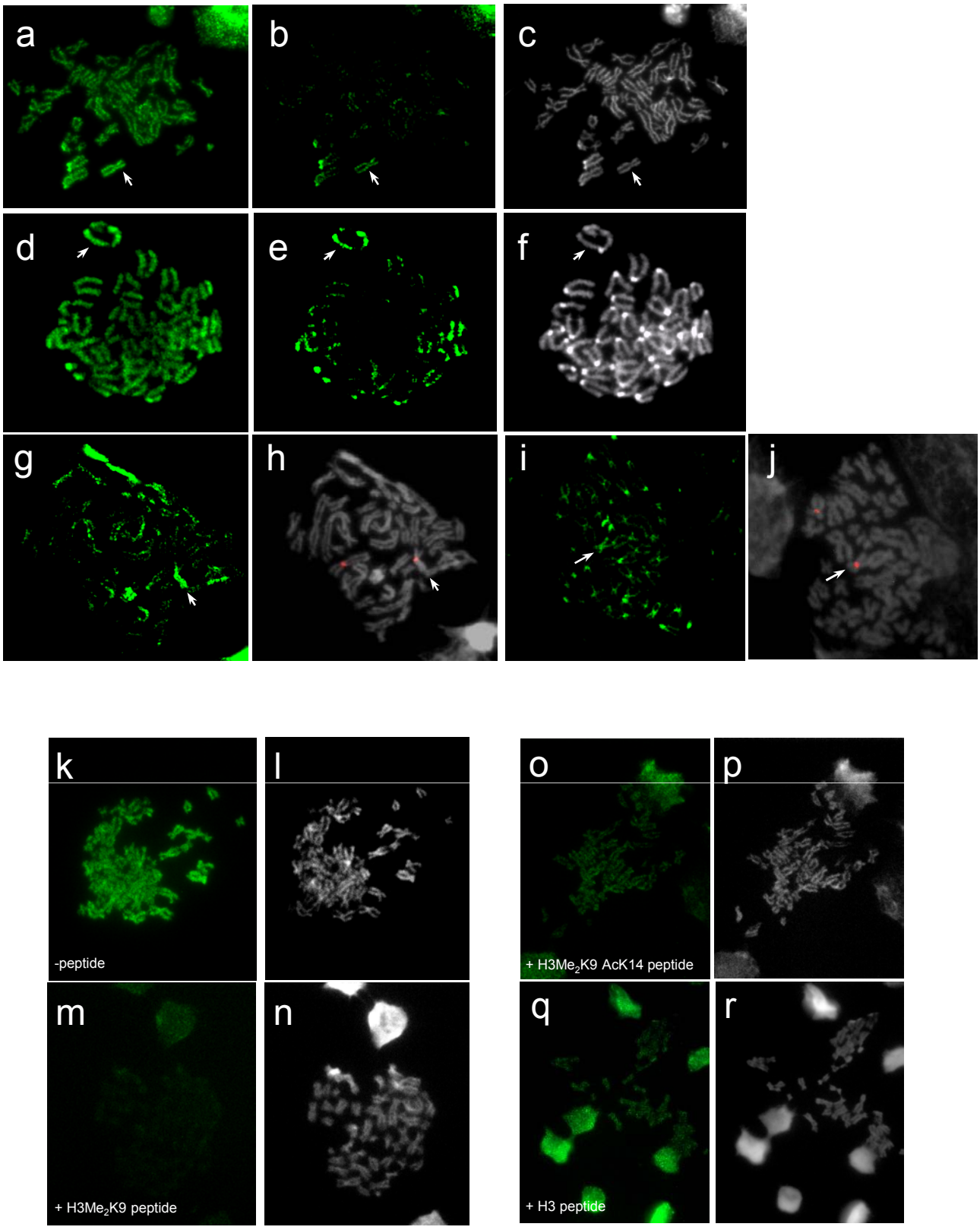

Figure 14. Metaphase spreads were prepared from human lymphoblastoid cell line GM12616 (a, g, i) and PMEFs (d) and immunolabelled using αH3 Me_2K9 (a, b, d, e ,g) and αH3 Me_3K9/27 (i). In a proportion of spreads (~10%) a chromosome was distinguishable based on its higher levels of lysine 9 di- and tri-methylation (a, d). This could be artificially enhanced by altering the threshold level of the imaging software (b, e, g, i). The brightly stained chromosome was confirmed as one of the X chromosomes using X-specific centromeric FISH (h).

Immunofluorescence was performed on cell line GM12616 using antiserum against H3 Me_2K9 under peptide inhibition conditions. The antiserum was incubated with peptides against H3Me_2K9 (m), H3Me_2K9 AcK14 (o) or an unmodified H3 peptide (q) prior to the immunolabelling of metaphase spreads. A no-peptide control was included and is shown in k. Images were captured under fixed timing conditions.

influence the binding efficiency of the antisera (Turner *et al.*, 1989; Clayton *et al.*, 2000). I wanted to test the hypothesis that the enrichment detected on Xi was on account of its depletion of acetylation at H3 lysine 14. This is absent from Xi but not the other chromosomes and if acetyl-lysine at position 14 was influencing the accessibility of binding to lysine 9, this would generate an altogether unrealistic impression of an enrichment of di-methylation at lysine 9 on Xi. Interestingly ELISA showed that the Upstate antiserum displayed significantly less inhibition of antibody binding to immobilised histones by a peptide acetylated at lysine 14 and di-methylated at lysine 9 than a peptide di-methylated at lysine 9 alone (data not shown). No such interference was observed by the Birmingham antibody (data not shown). This was confirmed through peptide inhibition by immunofluorescence. Immunolabelling was performed using the Upstate antiserum following incubation of the antiserum with four different peptides at a dilution confirmed by ELISA to give total inhibition by the H3Me$_2$K9 peptide. The peptides used were; a no peptide control (figure 14k), a synthetic peptide with di-methyl lysine at position 9 (figure 14m), a peptide with di-methyl lysine at position 9 and acetyl-lysine at position 14 (figure 14o) and an unmodified H3 peptide (figure 14q). The exposure time of the camera was fixed such that differences in fluorescence (antibody binding) were readily detectable. The antiserum showed strong binding in the absence of any peptide which was almost entirely blocked by a prior incubation with the H3Me$_2$K9 peptide. In contrast the peptide di-methylated at lysine 9 and acetylated at position 14 displayed significantly less inhibition. The doubly modified peptide displayed inhibition analogous to the unmodified H3 peptide and confirms that the Upstate antiserum is influenced by acetylation at position 14. Furthermore this suggests that the enrichment of Xi for H3Me$_2$K9 detected by Heard *et al.,* (2001) and Boggs *et al.,* (2002) may be a

consequence of its depletion for acetylated H3 at position 14. The $H3Me_3K9/27$ antiserum remains untested by peptide inhibition.

3.2.5.2 Immunodetection using antiserum against $H3Me_2K9_{BCH}$; raised using a branched hexameric peptide

Close inspection revealed that the publications reporting the most convincing enrichment for H3 di-methylation at lysine 9 (Mermoud *et al.*, 2002; Peters *et al.*, 2002) performed immunodetection on formaldehyde fixed metaphase spreads using an antibody raised against a "branched" hexameric synthetic peptide. This antibody, referred to here as $H3Me_2K9_{BCH}$ has a preference for chromatin that is of a more closed nature when compared to antibodies raised with a single synthetic peptide and a carrier protein such as ovalbumin. An analysis of the specificity of the antibody and the bias for closed chromatin structure has been discussed elsewhere (Maison *et al.*, 2002). I wanted to investigate whether the cross-linking of chromatin was biasing the target of the antibody given that cross-linking with formaldehyde can change chromatin structure and thus influence the availability of the antigen.

Mermoud *et al.,* (2002) reported that the frequency of female ES cells displaying a strongly labelled chromosome, identified previously as Xi, increased rapidly after two days of differentiation. Following seven days of differentiation almost 100% of cells displayed a strongly stained Xi. Therefore metaphase chromosomes were prepared from ES cells differentiated for seven days and immunolabelled using cross-linking (Mermoud *et al.*, 2002) and non cross-linking (Keohane *et al.*, 1996) conditions.

Consistent with the data in Mermoud *et al.,* (2002) under cross-linking conditions □H3Me$_2$K9$_{BCH}$ labelled the centric heterochromatin strongly and almost uniquely (arrowhead in figure 15a). Also in agreement with Mermoud *et al.,* (2002) a strongly stained chromosome was detected, although in only 26% of metaphase spreads (11/42) (arrow in figure 15a). The selective staining of constitutive and facultative heterochromatin is surprising given the reported ubiquity of H3 methylation (Duerre and Chakrabarty, 1975; Thomas *et al.*, 1975). In contrast immunodetection under non cross-linking conditions resulted in staining that was ubiquitous across all of the chromosomes and included the centric heterochromatin (arrowhead in figure 15c). This was consistent with immunolabellings performed using the □H3Me$_2$K9 antibody shown in section 3.2.2, and the antiserum obtained from Upstate, both raised in the same manner using a linear peptide conjugated to a carrier protein. Thus the selective staining of constitutive and facultative heterochromatin by □H3Me$_2$K9$_{BCH}$ is dependent upon formaldehyde fixation.

3.2.6 The loss of H3Me$_3$K4 is an early event in the process of X inactivation and precedes the loss of H3Me$_2$K4 which occurs concurrently with core histone deacetylation

Following the identification of new epigenetic marks that characterise the facultative heterochromatin of Xi, I wanted to determine the temporal order these histone modifications as they become established in female ES cells.

Given that the timing in ES cells was unknown and that these antibodies had not previously been used to immunostain mouse cells, I chose to immunolabel terminally differentiated mouse somatic cells. Therefore metaphase spreads were prepared from

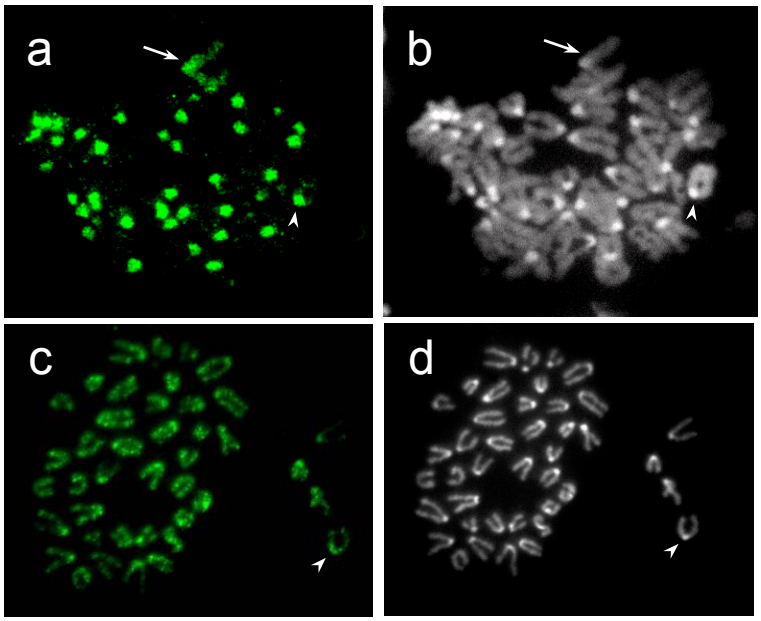

Figure 15. Metaphase chromosomes were prepared from female ES cells differentiated for 7 days and immunolabelled with αH3 Me_2K9_{BCH} using formaldehyde cross-linking (a) or non cross-linking (c) conditions. Under cross-linking conditions αH3 Me_2K9_{BCH} strongly labelled both the centric heterochromatin (arrowhead) and a single chromosome (arrow). Immunodetection performed using non cross-linked conditions stained all of the chromosomes including the centric heterochromatin (arrowhead). The DAPI counterstain is shown pseudocoloured as white on the right of each image.

primary mouse embryonic fibroblasts (PMEFs) and immunostained using $H3Me_2K4$ (figure 16a) and $H3Me_3K4/9$ (figure 16g). Both antisera identified a pale staining chromosome that was only visible on account of the DAPI counterstain (see arrows). The X chromosomes were identified using whole chromosome FISH (shown in green; figures 16b and h). The inactive X chromosome was pale staining along its entire length and never showed the localised methylation seen in the human lymphoblastoid cell line described in section 3.2.2. This may be attributable to the fact that the murine inactive X chromosome has significantly fewer genes that escape X inactivation (Ashworth *et al.*, 1991; Perry *et al.*, 2001).

To determine the order of events in ES cells metaphase chromosomes were prepared from cells differentiated for the specified number of days and immunostained using antisera against $H3Me_2K4$, $H3Me_3K4/9$ and $H3Me_3K4$. The percentage of metaphase spreads displaying a pale staining chromosome was determined and is represented graphically in figure 17. For all three antisera, a pale staining chromosome was observed at low frequency in undifferentiated cells ($H3Me_2K4$; figure 16c and $H3Me_3K4/9$; figure 16i). Immunolabelling with $H3Me_2K4$ revealed that between 3 and 4 days of differentiation there was rapid increase in the frequency of metaphase spreads displaying a pale staining chromosome. The frequency continued to increase until day 7, the last time point analysed. The temporal pattern is remarkably similar to that of the deacetylation of the core histones described in section 3.1.1. The graph in figure 7 showing the concurrent core histone deacetylation is included in figure 17 for direct comparison.

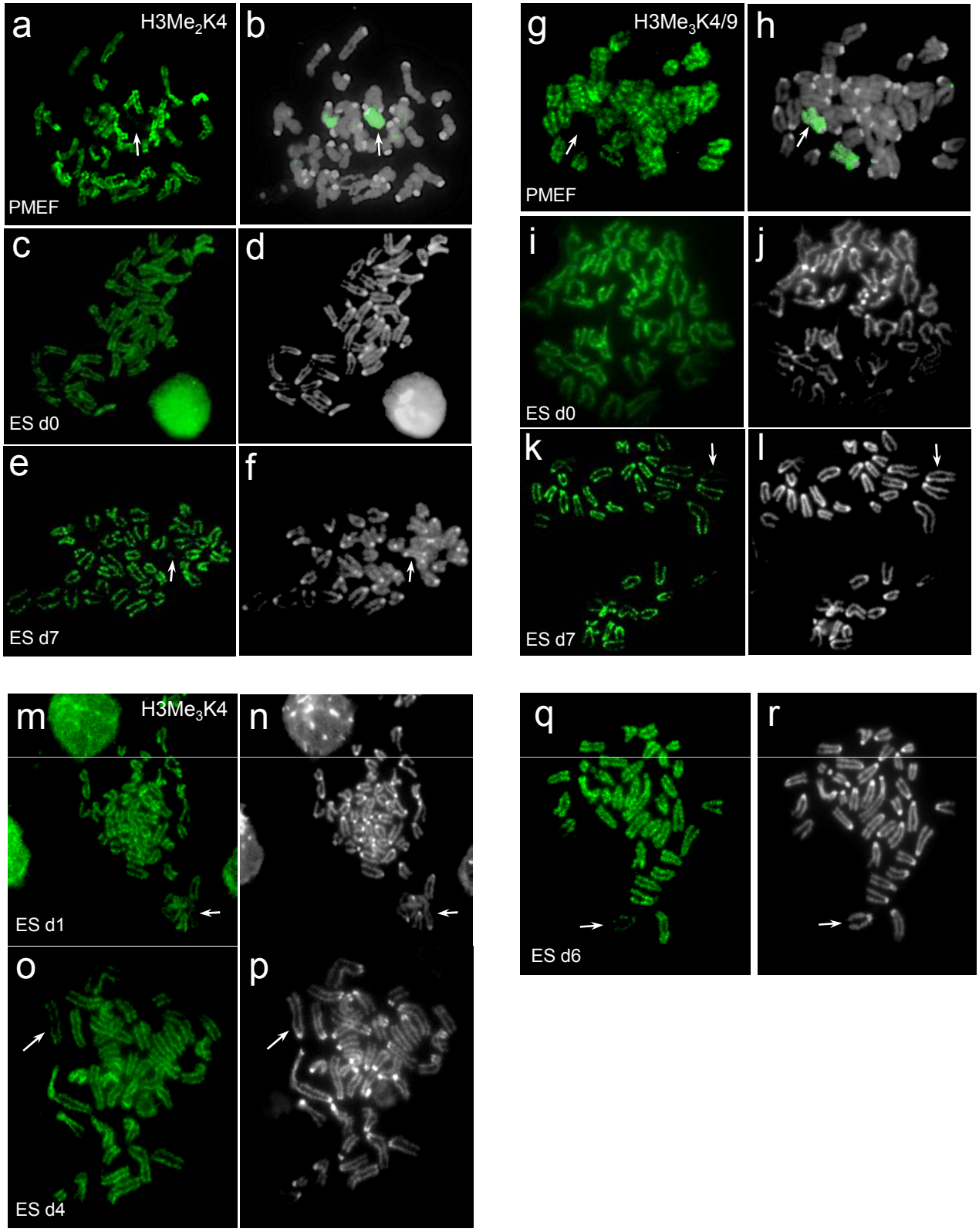

Figure 16. Metaphase spreads were prepared from primary mouse embryonic fibroblasts (PMEFs) (a, g) and undifferentiated (c, i) and differentiated (e, k, m, o, q) female ES cells. Spreads were immunolabelled using antisera to $H3Me_2K4$ (a, c, e), $H3Me_3K4/9$ (g, i, k) and $H3Me_3K4$ (m, o, q). The DAPI counterstain is shown pseudocoloured as white on the right of each image. A pale staining chromosome was identified following immunolabelling of the PMEFs using antisera against $H3Me_2K4$ (arrow in a) and $H3Me_3K4/9$ (arrow in g). The chromosome was subsequently shown to be one of the two X chromosomes using whole X chromosome FISH (b, h) (performed by Dr. G. Fews).

In contrast immunolabelling with antisera against $H3Me_3K4/9$ and $H3Me_3K4$ detected a pale staining chromosome as early as day 1 of differentiation ($H3Me_3K4$; figure 16m). The frequency of metaphase spreads displaying a pale staining chromosome using antiserum against $H3Me_3K4$ was almost 30% by day 2 (figure 17). By day six of differentiation the frequency had reached 52%. The timing of the loss of tri-methylated lysine 4 as determined by antiserum against $H3Me_3K4/9$ is very similar although it could be argued that the timing is one day later given that the biggest increase in the frequency occurs between days two and three of differentiation. I attribute this to its recognition of tri-methylated lysine 9 of H3 which may be lost subsequent to tri-methylated lysine 4. This would create a "dilution" effect such that some metaphase spreads would not be scored due to the retention of tri-methylation at lysine 9 during the initial stages of ES cell differentiation. Consistent with this it was noticeable that there was variability in the degree of paleness of Xi using this antiserum (see figure 16k). Hence the retention of tri-methylated lysine 9 early in differentiation made the detection of a chromosome based on its depletion of tri-methylated lysine 4 difficult.

In conclusion the loss of $H3Me_3K4$ is a relatively early event in the process of X chromosome inactivation occurring following just two days of differentiation, during a time period of *Xist* up-regulation, late replication and gene silencing (Keohane *et al.*, 1998). In contrast the loss of $H3Me_2K4$ occurs during a time period of core histone deacetylation. The data here suggests that there is functional significance to the level of lysine 4 methylation and is consistent with recently published data (Santos-Rosa *et al.*, 2002).

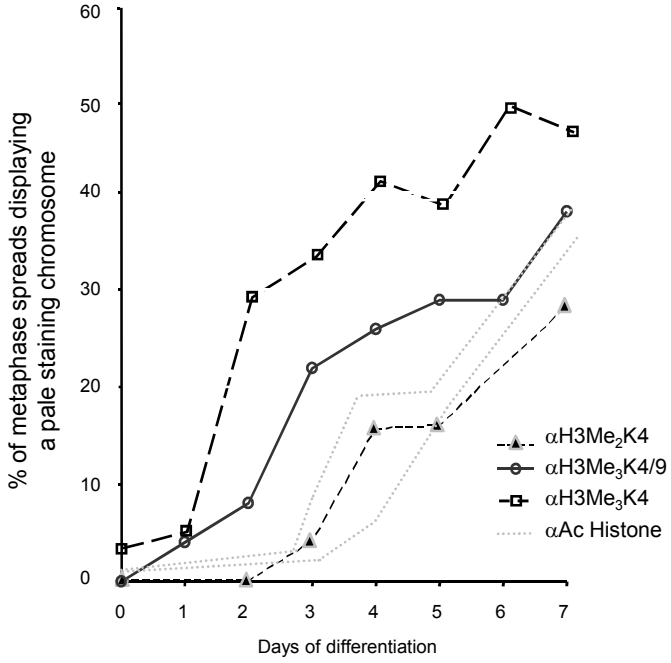

	n							
αH3Me$_2$K4	55	ND	50	50	51	50	53	52
αH3Me$_3$K4/9	50	45	54	47	58	51	58	41
αH3Me$_3$K4	51	53	58	56	41	51	48	61

Figure 17. Immunofluorescence was performed on metaphase spreads prepared from ES cells differentiated for the specified number of days using antisera against αH3Me$_2$K4, αH3Me$_3$K4/9 and αH3Me$_3$K4 Spreads were scored for the presence of a pale staining chromosome. The results are represented graphically. Total numbers of cells counted (n) are indicated beneath each day point.

3.2.7 TSA prevents the loss of H3Me$_2$K4 but not H3Me$_3$K4 on Xi if present throughout ES cell differentiation

In section 3.1.2 it was demonstrated that culturing ES cells in low concentrations of TSA induced histone hyperacetylation and importantly prevented the appearance of a hypoacetylated Xi. Here I wanted to determine whether TSA additionally prevented the appearance of a pale staining chromosome using antisera against H3Me$_2$K4 and H3Me$_3$K4.

Female ES cells were differentiated for 8 days in medium supplemented with or without TSA as detailed in section 3.1.2. Metaphase spreads were prepared and immunolabelled using antisera against H3Me$_2$K4 and H3Me$_3$K4.

Antiserum to H3Me$_2$K4 identified 52% (23/52) of the metaphase spreads as displaying a pale staining chromosome in control cells differentiated in the absence of TSA. In contrast cells differentiated for 8 days in the presence of the inhibitor displayed a pale staining chromosome in only 6% of the metaphases (3/47) analysed.

Experiments performed using antiserum against H3Me$_3$K4 identified a pale staining chromosome in 48% (29/60) of the control cells. Surprisingly, a pale staining chromosome was identified in 44% (24/54) of metaphase spreads prepared from cells cultured in the presence of TSA. Therefore supplementing the culture medium with the histone deacetylase inhibitor prevents the loss of H3Me$_2$K4 but not of H3Me$_3$K4. This suggests that the removal of di- and tri-methylated lysine 4 of H3 from Xi is regulated in a differential manner, as defined by their sensitivity to the presence of TSA.

To determine whether TSA was having a direct effect on the global levels of histone methylation histones were acid extracted from ES cells differentiated for 8 days in the presence or absence of TSA. Equal amounts of protein were electrophoresed using SDS containing polyacrylamide gels and western blotted using antisera to $H3Me_2K4$ and $H3Me_2K9$. Antiserum against $H3Me_2K9$ served as a control for the immunoblotting given a recent report showing no detectable increase in the level of di-methylated lysine 9 of H3 in cells cultured in TSA (Maison *et al.*, 2002).

The results are displayed in figure 18. There was a detectable increase in $H3Me_2K4$ in the cells cultured in TSA when compared to the control cells cultured without. In contrast and consistent with published data there was no change in the level of $H3Me_2K9$ following the culturing of cells in the presence of the inhibitor (Maison *et al.*, 2002).

Therefore differentiating ES cells in medium supplemented with TSA prevents the loss of $H3Me_2K4$ but not $H3Me_3K4$ on Xi and increases the global level of lysine 4 (but not 9) di-methylation.

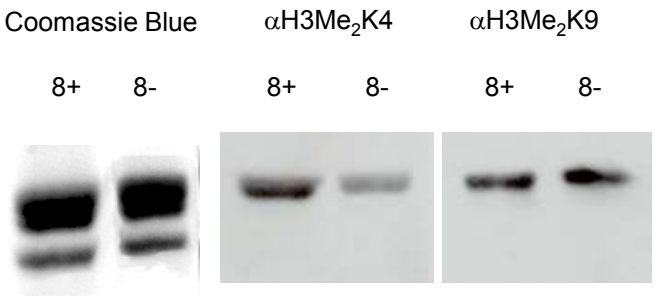

Figure 18. Histones were acid extracted from ES cells differentiated for 8 days in the presence (8+) or absence (8-) of TSA. The histones were separated using SDS polyacrylamide gel electrophoresis and western blotted using antisera against $H3Me_2K4$ and $H3Me_2K9$. The Coomassie Blue stained gel served as a loading control between the samples.

4 RESULTS - CHAPTER FOUR

4.1 IMMUNO-FISH ANALYSIS OF THE SPREAD OF X INACTIVATION IN X;AUTOSOME TRANSLOCATIONS

Cases of X;autosome translocation provide an opportunity to analyse how the spread of X-inactivation as determined by gene transcriptional analysis or the severity of the clinical phenotype compare with the properties that accompany transcriptionally silent genes. Here we were interested in the relationship between transcriptional silencing due to the spread of X-inactivation and the timing of DNA replication and the extent of spread of the histone modifications. The report that follows has analysed the spread of X inactivation in five cases of unbalanced human X;autosome translocation.

In cases of X;autosome translocation the X inactivation signal can spread variably into the attached autosomal segment, with the translocated portion of the chromosome adopting some of the features of the adjacent inactivated chromatin. Many reports have demonstrated that the translocated autosomal material can become delayed in its replication timing, a characteristic feature of Xi (Kulharya *et al.*, 1995). Indeed this has often been used as a marker to define the extent of spread of X inactivation. However, in general reports have failed to address how the spread of late replication actually relates to the extent of transcriptional silencing in the translocated autosomal segment. In many cases there is good correlation between the spread of late replication, the silencing of a single autosomal gene and the severity of the clinical phenotype (Couturier *et al.*, 1979; Mohandas *et al.*, 1982). It is presumed that a mild phenotype results from the transcriptional silencing of translocated autosomal genes that are trisomic. However, in contrast there are also reports of individuals with unexpectedly mild phenotypes possibly attributable to the spread of gene silencing in

which there was no detectable spread of late replication (Keitges and Palmer, 1986; Garcia-Heras *et al.*, 1997; Keohane *et al.*, 1999). Indeed it was recently demonstrated that late replication can be a poor correlate of the spread of gene silencing (Sharp *et al.*, 2001).

There are very few studies that have analysed the distribution of histone hypoacetylation in X;autosome rearrangements, and the cases studied appear to suggest little or no spreading into the autosomal segment (Keohane *et al.*, 1999).

The following data is the result of a collaboration with A. J. Sharp (Wessex Regional Genetics Laboratory, Salisbury). We have examined how the spread of late replication, chromatin depleted in acetylated H3/H4 and in H3 di-methylated at lysine 4 relates to the actual extent of transcriptional silencing in the autosomal segment. Using data from the human genome mapping project A. J. Sharp performed allele-specific reverse transcription PCR enabling us to accurately determine the transcriptional status of genes in the autosomal segment of the translocated chromosome. Immunocytochemistry experiments performed in Birmingham established how the spread of gene silencing compared with the extent of spread of the histone modifications that characterise the facultative heterochromatin of the inactive X chromosome.

All five cases were unbalanced translocations shown to have a completely skewed X inactivation pattern towards the translocated X chromosome.

4.1.1 Case 1 - SP, 46,X,der(X)t(X;11)(q26.3;p12) de novo (pat)

Heterozygous polymorphisms were identified in eleven genes spanning the majority of the translocated segment 11p12-pter in the patient SP and were used for allele-specific RT-PCR. The transcriptional status of these genes was analysed using RNA extracted from peripheral blood and from EBV-transformed lymphoblasts. Both gave concordant results. The analysis demonstrated a continuous spread of gene silencing across nearly the entire translocated 11p segment.

A fluorescent late-pulse BrdU assay combined with *in situ* hybridisation using whole chromosome 11 paint was performed to determine the extent of spread of late-replication into the autosomal segment. In each of 50 cells examined in both peripheral blood and lymphoblasts there was partial spreading of late-replication into the translocated 11p segment. The late replicating region extended from the X chromosome across approximately half to two-thirds of the autosomal chromatin.

To analyse the spread of histone modifications, metaphase chromosomes were prepared from EBV-transformed lymphoblastoid cells and immunolabelled using antisera against H4 AcK8 (figure 19a), H3 AcK14 (figure 19d), and H3Me_2K4 (figure 19g). Immunolabelling was combined with *in situ* hybridisation using a whole chromosome 11 paint (red) and is shown with the DAPI counterstain in blue (figure 19b, e and h). Superimposed images of the immunolabelling and FISH are shown (figure 19c, f and i) to give a true assessment of the spread of each of the histone modifications into the autosomal segment. In each of the 36 cells examined, the 11p segment was clearly hypoacetylated for H3 and H4 and depleted in chromatin di-methylated at H3 lysine 4 (H3Me_2K4) along almost its entire length. However, in

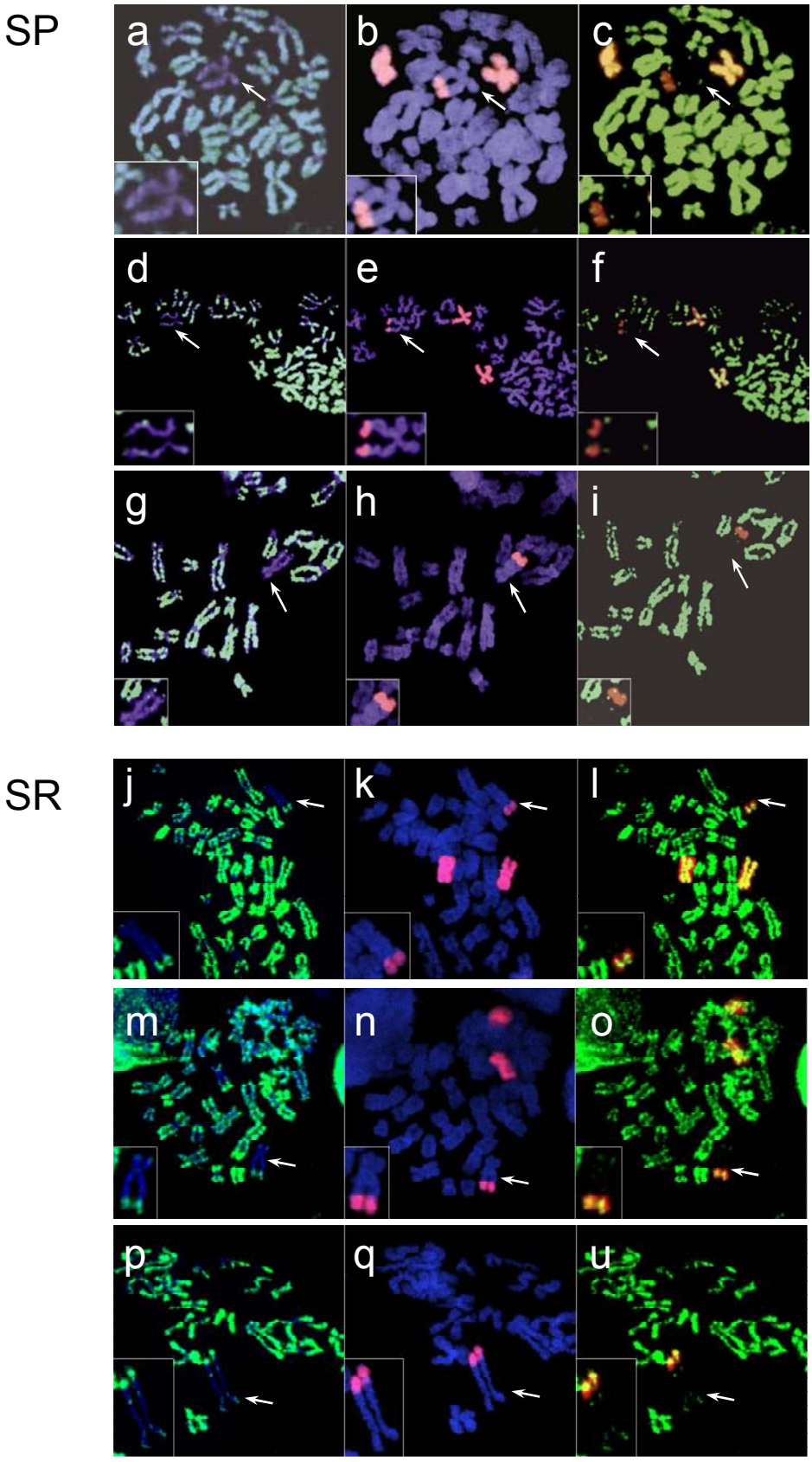

Figure 19. Combined immuno-FISH analysis of X;autosome translocation cases SP (a-i) and SR (j-u). Metaphase chromosomes were prepared from lymphoblastoid cells and immunolabelled using antisera to H4 AcK8 (a, j), H3 AcK14 (d, m), and H3Me_2K4 (g, p) combined with *in situ* hybridisation using a whole chromosome 11 (SP; b, e, h), or 7 paint (SR; k, n, q). DAPI counterstain is shown as blue. The immunolabelling and FISH have been superimposed in order to asses the degree of spread of each of the histone modifications (c, f, i, l, o, u).

every cell examined a small punctate region of H3/H4 acetylation and H3 lysine 4 di-methylation was clearly visible at the distal tip of the translocated segment of 11p. In a proportion of cells, similar punctate staining was also apparent using these antisera at the distal tip of Xp, corresponding to the pseudoautosomal region (PAR), and on the long arm of the X chromosome at approximately Xq22-25, consistent with previous observations (Belyaev *et al.*, 1996; Boggs *et al.*, 2002) and the data shown in section 3.2.2. In brief the analysis of SP revealed a continuous spread of gene silencing over almost the entire translocated segment, accompanied by only a partial but variable spread of late replication and an almost complete spread of chromatin depleted in acetylated H3/H4 and H3 di-methylated at lysine 4.

4.1.2 Case 2 - SR, 46,X,der(X)t(X;7)(q27.3;q22.3) mat

Heterozygous polymorphisms were identified in three genes within the translocated segment 7q22.3-qter in SR. Allele-specific RT-PCR showed that a gene approximately 4Mb into the autosomal segment was transcriptionally silent and a gene 40Mb into the translocated region displayed around 30% of the expression seen in normal control cells. In contrast a gene 42.5Mb from the autosomal breakpoint was shown to display normal expression. Therefore the spread of gene silencing was both partial and continuous.

Replication timing analysis was performed using peripheral blood and lymphoblastoid cells and revealed that 49/54 peripheral blood and 30/35 lymphoblasts showed a partial, continuous spread of late replication across approximately one third of the 7q segment. However, in the remaining cells the late replicating region only extended as

far as the X;autosome boundary and did not visibly spread into the translocated 7q segment.

The spread of the histone modifications was studied by performing immuno-FISH using antisera against H4 AcK8 (figure 19j, k, l), H3 AcK14 (figure 19m, n, o), and $H3Me_2K4$ (figure 19p, q, u) combined with a whole chromosome 7 (red) paint. In each of the 27 lymphoblastoid cells examined there was a continuous spread of hypoacetylated H3 and H4 together with chromatin depleted in $H3Me_2K4$ across approximately one third of the 7q segment. Residual antibody staining was also observed using all antisera at the tip of Xp corresponding to the PAR. Antibodies against $H3Me_2K4$ also revealed a di-methylated region at Xq22-25, consistent with the data shown in section 3.2.2.

In summary SR displayed a partial and continuous spread of gene silencing which correlated well with both the spread of late replication and chromatin depleted in acetylated H3/H4 and $H3Me_2K4$.

4.1.3 Case 3 - AL0044, 46,X,der(X)t(X;6)(p11.2;p21.1) mat

The AL0044 case has been reported previously (Keohane *et al.*, 1999). This study reported an apparent exclusion of late replication and hypoacetylated H4 from the translocated segment of 6p.

Heterozygous polymorphisms were identified in nine genes within the translocated segment 6p21.1-pter in AL0044, which were used for allele-specific RT-PCR. In brief

the results showed a discontinuous spreading of gene silencing across the entire translocated segment of 6p, with active genes interspersed among inactive genes.

Late replication analysis revealed that 20/50 lymphoblastoid cells displayed a complete absence of spreading of late replication into the 6p segment. In the remaining 30/50 cells there was a discontinuous spread of late replication into the translocated 6p segment. In these cells there was a region of late replication of variable size visible on the 6p telomere, with no detectable late replicating DNA on the intervening segment.

Immuno-FISH analysis was performed using antisera against H4 AcK8 (figure 20a, b, c), H3 AcK14 (figure 20d, e, f), and H3Me_2K4 (figure 20g, h, i) combined with a whole chromosome 6 (red) paint. In each of the 23 lymphoblastoid cells examined there was a discontinuous spread of hypoacetylated H3/H4 and chromatin depleted in H3Me_2K4 into the 6p segment. However, the proximal portion of the translocated 6p chromatin was indistinguishable from the corresponding regions of the chromosome 6 homologues. The distal portion of the autosomal segment, depleted in both acetylated H3/H4 and di-methylated lysine 4 of H3 varied in size and in some instances covered almost one third of the 6p.

4.1.4 Case 4 - BO0566, 46,X,der(X)t(X;6)(q28;p12) de novo (pat)

Heterozygous polymorphisms were identified in seven genes within the translocated segment 6p12-pter in BO0566, and were analysed using allele-specific RT-PCR. The results showed a discontinuous spreading of gene silencing across the translocated segment of 6p, with active genes interspersed among inactive genes.

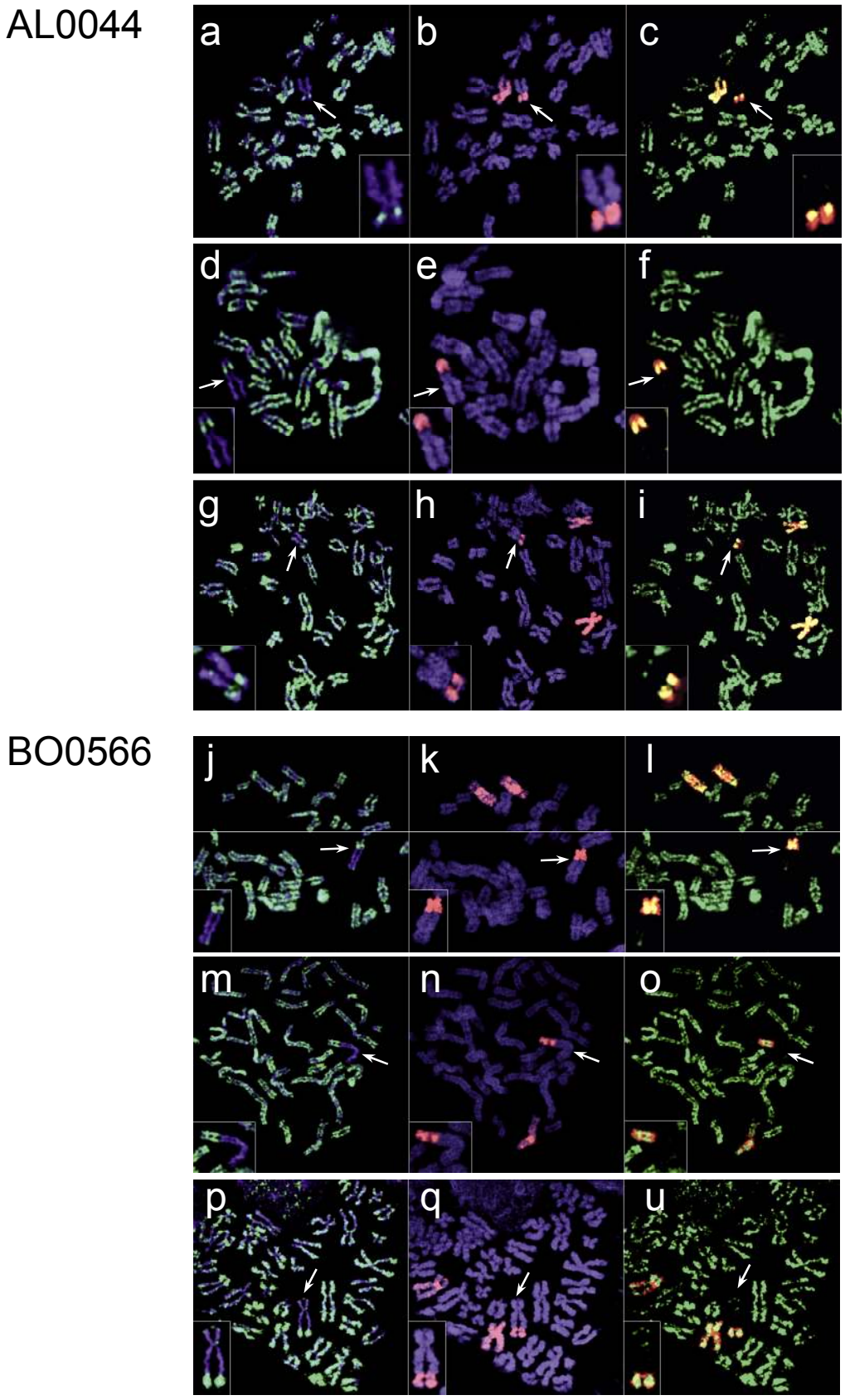

Figure 20. Immuno-FISH analysis of X;autosome translocation cases AL0044 (a-i) and BO0566 (j-u). Lymphoblastoids were immunostained using antisera against H4 AcK8 (a, j), H3 AcK14 (d, m), and $H3Me_2K4$ (g, p) combined with *in situ* hybridisation using a whole chromosome 6 paint (b, e, h, k, n, q). DAPI counterstain is shown as blue. The immunolabelling and FISH have been superimposed in order to asses the degree of spread of each of the histone modifications (c, f, i, l, o, u).

Replication timing analysis in lymphoblastoids revealed that in each of the 50 cells examined there was no detectable spread of late replication into the translocated segment. The late replicating region appeared to define the boundary between X and autosomal chromatin.

The extent of spread of each of the histone modifications was analysed by performing immuno-FISH on metaphase chromosomes prepared from lymphoblastoids using antisera against H4 AcK8 (figure 20j, k, l), H3 AcK14 (figure 20m, n, o), and $H3Me_2K4$ (figure 20p, q, u) and a whole chromosome 6 (red) paint. In each of the 24 cells examined there was a complete absence of spreading of any of the histone modifications. The chromatin that was depleted in H3/H4 acetylation and H3 di-methylation at lysine 4 appeared to define the X;autosome boundary. In a proportion of cells punctate staining was observed using all of the antisera at the distal tip of Xp corresponding to the pseudoautosomal region (PAR).

In summary AL0044 and BO0566, both X;6 translocations showed a discontinuous spread of gene silencing. However, the cytogenetic observations differed between each case. AL0044 showed a discontinuous spread of late replication and chromatin depleted in acetylated H3/H4 and $H3Me_2K4$ whereas BO0566 displayed little or no spread of late replication or the histone modifications.

4.1.5 Case 5 - AH, 46,X,der(X),t(X;10)(q26.3;q23.3) mat

Replication timing and gene expression analysis of the translocated portion in the AH case has been reported previously (Sharp *et al.*, 2001). These studies demonstrated an apparently continuous but incomplete spread of gene silencing, covering the majority

AH

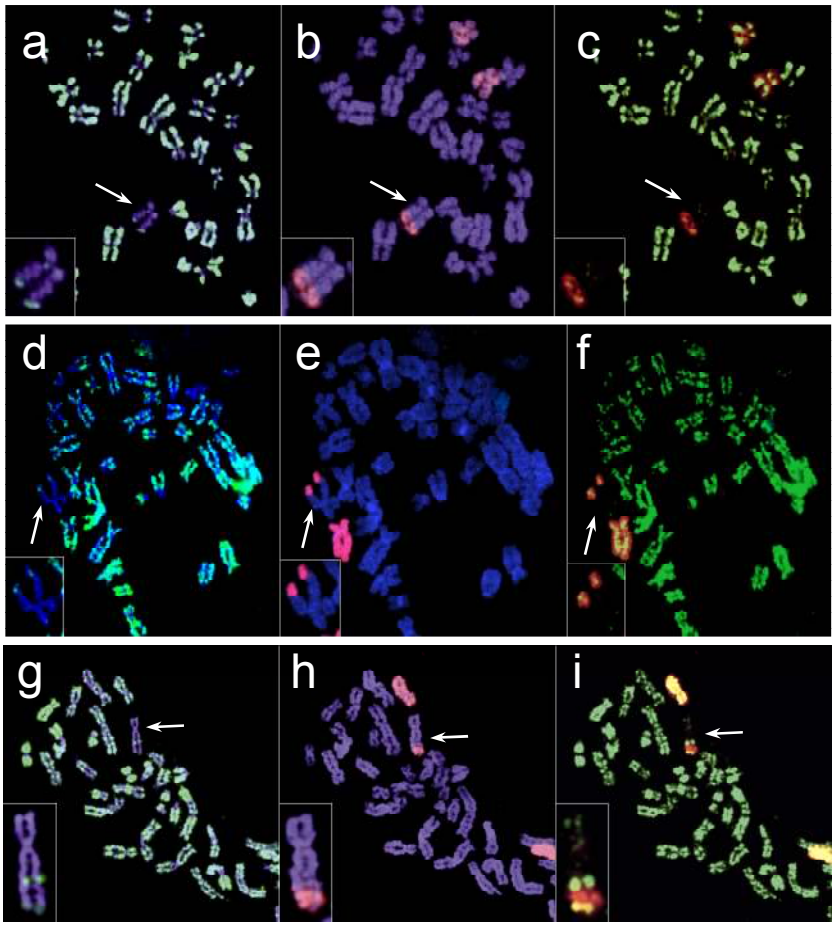

Figure 21. Combined immuno-FISH analysis of AH. Metaphase chromosomes were prepared from lymphoblastoid cells and immunolabelled using antisera to H4 AcK8 (a), H3 AcK14 (d), and H3Me_2K4 (g) combined with *in situ* hybridisation using a whole chromosome 10 paint (b, e, h). DAPI counterstain is shown as blue. The immunolabelling and FISH have been superimposed in order to asses the degree of spread of each of the histone modifications (c, f, i).

of the translocated 10q segment. In contrast to the spread of transcriptional silencing the late replicating region only extending as far as the X;autosome boundary.

Results gained by immuno-FISH using antisera against H4 AcK8 (figure 21a), H3 AcK14 (figure 21d), and H3Me$_2$K4 (figure 21g) combined with *in situ* hybridisation using a whole chromosome 10 (red) paint revealed a continuous and almost complete spread of chromatin depleted in acetylated H3/4 and H3 di-methylated at lysine 4 in each of the 32 cells examined. This was in direct contrast to the results gained by the replication analysis where the late replicating DNA was confined by the X;autosome boundary. However, in every cell examined a small region of H3/H4 acetylation and H3Me$_2$K4 was visible at the distal end of the translocated segment of 10q. Similar punctate staining was occasionally observed using all antisera at the distal tip of Xp (PAR). Immunolabelling using the antibody against H3Me$_2$K4 additionally revealed a brightly stained region at approximately Xq22-25 which was consistent with previous observations.

In the AH case the spread of gene silencing correlated well with the degree of spread exhibited by the histone modifications but not with the spread of late replication.

4.1.6 Relationship between the spread of gene silencing, late replication and chromatin depleted in acetylated H3/4 and H3Me$_2$K4 in cases of X;autosome translocation

When all five cases are considered collectively we can make various conclusions. Firstly we have shown that the spread of gene silencing can occur in a variable manner, suggesting that the factors responsible for the spread of X inactivation are not

unique to the X chromosome. However, this spread occurred in either an incomplete or discontinuous fashion, suggesting that autosomal chromatin does not transmit or maintain the X inactivation signal as efficiently as the X chromosome.

In this study we have shown that the spread of X inactivation can occur with or without the cytogenetic features normally associated with the inactive X; such as late replication and chromatin depleted in acetylated H4/H3 and H3 di-methylated at lysine 4. This is most striking in AL0044 and BO0566, both X;6 translocations with a discontinuous spread of gene silencing. However, the cytogenetic observations differed between each case; in the AL0044 case we observed a discontinuous and variable spread of gene silencing that was accompanied by chromatin depleted in acetylated H3/4 and $H3Me_2K4$, whereas the BO0566 case displayed no detectable spread of the histone modifications or late replication. Collectively these two cases illustrate the necessity for gene transcriptional analysis in cases of X;autosome translocation.

Whilst late replication appears to be a poor correlate of gene activity in some of these cases, all autosomal genes located within cytogenetically late replicating regions were inactive. One might propose that these domains are retained transcriptionally inert in a more stable fashion.

Immuno-FISH analysis revealed that in general chromatin depleted in acetylated H3/4 and $H3Me_2K4$ is a good correlate of gene inactivity in all of the cases except BO0566. Furthermore in the BO0566 case there may have been localised regions of chromatin, depleted in acetylated H3/4 and $H3Me_2K4$ that accompanied gene inactivity, but

remained undetectable using a cytogenetic approach. For a more informative analysis chromatin immunoprecipitation must be employed to determine the acetylation and $H3Me_2K4$ status of the inactive genes in the autosomal portion of the translocated chromosome. In conclusion the histone modifications that distinguish the inactive X chromosome appear to be superior cytogenetic measures of the spread of X inactivation than late replication.

5 RESULTS - CHAPTER FIVE

5.1 THE ANALYSIS OF CLASS I HISTONE DEACETYLASE DISTRIBUTION BY IMMUNOPRECIPITATION OF FORMALDEHYDE CROSS-LINKED CHROMATIN

The *Xist* (Xi-specific transcript) gene is an absolute requirement for the process of X chromosome inactivation (Penny *et al.*, 1996; Marahrens *et al.*, 1997). *Xist* produces a non-coding RNA transcript that is expressed exclusively by the inactive X chromosome in female somatic cells (Brockdorff *et al.*, 1991). Using embryonic stem cells it was demonstrated that following differentiation there is a transition from low level biallelic *Xist* expression to high level monoallelic expression. This was proposed to be regulated through the stabilisation of the transcript and results in its accumulation on the inactive X (Panning *et al*., 1997; Sheardown *et al.,* 1997). Given its involvement in the process of X chromosome inactivation, it was interesting to discover the dramatic changes in the level of H4 acetylation that occur local to the *Xist* promoter region early in female ES cell differentiation (figures 22a and b) (O'Neill *et al.*, 1999). Chromatin immunoprecipitation (ChIP) on undifferentiated and differentiated ES cells using antibodies to acetylated H4 identified a region of H4 hyperacetylation that extended up to 120kb upstream of the P1 promoter (MP to NM18B) and included the *Enox* gene, the *Xist* minimal promoter region but not the coding domain of *Xist* (W7D and W5i). The hyperacetylated region was not observed in male undifferentiated cells and was lost in female cells following seven days of differentiation, a time point when *Xist* is expressed at high levels from the inactive X chromosome. Interestingly ChIP performed on female ES cells differentiated for just one day showed a detectable fall in H4 acetylation in the region HH1.5, 5' of the *Xist* P1 promoter region suggesting that local deacetylation events occur early in process of X chromosome inactivation.

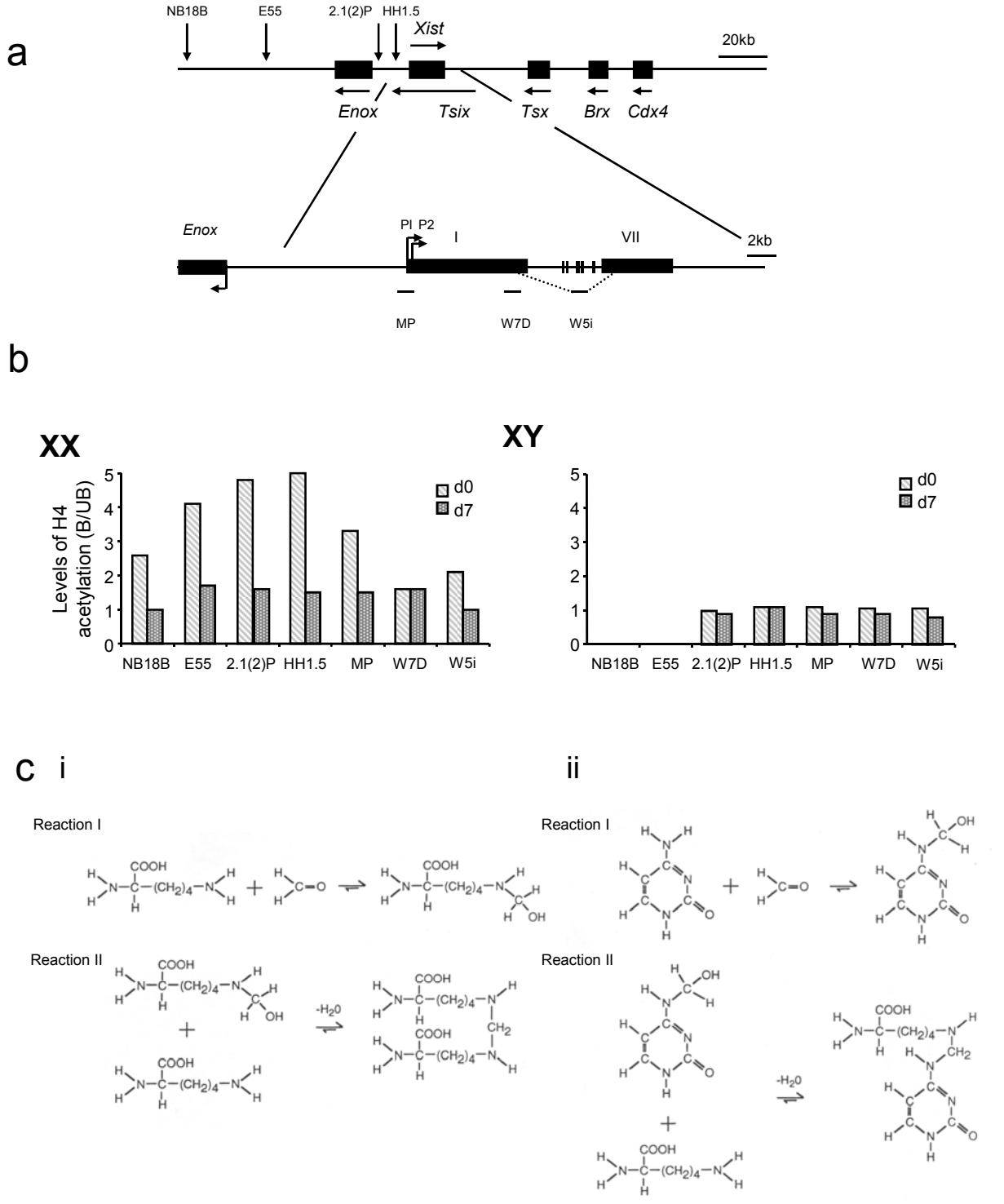

Figure 22. NChIP identified a region of H4 hyperacetylation extending up to 120kb upstream of the *Xist* P1 promoter in female undifferentiated cells (a & b); probes MP to NB18B. The hyperacetylated domain was not seen in male cells and lost in female cells following seven days of differentiation. Adapted from O'Neill *et al.,* (1999).

Chemical cross-linking of protein-protein (ci) and DNA-protein (cii) by formaldehyde. Amino and imino groups of proteins (e.g. lysine) and nucleic acids (e.g. cytosine) react with formaldehyde leading to the formation of a Schiff base (reaction I). This intermediate can react with a second amino group in a condensation reaction (reaction II). Adapted from Orlando *et al.,* (1997).

Given this developmental fall in histone acetylation in differentiating female ES cells, it was my intention to analyse the distribution of the histone deacetylases (Hdacs) during female ES cell differentiation. This was undertaken based on the hypothesis that the fall in H4 acetylation 5' to the *Xist* promoter region was due to a coordinated recruitment of an enzyme complex capable of histone deacetylation. However, other possibilities are conceivable given that a fall in histone acetylation can theoretically be generated by the recruitment of a histone deacetylase or a selective loss of associated histone acetyltransferases.

In addition to the *Xist* promoter region, the chromatin of the X-linked gene *Pgk-1* and a region rich in L1 elements were studied on account of them being putative targets for histone deacetylases owing to their histone hypoacetylation (Jeppesen and Turner, 1993; Johnson *et al.*, 1998). Additionally the housekeeping gene *Tuba6* was analysed as a negative control based on an expected depletion of deacetylases in a region of constitutive expression.

Aside from the recovery of DNA associated with a particular histone modification, native chromatin immunoprecipitation (NChIP) has been used to assay the genomic distribution of MeCP2, a protein that binds methylated DNA (Gregory *et al.*, 2001). Therefore the deacetylase antibodies were initially tested for the precipitation of chromatin using NChIP. However, the immunoprecipitation experiments rarely recovered more chromatin than the no-antibody control. This was largely expected because the histone deacetylases do not bind the DNA directly and require trans-acting factors to bring them into association with their substrate, the histone N-terminal tails. It was thus necessary to chemically cross-link the deacetylases to the

chromatin fibre prior to the immunoprecipitation step. Therefore the technique of formaldehyde cross-linking chromatin immunoprecipitation (XChIP) was employed.

The XChIP approach offers the ability to detect any protein at its *in vivo* binding site but also allows the study of proteins that do not bind DNA directly. Formaldehyde is a cross linking agent that creates tight (2Å) protein-protein (figure 22ci) and protein-nucleic acid (figure 22cii) cross-links *in vivo*. Amino and imino groups (lysines, histidines and arginines) of amino acids react with formaldehyde within minutes of its addition to living cells. The cross-links are reversible and following the immunoprecipitation of chromatin using an antibody targeted to the protein of interest the DNA can be recovered and analysed.

5.1.1 The technique of XChIP was analysed extensively using certain criteria

Initially to familiarise myself with formaldehyde cross-linking chromatin immunoprecipitation, the technique was examined using the following criteria:

Antibody specificity - The antibodies were raised against the human deacetylases and it was essential to test their antigen recognition in mouse ES cells using western blotting of whole cell extracts. Additionally the expression levels of the class II and Sir2 class deacetylases were examined using reverse transcription PCR to give a full complement of deacetylase expression in undifferentiated and differentiated ES cells.

Capacity of antibodies to immunoprecipitate - The antibodies were characterised with respect to the immunoprecipitation of deacetylase complexes. Co-precipitation experiments were performed using whole cells extracts and cross-linked chromatin.

Efficiency of cross-linking - The formaldehyde incubation time was examined to confirm that there was sufficient cross-linking of the chromatin and its associated factors. This was tested by isopycnic centrifugation of cross-linked chromatin.

Sonication shearing conditions - Sonication conditions were optimised to guarantee sufficient resolution of the starting material such that a precipitated DNA fragment did not encompass more than one region of interest.

Size range of DNA following XChIP - The size range of the DNA fragments recovered following XChIP was analysed to examine the potential bias by the antibodies for high or low molecular weight chromatin.

Multiplex PCR - The technique of multiplex PCR was optimised for the analysis of five regions of *Xist* in the immunoprecipitated DNA.

In what follows there will be brief explanations regarding how each of these criteria was satisfied.

5.1.1.1 Embryonic stem cells express histone deacetylases Hdac 1, 2, 3, 4, 5, 6, 7, Sir2α, Sirt1, Sirt2 and Hdac associated protein RbAp48 with no detectable changes in expression following differentiation for 8 days

In order to analyse the epitope recognition of the antibodies and examine the protein expression levels of *Hdacs 1, 2, 3, 4, Sir2α and RbAp48* before and after the global deacetylation of Xi has occurred, whole cell extracts were prepared from undifferentiated female ES cells and from cells differentiated for 8 days. Total protein was electrophoresed and western blotted. The results are shown in figure 23a. Although the antibodies to Hdacs 1, 2, 3 and Hdac associated protein RbAp48 were each raised using a synthetic peptide derived from the human sequence they

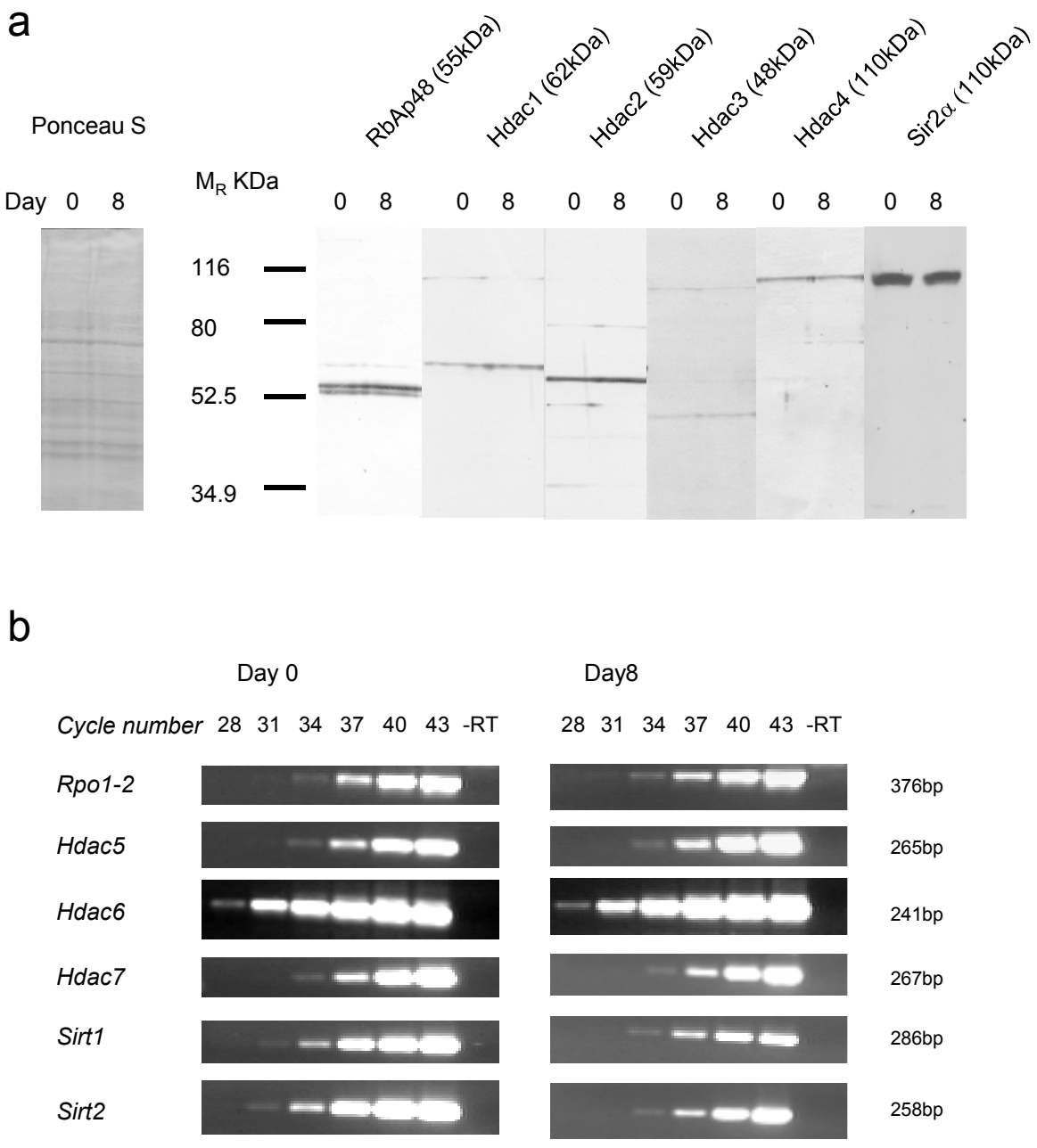

Figure 23. Whole cell extracts were prepared from undifferentiated (day 0) and differentiated (day 8) female ES cells and electrophoresed using 7.5% SDS polyacrylamide gels together with low molecular weight markers. The protein was transferred and immunoblotted using antisera raised against Hdac1, 2, 3, 4, Sir2α and the Hdac associated protein RbAp48 (a). A Ponceau S stained membrane is shown as a loading control.

The expression of Hdac5, 6, 7, Sirt1 and 2 was assayed using RT-PCR (b). Aliquots were taken at cycles 28, 31, 34, 37, 40 and 43. Samples were analysed using agarose gel electrophoresis. An image of the ethidium bromide stained gel is shown in b. PCR using RNA not subjected to reverse transcription (-RT) shows that the amplification was cDNA specific. PCR was performed on cDNA derived from the housekeeping gene *Rpo1-2* to control for differences in input RNA.

consistently recognised a single protein band of the appropriate size in mouse ES cells. The exception was RbAp48 where a protein doublet was evident. This was most likely due to recognition of RbAp46, an orthologue of RbAp48. There were no detectable differences in protein expression levels using any of the deacetylase antibodies including antiserum against Hdac4 obtained from Dr. A. Wang and Sir2α obtained commercially.

To examine the levels of mRNA transcripts of the remaining published mouse deacetylases; *Hdacs 5, 6, 7, Sirt1 and Sirt2*, semi-quantitative RT-PCR was performed on undifferentiated cells and cells differentiated for 8 days. Results are shown in figure 23b. The transcript encoding the second largest subunit of mouse RNA polymerase II (*Rpo1-2*) was used to control for differences in input RNA. *Rpo1-2* was used in preference to the housekeeping gene *Tuba6 (α-tubulin)* on account of transcripts derived from *Tuba6* being detectable as early as cycle 18.

There was obvious variation in the absolute levels of the deacetylase transcripts. *Hdac6* in particular was detected at a high level in undifferentiated and differentiated cells relative to the other deacetylases examined. However, there were no detectable differences in any of the deacetylases between the day points analysed.

5.1.1.2 Antibodies to Hdacs 1, 2, 3 and RbAp48 can immunoprecipitate histone deacetylase complexes under non cross-linking and cross-linking conditions

The antibodies were tested for their capacity to immunoprecipitate deacetylase complexes under non cross-linking conditions. Whole cell extracts were prepared from ES cells differentiated for 8 days and HeLa cells which served as a positive control. The immunocomplexes were isolated using protein A-Agarose (PAA). Protein A-Agarose was used in preference to protein A-Sepharose because the elution of the immunocomplex from Sepharose beads resulted in significant protein A leaching and made immunodetection by western blot almost impossible. The deacetylase complexes were electrophoresed using SDS-containing polyacrylamide gels and western blotted. For the immunodetection by western blotting a mouse monoclonal antibody was used that was obtained from BD Transduction Laboratories. Whilst it was characterised as recognising Hdac3, I subsequently show here that it also recognises Hdac1 and 2. The results are shown in figure 24a.

The commercial antibody recognised three bands in the input control lanes corresponding to Hdacs 1, 2 and 3 as indicated by the arrows. In both cell types the protein targeted by the antibody during the immunoprecipitation was clearly detectable. All antibodies consistently behaved with similar efficiency except during the immunoprecipitation of Hdac1 in ES cells. Antiserum to Hdac1 was more efficient at immunoprecipitation in HeLa cells, possibly due to subtle differences in the amino acid sequence of mouse Hdac1 that influences the efficiency of antigen recognition. Immunocomplexes prepared with antibodies to Hdac2 and RbAp48 contained Hdac1 and 2 in both cell types. This was consistent with published data (Zhang *et al.*, 1998b; Khochbin *et al.*, 2001; Johnson *et al.*, 2002) and confirms that some deacetylase complexes contain both these enzymes together with the Hdac associated protein RbAp48. However, there was significantly less Hdac1 in the

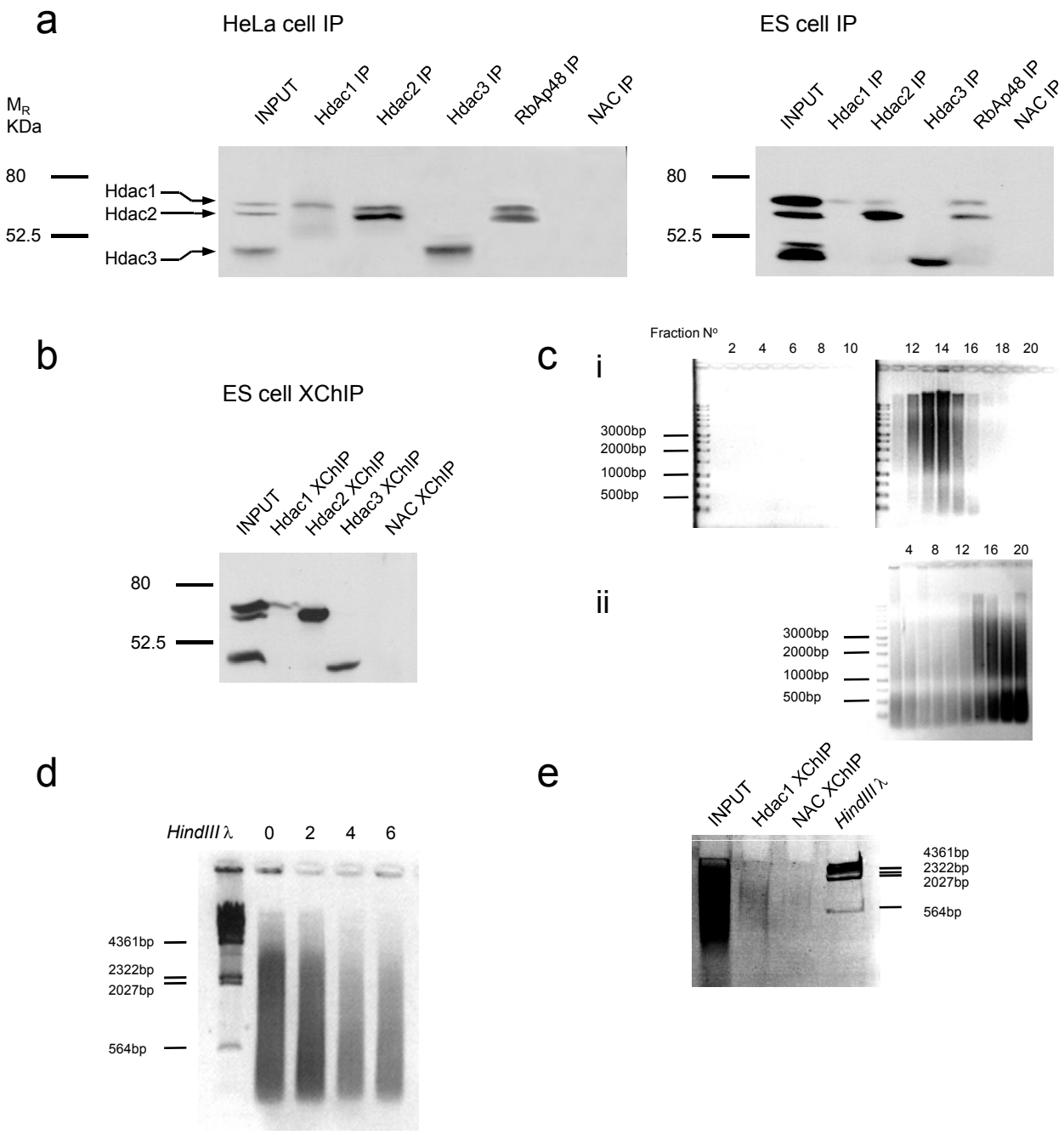

Figure 24. Whole cell extracts were prepared from HeLa cells or ES cells differentiated for 8 days (a) and immunoprecipitated using antibodies against Hdac1, 2, 3 and RbAp48. The immunocomplexes were electrophoresed using 7.5% SDS-polyacrylamide gels, transferred and western blotted using an antibody that recognises Hdac1, 2, and 3 (arrows). A similar co-precipitation approach was performed on sonicated cross-linked chromatin prepared from undifferentiated ES cells using antisera against Hdac1, 2 and 3 (b).

Formaldehyde cross-linked chromatin was prepared from ES cells differentiated for 6 days (c i) or *Drosophila* SL2 cells (c ii) and separated using isopycnic centrifugation. The fractions were collected, the cross links were reversed and the DNA was analysed using 0.8% agarose gel electrophoresis. A negative image of the ethidium bromide stained gel was recorded.

Sonicated cross-linked chromatin was prepared from undifferentiated ES cells or cells differentiated for 2, 4, or 6 days. The DNA was recovered following cross-link reversal and 2μg was electrophoresed using a 0.8% agarose gel. *HindIII* λ molecular weight standards were also included. A negative image of the ethidium bromide stained gel shown in d.

XChIP was performed on undifferentiated ES cells using antisera against Hdac1. The total DNA recovered following immunoprecipitation using Hdac 1 antisera was electrophoresed together with the no-antibody control (NAC) and 2μg of INPUT DNA using a 5% polyacrylamide gel. A negative image of the ethidium bromide stained gel was recorded.

immunocomplexes prepared from ES cells suggesting that Hdacs 1 and 2 do not associate with such affinity in these cells. The finding that material precipitated with antibodies to Hdac1 contained only the Hdac1 subunit in both cell types confirms that complexes with just this subunit do exist, but also raises the question why this antibody fails to precipitate any Hdac2 whatsoever. It is conceivable that the binding of Hdac2 obscures the epitope recognised by the anti-Hdac1 antibody.

The same co-precipitation approach was performed using formaldehyde cross-linked chromatin immunoprecipitation of ES cells differentiated for 8 days. The results are displayed in figure 24b. This was important to confirm the antibodies were compatible with the XChIP buffers and retained the ability to recognise their antigens in fixed material. An INPUT control prepared from cross-linked chromatin was electrophoresed adjacent to a whole cell extract lane and stained using Coomassie Blue in order to determine whether the cross-links had been successfully reversed (data not shown). The results were consistent with the non cross-linked data in that Hdac2 consistently failed to immunoprecipitate significant amounts of Hdac1.

5.1.1.3 Incubating cells in 1% formaldehyde for 8 minutes is sufficient to cross-link DNA and protein

Efficient cross-linking of a protein to DNA is essential for the XChIP technique. Prolonged fixation can lead to reduced antigen availability, especially important when considering histone modifications that maybe lost through the engagement of lysines and other formaldehyde reactive sites. However, insufficient cross-linking will result in poor yield following immunoprecipitation and generates cells that are refractory to sonication. During a visit to the laboratory of Dr. V. Orlando (Institute of Genetics

and Biophysics, CNR, Via G. Marconi, Napoli, Italy), I wanted to determine whether ES cells fixed in 1% formaldehyde for 8 minutes at 37^{o}C had sufficient DNA-protein cross-links such that the immunoprecipitation would generate a satisfactory yield of DNA. Therefore sonicated chromatin was prepared from cross-linked female ES cells differentiated for 6 days and poorly cross-linked *Drosophila* SL2 cells (prepared by Dr. A. Breiling). The chromatin was separated by isopycnic centrifugation using a $CsCl_2$ step gradient. Samples were taken following centrifugation by drawing fractions from the bottom of the column using vacuum apparatus. Isopycnic gradients permit the separation of high density material such as free DNA which migrates to the bottom of the tube from cross-linked chromatin, which locates higher on the gradient on account of its lower density. The DNA from each fraction was recovered and analysed using agarose gel electrophoresis (figure 24c).

The ES cell chromatin (i) is strictly confined to fractions 11 to 16. Given that the DNA recovered from these fractions must have been associated with protein; it confirms that the formaldehyde is efficiently cross-linking the DNA to its associated protein. In contrast, whilst the SL2 cells (ii) have cross-linked chromatin that is largely confined to fractions 14 to 20 there is also detectable DNA in all of the other fractions. This suggests inefficient cross-linking as the DNA in the lower fractions (1-8) is likely to be free of associated protein.

5.1.1.4 Sonication can generate chromatin fragments with an average size of 500bp and a maximum of 2kb

Given that five distinct regions of the *Xist* gene were to be examined for the presence or absence of histone deacetylases it was essential to optimise sonication conditions

such that a chromatin fragment precipitated on account of its association with a deacetylase was not amplified by more than one primer set. This would cause a dilution of any specific enrichment detected.

Sonicated chromatin from undifferentiated ES cells and cells differentiated for 2, 4, and 6 days was generated as described in the method (section 2.12). To determine the extent of shearing, aliquots of the chromatin were taken and the cross-links were reversed and the DNA recovered using phenol: chloroform purification. DNA from each sample was separated using 0.8% agarose gel electrophoresis (figure 24d). The sonication conditions successfully shear the chromatin equally in all of the day points analysed. The majority of the chromatin (approximately 90%) was below 2kb in size with an average of 500bp. Therefore to be certain that more than one primer set is not amplifying the same DNA fragment the primers must amplify regions that are separated by at least 2kb.

5.1.1.5 Gel electrophoresis shows that the DNA precipitated is representative of the starting material

In order to ascertain whether the antisera were favouring high or low molecular weight chromatin during the immunoprecipitation, XChIP was performed on undifferentiated ES cells using the antibody against Hdac1. The total DNA recovered was analysed using polyacrylamide gel electrophoresis (figure 24e).

The DNA precipitated following XChIP has a similar size range to that of the starting INPUT material and the amount precipitated is clearly more than the no-antibody

control. Therefore in conclusion there was no detectable bias by the antibody towards high or low molecular weight chromatin.

5.1.1.6 Multiplex PCR analysis of precipitated DNA permits the simultaneous analysis of five regions of Xist

After DNA purification from immunoprecipitated chromatin the enrichment of given genomic regions can be determined in a number of ways. Conventional slot blotting has been performed in the past whereby the immunoprecipitated DNA is applied to a membrane and hybridised using the DNA regions of interest (Dedon *et al.*, 1991). An alternative approach is to use the precipitated DNA as the probe in Southern Blot analysis (Orlando *et al.*, 1997). This permits the identification of binding sites within large genomic regions without relying on multiple hybridisations or PCR reactions. However, the amount of DNA obtained by XChIP is usually in the range of a few nanograms and often below the threshold level of DNA hybridisation. Indeed additional steps were taken in the later case whereby the immunoprecipitated DNA was ligated to a synthetic linker and PCR amplified prior to hybridisation.

The analysis of immunoprecipitated DNA using a PCR based strategy is very popular and provides effective answers to questions concerning the association of a transcription factor with a genomic region (Gilbert and Sharp, 1999; Breiling *et al.*, 2001; Boggs *et al.*, 2002; Drewell *et al.*, 2002). However, too often only one genomic region is tested using a single antibody, providing a somewhat limited picture (Drewell *et al.*, 2002). Multiplex PCR of the precipitated DNA, whereby all primers amplify at the same time has given a more informative analysis (Strahl-Bolsinger *et al.*, 1997; Hecht and Grunstein, 1999).

It was my intention to use the technique of multiplex PCR followed by DNA polyacrylamide gel electrophoresis to analyse the precipitated DNA for the enrichment of five genomic regions surrounding the *Xist* promoter simultaneously. The primer positions relative to *Xist* are shown in figure 25. It was essential that each primer set amplified independently with no detectable influence on the efficiency of the other primers. It was equally as important to verify that the all of the primer sets were amplifying in the same linear fashion such that all five products in the reaction could be sampled with the confidence that they were each within the linear range. To achieve these goals pilot experiments were performed using DNA purified from sonicated chromatin. The first criterion was satisfied by experiments designed such that each primer pair amplified the DNA independently in separate tubes but also collectively as a pentaplex reaction. For example in figure 25a I have analysed the effect of primer pairs X8u and X4u on the multiplex PCR reaction. The PCR was sampled in the linear range, with X8u and X4u amplifying independently (lanes 2 & 3) and collectively as tetraplex (4 & 5) or pentaplex reactions (1).

The rate of accumulation of each primer pair was analysed individually and collectively by sampling in a semi-quantitative manner, removing aliquots from the PCR master mix every three cycles and separating the products using polyacrylamide gel electrophoresis. For example in figure 25b I show that all five PCR primer sets co-amplify in the same manner, with no significant bias towards any one of the PCR products. I was therefore able to conclude that in my *Xist* pentaplex reaction all of the

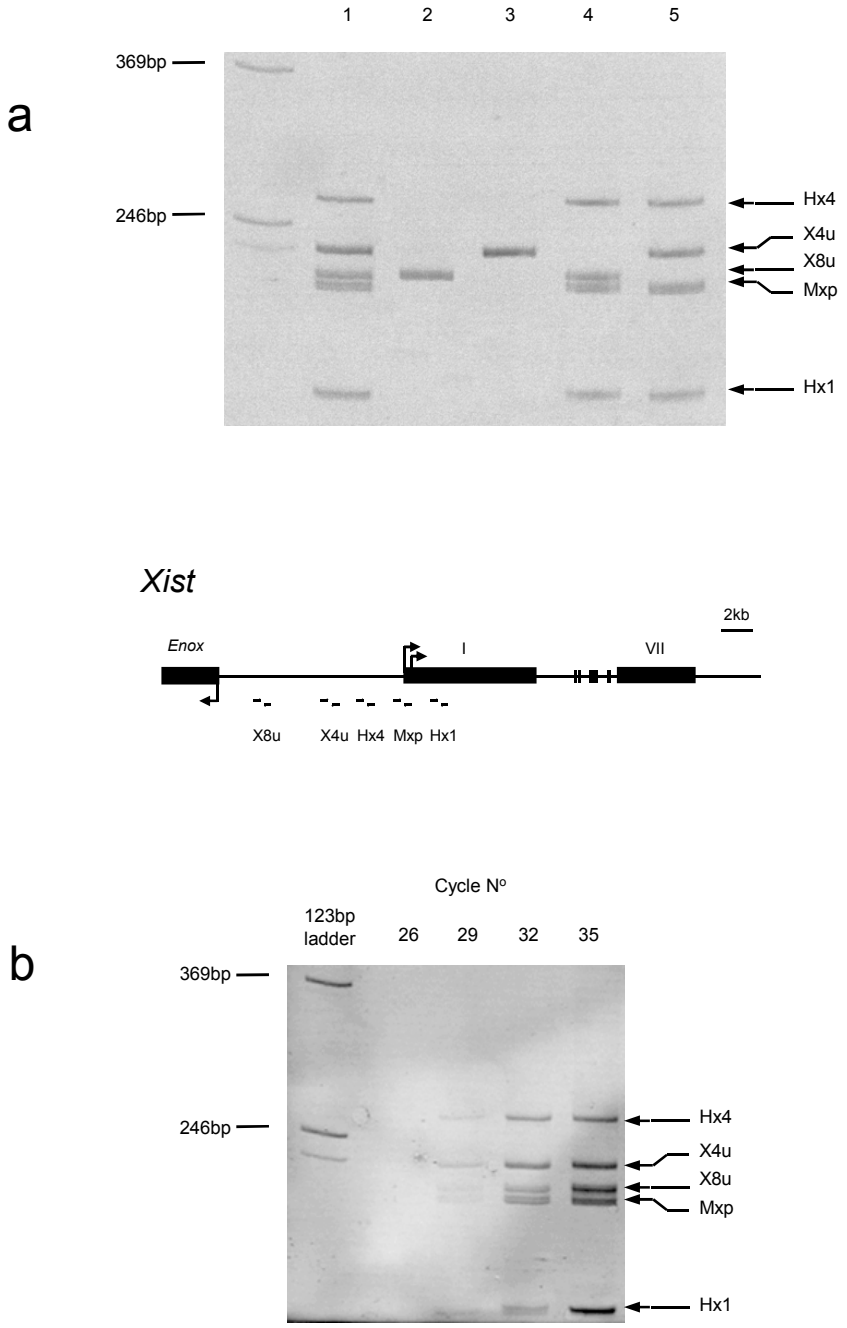

Figure 25. Optimising conditions for multiplex PCR. Each primer pair was tested for its influence on the multiplex PCR reaction (a). For example primer pairs X8u and X4u were tested independently (lanes 2 & 3 respectively) and collectively as tetraplex (4 & 5) and pentaplex (1) reactions. PCR was performed within the linear range, as determined by pilot experiments and the products were separated using DNA polyacrylamide gel electrophoresis. A negative image of an ethidium bromide stained gel is shown.

The rate of accumulation of each primer pair during multiplex PCR was analysed by amplifying 75ng of DNA purified from sonicated chromatin and sampling in a semi-quantitative manner by removing aliquots at cycles 26, 29, 32 and 35. The products were separated using DNA polyacrylamide gel electrophoresis (b). A negative image of an ethidium bromide stained gel is shown.

primers behaved the same individually as they did collectively and co-amplified sonicated DNA in the same linear fashion.

5.1.2 XChIP shows ubiquitous association of the class I histone deacetylases with the chromatin template throughout ES cell differentiation

Cross-linked chromatin fragments were prepared from female undifferentiated ES cells or cells differentiated for 2, 4, or 6 days and immunoprecipitated using antisera against Hdacs 1, 2, 3 and RbAp48 as described previously (Ferreira *et al.*, 2001). To examine the relative enrichment of the DNA recovered from the immunoprecipitated chromatin for five genomic regions spanning the *Xist* promoter domain (figure 26b), pentaplex PCR was performed as described in section 5.1.1.6. The X-linked *Pgk-1* gene was analysed using duplex PCR whereby the promoter and coding regions were co-amplified in the same reaction (figure 26c). In addition the constitutively expressed housekeeping gene *Tuba6* and a region rich in L1 elements (X141) corresponding to the A3 Giemsa dark band on the mouse X chromosome were amplified as single reactions. The PCR reactions were performed in the presence of α^{32}P dCTP and separated using DNA polyacrylamide gel electrophoresis. Representative gels are shown in figure 26a. Pilot experiments were performed initially to determine the cycle number when 75ng of INPUT DNA was being amplified in the linear range. Following PCR and gel electrophoresis the INPUT DNA consistently yielded a more intense product than the material recovered from the precipitated chromatin. This confirmed that PCR was always performed within the linear range. The relative enrichment of the deacetylases at the *Xist*, *Pgk-1* and *Tuba6* genes were quantified by PhosphorImager analysis of the appropriate PCR band. The degree of enrichment of a genomic region was expressed a ratio of BOUND divided by the INPUT (figures 26d-

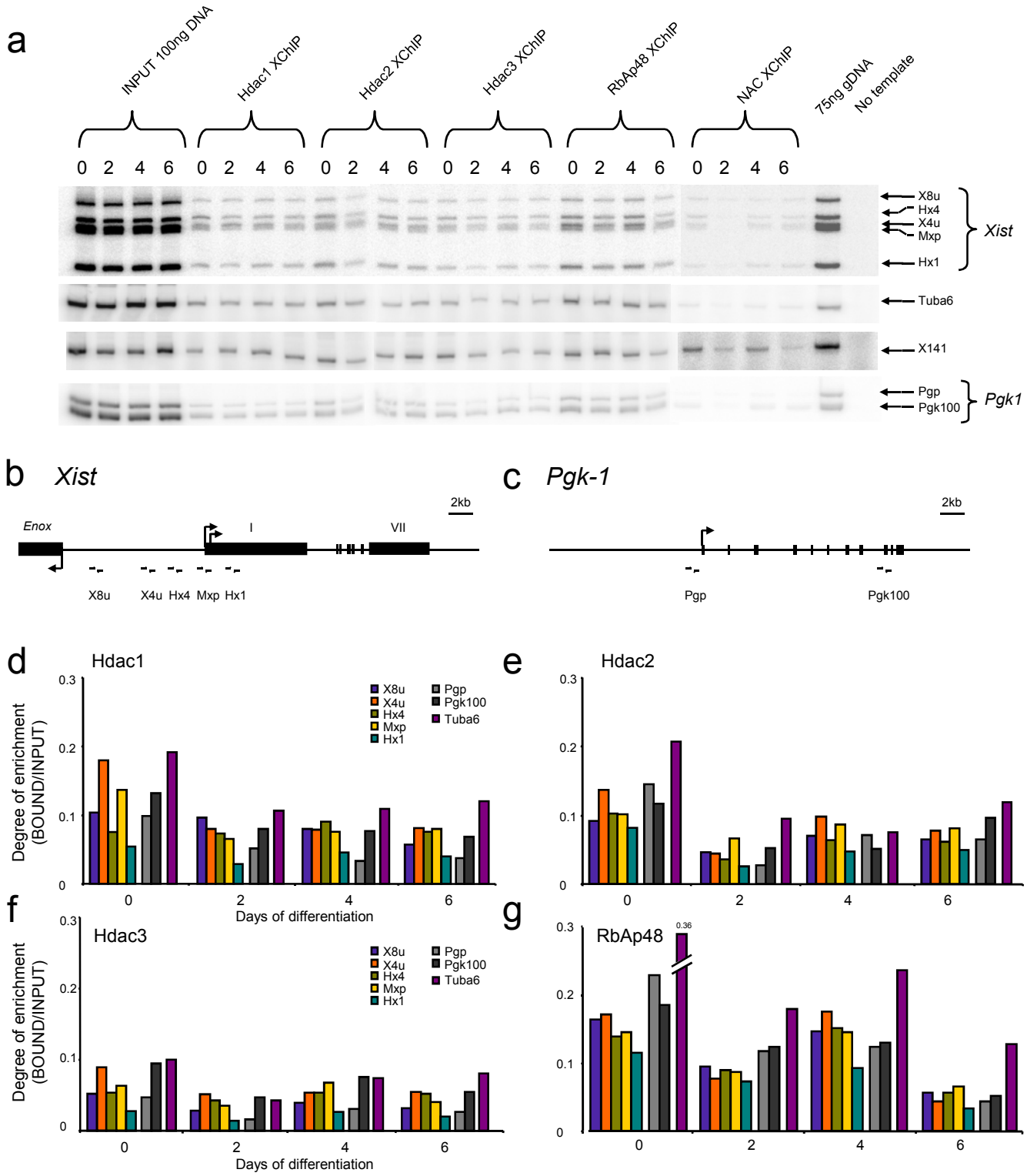

Figure 26. XChIP was performed on undifferentiated female ES cells or cells differentiated for 2, 4, or 6 days using antisera against Hdac1, 2, 3 and RbAp48. The immunoprecipitated DNA was analysed for the enrichment of specific genomic regions using PCR performed within the linear range. Five regions of *Xist* (b) were examined using pentaplex PCR and the promoter and coding regions of X-linked *Pgk-1* (c) using duplex PCR. The *Tuba6* housekeeping gene and a region rich in L1 elements (X141) were analysed as single PCR reactions. Following PCR the products were separated using DNA polyacrylamide gel electrophoresis (a) and quantified using a PhosphorImager (d-g). The relative enrichment of a genomic region is expressed as intensity of immunoprecipitated material (BOUND) divided by intensity of the INPUT. This controlled for variability in primer efficiency during multiplex PCR.

g). This controlled for variability in the primer efficiencies during the multiplex reactions.

Antisera against Hdac1 (figure 26d), Hdac2 (figure 26e), Hdac3 (figure 26f), and RbAp48 (figure 26g) precipitated levels of chromatin from all regions of *Xist*, *Pgk-1* and the coding region of *Tuba6* that consistently exceeded that recovered from the no-antibody control (NAC). The inability to precipitate levels of chromatin that surpassed that recovered from the no-antibody control from a region rich in L1 elements (X141) corresponding to the A3 Giemsa dark band on the mouse X chromosome (Nasir *et al.*, 1991) using any of the antibodies was more likely to be due to the stringent PCR conditions that were enforced in order to prevent cross amplification of more that one region. This is reflected by only minor differences between 75ng of INPUT material and the precipitated chromatin after 37 cycles.

Hdacs 1, 2, 3 and RbAp48 were shown to be distributed throughout the promoter and coding regions of *Pgk-1* and *Xist* in addition to the coding region of *Tuba6* in three independent experiments. Analysis of *Xist* reveals that the region with the biggest depletion in deacetylases at all of the time points analysed was Hx4, corresponding to exon I. This is in contrast to *Pgk-1* where if anything the deacetylases are more enriched in the coding domain than at the promoter. In undifferentiated cells there was enrichment for Hdacs 1, 2 and 3 at the X4u region of *Xist*. However, in general the deacetylases were found globally distributed across *Xist*, *Pgk-1* and *Tuba6* with no enrichment that exceeded two times that of an adjacent genomic region.

There appears to be a general drop in the association of all of the deacetylases at all of the genomic regions tested following differentiation. However, this is difficult to verify given that there is no internal standard within the multiplex reactions and *Tuba6*, a constitutively expressed housekeeping gene also follows the general trend of a fall in Hdac association following differentiation. It is apparent that the most informative analysis comes from the multiplex PCR reactions of *Xist* and *Pgk-1* whereby different regions of the same gene can be compared with confidence. However, to address the question concerning whether class I Hdacs are targeted to the X chromosome during ES cell differentiation the enrichments across the X-linked genes *Pgk-1* and *Xist* can be normalised against *Tuba6* (figure 27). For example in the event that Hdac 1 is driving global histone hypoacetylation on the inactive X chromosome one would expect a dramatic increase in the deacetylase enrichment at *Pgk-1* and *Xist* relative to *Tuba6* following differentiation. Analysis of figure 27 reveals that there are no significant changes in the enrichment of the class I Hdacs or RbAp48 following six days of differentiation, a time point of histone hypoacetylation along Xi (see section 3.1.1), suggesting that these changes are driven by another mechanism.

In conclusion Hdacs 1, 2, 3 and RbAp48 retain an intimate and ubiquitous association with the chromatin template throughout ES cell differentiation in a manner that does not correlate with the reported distribution of H4 acetylation at the *Xist* promoter region (O'Neill *et al.*, 1999) or along the chromatin of Xi. This is consistent with previous reports in yeast (Vogelauer *et al.*, 2000) and *Drosophila* (Breiling *et al.*, 2001). Additionally there was no apparent relationship between the enrichment of the

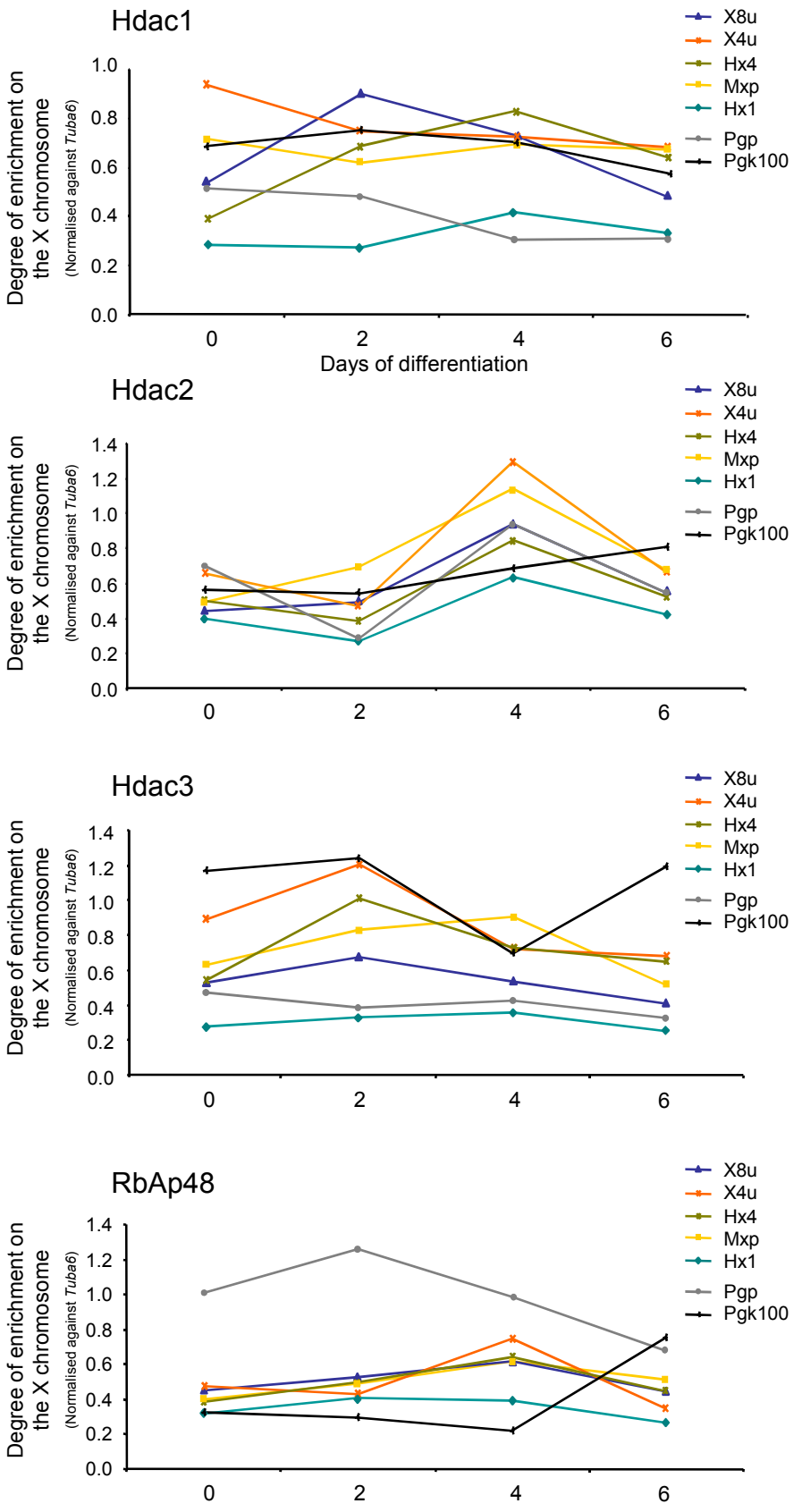

Figure 27. A graphical representation of the degree of enrichment of the class I Hdacs and RbAp48 on the X chromosome during ES cell differentiation. The enrichments across the X-linked genes *Xist* and *Pgk-1* were normalised against the autosomal housekeeping gene *Tuba6.*

class I deacetylases and the loss of H4 hyperacetylation 5' to the promoter region following differentiation (O'Neill *et al.*, 1999).

5.1.3 XChIP identifies a region 8kb upstream of Xist that is enriched for H3 di-methylated at lysine 4 and acetylated H3 in undifferentiated ES cells

It was my intention to further characterise the *Xist* promoter region with respect to acetylated H3 and di-methylated lysine 4 of H3 and examine how this compares to the reported H4 acetylation (O'Neill *et al.*, 1999). Therefore chromatin fragments were prepared from female undifferentiated ES cells and cells differentiated for 2, 4, or 6 days and immunoprecipitated using antisera against acetylated H3 (H3 AcK14) and H3Me_2K4. Using the technique of XChIP, antisera prepared against acetylated H4 consistently failed to immunoprecipitate levels of chromatin that exceeded the no-antibody control and was therefore not used in this study. The DNA recovered from the immunoprecipitated chromatin was analysed for its relative enrichment at the *Xist*, *Pgk-1*, and *Tuba6* regions in addition to a region rich in L1 elements (X141) as outlined in section 5.1.2. Each immunoprecipitation was performed at least twice and the results obtained using the multiplex PCR analysis were shown to be consistent following repeat experiments. Representative DNA polyacrylamide gels are shown in figure 28a.

Once again the region rich in L1 elements amplified by the primer pair X141 failed to reveal anything informative and displayed levels of chromatin that only just exceeded the no-antibody control (NAC). Whilst this may have been on account of its low levels of H3 AcK14 and H3Me_2K4 given previous reports showing a significant depletion of acetylated H4 in L1 elements (Johnson *et al.*, 1998; McCabe *et al.*,

1999), it was noticeable from the data in section 5.1.2 that the PCR conditions and the nature of the repeat element were not suited to this type of analysis.

However, the primer pairs amplifying *Xist*, *Pgk-1* and *Tuba6* revealed a clear distinction between the levels of chromatin precipitated using the antibodies and the no-antibody control (NAC). There was also notable variability in the distribution of both of these modifications across the *Xist* and *Pgk-1* genes.

Immunoprecipitations with antiserum to H3 di-methylated at lysine 4 (figure 28d) showed that in undifferentiated cells the *Xist* gene displayed high levels $H3Me_2K4$ in a region 8kb upstream of the *Xist* P1 promoter (PCR primer pair X8u). Similar levels of H3 di-methylated lysine 4 were also detected at the minimal promoter region (Mxp) and at the 5' end of exon I (Hx1). Perhaps the most striking feature of all was the dramatic drop in $H3Me_2K4$ that occurs between X8u and Mxp. Regions Hx4 and X4u, 2kb and 4kb upstream of the *Xist* P1 promoter respectively were significantly depleted in chromatin di-methylated H3 lysine 4. Indeed X8u displayed levels of $H3Me_2K4$ that was almost 8 times that of Hx4. A similar pattern of H3 di-methylation at lysine 4 was observed across *Xist* following 2, 4, and 6 days of differentiation.

There was a notable fall in $H3Me_2K4$ at X8u and Mxp relative to the housekeeping gene *Tuba6* following 2 days of differentiation. Indeed following 6 days of differentiation X8u had fallen over two fold relative to *Tuba6*. Note that whilst the *Tuba6* gene can be used as a comparison for the relative changes that occur in the *Xist*

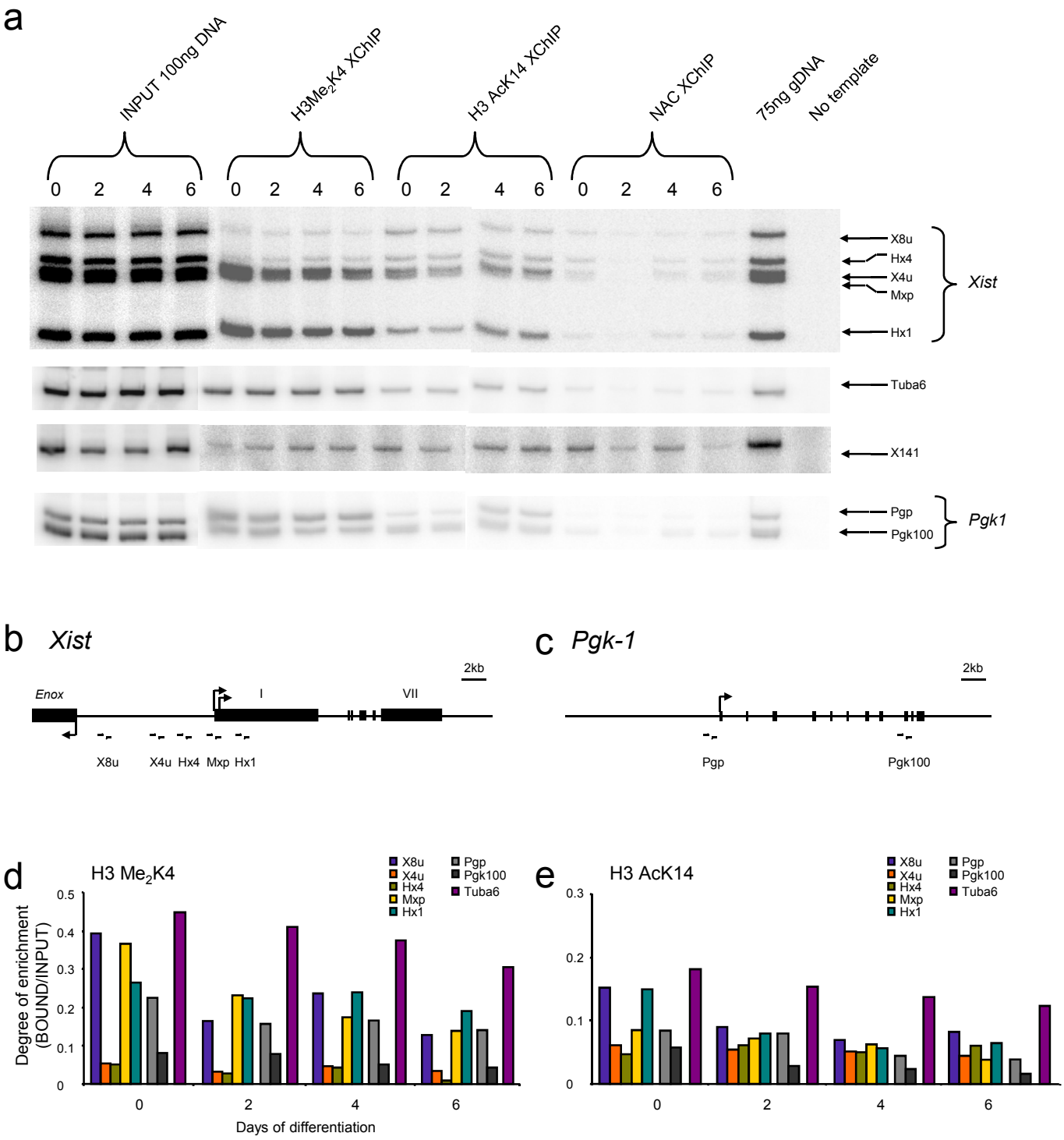

Figure 28. XChIP was performed on undifferentiated female ES cells or cells differentiated for 2, 4, or 6 days using affinity purified antisera against H3Me$_2$K4 and acetylated H3 (H3 AcK14). The immunoprecipitated DNA was analysed for the enrichment of specific genomic regions using PCR performed within the linear range. Five regions of *Xist* (b) were examined using pentaplex PCR and the promoter and coding regions of X-linked *Pgk-1* (c) using duplex PCR. The *Tuba6* housekeeping gene and a region rich in L1 elements (X141) were analysed as single PCR reactions. Following PCR the products were separated using DNA polyacrylamide gel electrophoresis (a) and quantified using a PhosphorImager (d, e). The relative enrichment of a genomic region is expressed as intensity of immunoprecipitated material (BOUND) divided by intensity of the INPUT. This controlled for variability in primer efficiency multiplex PCR.

and *Pgk-1* genes, the actual levels of H3Me$_2$K4 are not directly comparable. This is on account of the *Tuba6* primer set behaving in a manner that differed significantly from the *Xist* and *Pgk-1* primers. Indeed it was for this reason that the *Tuba6* gene was not amplified as part of a multiplex reaction.

The *Pgk-1* promoter region displayed enrichment for H3 di-methylated at lysine 4 relative to its coding domain at all of the time points analysed, as expected. The degree of enrichment varied from 2.0 fold after two days of differentiation to 3.3 fold at day six. The enrichment of H3Me$_2$K4 relative to *Tuba6* fell in both the coding and promoter regions following differentiation as expected, and was consistent with the data in section 3.2.2.

Immunoprecipitation experiments performed using antiserum against acetylated H3 revealed a similar distribution to that of H3Me$_2$K4 consistent with previous reports (Litt *et al.*, 2001). Undifferentiated cells displayed high levels of H3 acetylation at X8u and Hx1, that decreased relative to *Tuba6* following 2 days of differentiation. By day 2 X8u and Hx1 displayed levels of acetylated H3 that were higher but analogous to the three intervening regions. Following 4 days of differentiation all five of the *Xist* regions displayed comparable levels of H3 acetylation.

As expected, the chromatin of the *Pgk-1* promoter region was enriched for acetylated H3 relative to the coding domain, with the degree of enrichment varying between 1.5 fold in undifferentiated cells to 2.8 fold in cells differentiated for two days. The level of acetylated H3 fell in both the promoter and coding regions of *Pgk-1* relative to

Tuba6 following ES cell differentiation as expected, consistent with the data in section 3.1.3.

5.1.4 The distribution of the class I histone deacetylases shows no correlation with the distribution of acetylated H3 and H3Me$_2$K4 across the Xist promoter region

Given the internally controlled multiplex PCR step, *Xist* can be used as an example to compare the distribution of the histone deacetylases (Hdac1; figure 29c) with acetylated H3 (figure 29b) and H3Me$_2$K4 (figure 29a). Hdac1 was chosen purely to represent the general distribution of the class I deacetylases across *Xist*. It is of interest to compare H3Me$_2$K4, despite the deacetylases having no reported role in the deposition or removal of this modification because of recent data showing significant correlation with the genomic distribution of acetylated H3 (Litt *et al.*, 2001). Indeed this study also suggests that the two modifications have a similar genomic distribution. In undifferentiated ES cells there appears to be a direct correlation between the relative enrichment of Hdac1 and chromatin depleted in acetylated H3 and H3Me$_2$K4 at region X4u. However, the enrichment for Hdac1 is lost following two days of differentiation whilst X4u continues to be depleted in acetylated H3 and H3Me$_2$K4 until day 6, the last time point analysed. In addition the fall in H3 acetylation and H3Me$_2$K4 at X8u does not correlate with any specific enrichment of Hdac1 at any of the day points analysed suggesting that this change is driven by a different mechanism.

In conclusion there is no obvious correlation between the distribution of the class I Hdacs and the histone modifications studied here suggesting that the patterns of

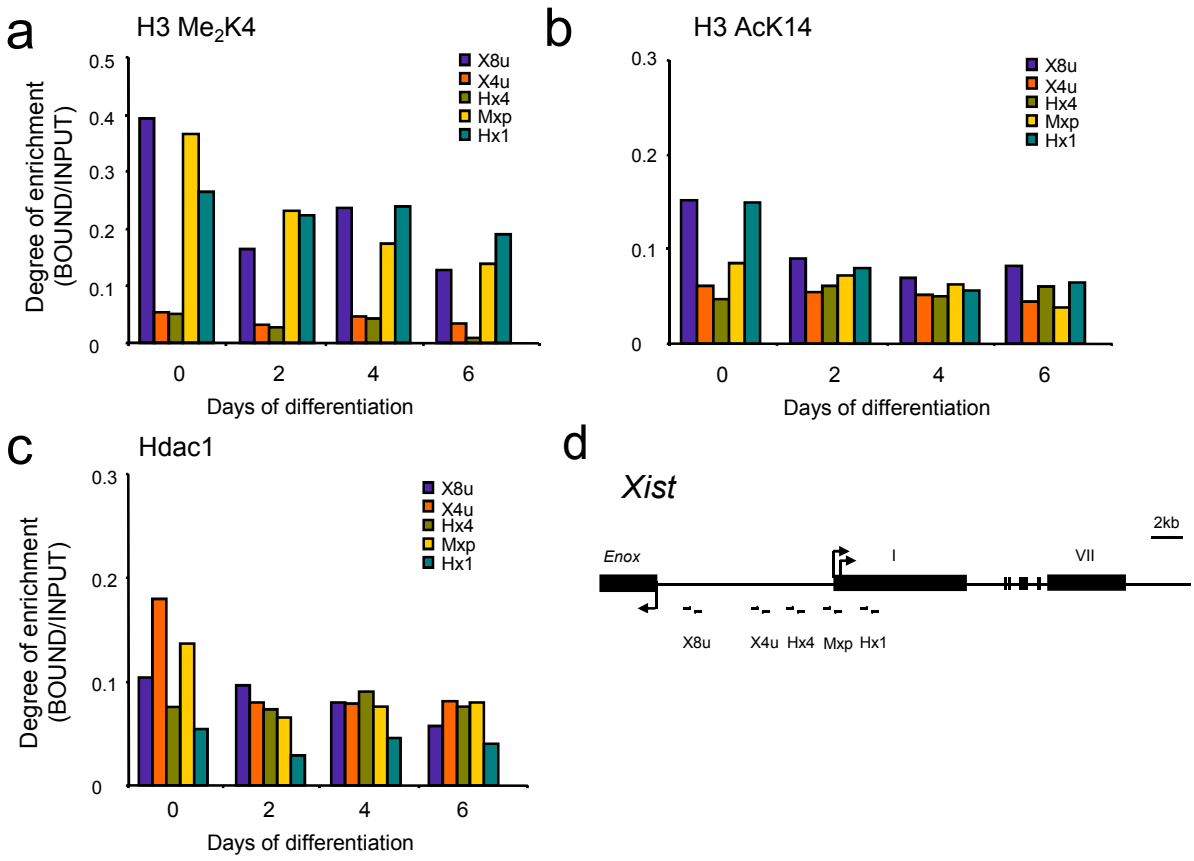

Figure 29. Analysis of the correlation between the distribution of the class I histone deacetylases, here represented by Hdac1 (c) and the histone modifications; acetylated H3 (b) and H3 Me_2K4 (a) across the *Xist* gene. The positions of the PCR primer pairs relative to *Xist* are shown in d.

modification are established by an as yet unidentified mechanism that occurs in a background of global histone deacetylase association.

6 DISCUSSION – CHAPTER SIX

6.1 HISTONE ACETYLATION AND X CHROMOSOME INACTIVATION

6.1.1 Concurrent histone deacetylation – a maintenance role in X chromosome inactivation

I have examined the global deacetylation that is associated with X chromosome inactivation in mouse embryonic stem cells. By immunolabelling metaphase chromosomes prepared from ES cells differentiated for specified numbers of days I have established the temporal pattern of H2A, H2B, H3 and H4 deacetylation. All four core histones were found to become deacetylated on the inactive X chromosome within a time period of two days following three to five days of differentiation. The loss of acetylated H4 has been analysed previously by Keohane *et al.,* (1996) and by an independent group using the same method (Mermoud *et al.*, 1999), both showing H4 deacetylation within the same time period as in this study. The data in this report supports the concurrent deacetylation of all four core histones as a maintenance role in the process of X chromosome inactivation. Indeed by day 2 of differentiation, a time point when the frequency of metaphase spreads with an underacetylated X chromosome is low; an up regulation of *Xist* RNA, a late replicating X chromosome and the silencing of X-linked genes are all readily detectable (Keohane *et al.*, 1996). In contrast to the data presented in this report, Heard *et al.,* (2001) have shown the timing of H3 and H4 deacetylation in ES cells to be significantly earlier. They showed a detectable hypoacetylation of H3 as early as day 1, and the hypoacetylation of H4, a little later following 2 days of differentiation. Heard *et al.,* (2001) suggest that the deacetylation of H3 and H4 are regulated by different histone deacetylases and occur during a time period when genes on the inactive X chromosome are subject to transcriptional silencing. Indeed it is not unreasonable to suggest that the histone

modifications are differentially regulated (Gregory *et al.*, 2001). However, the technical approach made in this report and by others (Keohane *et al.*, 1996; Mermoud *et al.*, 1999) differs significantly from the aforementioned study in that metaphase as opposed to interphase nuclei were scored for the presence or absence of a pale staining chromosome. Additionally the antiserum used to detect H3 hypoacetylation was specific for acetylated lysine 14 as opposed to lysine 9 in Heard *et al.,* (2001). It is plausible that lysines 9 and 14 are differentially regulated given that lysine 9 of H3 has the potential to be either methylated or acetylated; with deacetylation being a requirement for subsequent lysine 9 methylation (Rea *et al.*, 2000), an early event in the process of X inactivation (see section 6.2). However, the data in this report supports a deacetylation event that is not histone or lysine specific.

In our Birmingham laboratory we induce the differentiation of ES cells by the removal of LIF. However, it is also common practise to supplement the media with all-*trans*-retinoic acid during the first few days of differentiation (Smith, 1991). Indeed the later approach was used in the study by Heard *et al.,* (2001) and one might suggest that the earlier timing of H3 and H4 deacetylation was simply a consequence of a more synchronous differentiation induction such that the ES cells reached the time point of H3/4 deacetylation earlier. However, the Pgk12.1 ES cell line has been described previously and shown to successfully differentiate following the removal of LIF as determined by the down regulation of *Oct4* RNA levels (Norris *et al.*, 1994), an early marker for ES cell differentiation (Palmieri *et al.*, 1994).

Interestingly the percentage of metaphase spreads displaying a hypoacetylated chromosome never exceeded 50%, even after seven days of differentiation. This may

have been a consequence of the technique used given that I was scoring metaphase spreads for the presence of a negative mark i.e. spreads containing a pale stained, hypoacetylated chromosome. However, similar low percentages have been observed in the past using the Kanda staining method which allows the inactive X chromosome to be identified as a positive marker (Kanda, 1973; Rastan and Robertson, 1985). Kanda staining allows Xi to be identified based on its differential staining due to its degree of compaction. It is plausible that the same X chromosomes are acetylated or hypoacetylated from one cell cycle to the next; thereby lowering the percentage significantly. However, this is unlikely given the chromatin immunoprecipitation (NChIP) data reported in this study and previously (Keohane *et al.*, 1998) showing an almost two fold drop in the H4 acetylation of four X-linked genes following seven days of differentiation. This can only be accounted for if all of the cells undergo X chromosome inactivation and deacetylate one of their two X chromosomes.

6.1.1.1 The deacetylation of the inactive X chromosome occurs during a single cell cycle

Given the low percentage (<1%) of metaphase spreads displaying a chromosome that was pale along a proportion of its length, it seems likely that the process of concurrent histone deacetylation on the inactive X chromosome occurs during a single cell cycle. This is in contrast to the spread of *Xist* RNA on the inactive X which can be seen to spread from the *Xic* over several cell generations (Panning *et al.*, 1997) and to the progressive deacetylation of the centric heterochromatin observed in this study and previously (Keohane *et al.*, 1996) to occur over a period three or four days following the induction to differentiate. Whether the process of global histone deacetylation on the inactive X centres on the recruitment of histone deacetylase complexes (see

section 6.4) or through the selective proteolytic cleavage of the histone tails remains to be tested. Indeed the selective cleavage of H3 N-termini has been shown to occur *in vivo* in *Tetrahymena* (Allis *et al.*, 1980). This would explain the absence of immunostaining on the inactive X chromosome; owing to the unavailability of the antigen. However, this would require the removal of a significant portion of the histone tail given that the antibody against acetylated H3 recognises acetyl-lysine at position 14. Indeed the selective cleavage of the H3 tail can be discounted given a report documenting the presence of labelling on the inactive X chromosome using an antibody specific for the unacetylated form of H3 (Boggs *et al.*, 1996). This result also confirms that the absence of staining on the inactive X chromosome is not simply a consequence of antigen occlusion due to the binding of non-histone proteins, something that should be considered when using antibodies as molecular tools.

6.1.2 Trichostatin A establishes periods of "sensitivity" and "resistance" to the inhibition of the appearance of a hypoacetylated Xi in ES cells

In this study I have analysed the sensitivity of the appearance of a hypoacetylated Xi to the histone deacetylase inhibitor Trichostatin A (TSA) in ES cells. By differentiating ES cells in culture medium supplemented with low levels of the inhibitor I have shown that by day 8 of differentiation the percentage of metaphase spreads displaying a hypoacetylated Xi was significantly reduced, consistent with published data (O'Neill *et al.*, 1999). In contrast if the inhibitor was supplemented into the medium after three days of differentiation, the percentage of spreads with a hypoacetylated Xi was not significantly different from control cells grown in the absence of the inhibitor. This clearly establishes time periods when supplementing the medium with the inhibitor generates sensitivity or resistance to the abolition of a

hypoacetylated Xi after 8 days of differentiation. The pooled data suggests that the shift from TSA "sensitivity" to "resistance" occurs between days two and three when the frequency of spreads with a hypoacetylated Xi at day 8 dramatically increases and is not significantly affected by the presence of the inhibitor (figure 30).

The timing of the shift from TSA "sensitivity" to "resistance" compares well with published data from Wutz and Jaenisch, (2000) who studied the silencing capability of *Xist* transgenes on adjacent reporter genes using ES cells. It was shown that *Xist* could cause reversible gene inactivation by inducing its expression during the first two days of ES cell differentiation, i.e. gene reactivation occurred following the switching off of *Xist* expression (Wutz and Jaenisch, 2000). In contrast when *Xist* was expressed during the first three days of differentiation and switched off, the gene silencing of the reporter genes was shown to be irreversible. This report together with my data suggests that following three days of differentiation there are factors present that permit a commitment to X inactivation that cannot be reversed by either the switching off of *Xist* or the use of inhibitors such as TSA. The insensitivity of Xi to TSA following three days of differentiation is difficult to explain. However, the recruitment of a Sir2 deacetylase by Xi and subsequent core histone deacetylation may explain this finding in light of the group's resistance to the inhibitor (Imai *et al.*, 2000). An alternative explanation lies in the possibility that there a replacement mechanism that serves to introduce hypoacetylated histones onto Xi eliminating the requirement for the enzymatic removal of the acetyl groups. It follows that a mechanism protecting Xi from re-acetylation would serve to explain the insensitivity of Xi to Hdac inhibitors in female somatic cells.

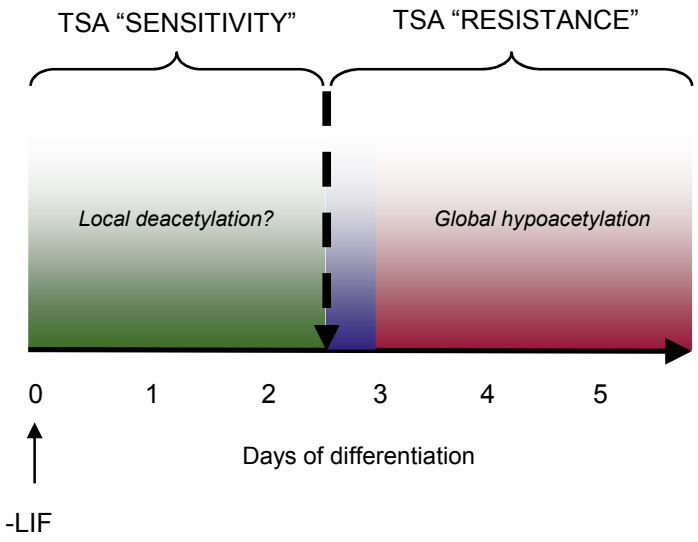

Figure 30. Experiments analysing the effect of the histone deacetylase inhibitor Trichostatin A on the appearance of a hypoacetylated Xi establish periods of TSA "sensitivity" (days 0-2) and "resistance" (days 3+) during ES cell differentiation. Supplementing the medium with the inhibitor prior to day three of differentiation inhibits the appearance of a hypoacetylated Xi at day 8. However, adding the inhibitor after day 2 (dashed arrow) results in the appearance of a hypoacetylated Xi at a frequency similar to control cells.

It is noticeable that the shift from TSA sensitivity to resistance occurs prior to the global deacetylation discussed in section 6.1.1 which occurs at day's three to five of differentiation. This suggests that in the first few days of differentiation there are TSA sensitive events, mandatory for the steps that lead to a hypoacetylated Xi. Indeed although the global deacetylation of the inactive X chromosome occurs relatively late in the process of X inactivation, we cannot discount the importance of local deacetylation events. For example the H4 deacetylation 5' of the *Xist* gene, shown to be detectable as early as day two of differentiation (O'Neill *et al.*, 1999). However, it remains to be seen whether this deacetylation event is sensitive to TSA or indeed important in the process of X inactivation. Data presented here certainly eliminates the possibility that class I Hdacs are recruitment to this region. This data also suggests that once a hypoacetylated Xi has become established, TSA cannot reverse the process to generate an acetylated chromosome. This was evident in human lymphoblastoid and PMEF cells where concentrations of TSA capable of histone hyperacetylation consistently failed to re-acetylate the inactive X chromosome (data not shown; Jeppesen and Turner, 1993). This is surprising given the dynamic equilibrium that exists between the histone acetyltransferases (HATs) and the histone deacetylases (HDACs). Indeed the inactive X chromosome has previously been shown to be remarkably resistant to TSA (Csankovszki *et al.*, 2001), although this study analysed the degree of gene reactivation by the inhibitor.

It remains unlikely that TSA causes the aberrant expression of genes responsible for negatively regulating the process of X inactivation (as proposed in male cells), given the low concentrations of the inhibitor used and the relatively small number of genes reactivated *in vivo* using similar deacetylase inhibitors (Butler *et al.*, 2002).

6.1.3 The inactive X chromosome is deacetylated at the coding and promoter regions of X-linked genes during ES cell differentiation

In collaboration with Dr. L. P. O'Neill I have shown that all four of the core histones are deacetylated on the inactive X chromosome using NChIP. This was largely as expected and was consistent with the data within this report and previous publications (Keohane *et al.*, 1998; O'Neill *et al.*, 1999). Moreover we have shown that both the coding and promoter regions are deacetylated on the mouse X chromosome following seven days of differentiation. This data demonstrates how native chromatin immunoprecipitation (NChIP) can be used to detect two fold differences in the level of histone acetylation. Given the level of acetylation at a particular genomic region is assayed as a BOUND (chromatin enriched for the histone modification) to UNBOUND (chromatin depleted) ratio we can have confidence in the smallest of differences generated using this tightly controlled assay.

The data presented here shows the loss of core histone acetylation across both promoter and coding regions of Xi. This in contrast to recently published data documenting a promoter-specific hypoacetylation of X-inactivated genes (Gilbert and Sharp, 1999). That is to say the difference between the active and inactive X chromosomes was the degree of H3 and H4 acetylation at the promoter regions of X-linked genes. The study made by Gilbert and Sharp, (1999) differed significantly from the one made here in that somatic cell hybrid cell lines were used containing either an active or an inactive human X chromosome. Additionally the technique of cross-linked chromatin immunoprecipitation (XChIP) was employed. Whilst we cannot discount the fact that human and mouse inactive X chromosomes are hypoacetylated to different degrees, it is difficult to imagine how Xi can stain differentially at

metaphase purely as a result of promoter-specific hypoacetylation. Given this, it was fortuitous to have access to the same somatic cell line. Indeed the immunolabellings in section 3.2.4 were performed on the same hybrid line used by Gilbert and Sharp, (1999). There is obvious hypoacetylation for H4 and all of the other core histones (data not shown) in this cell line. However, the degree of "paleness" that distinguished Xi was never as pronounced as in the human lymphoblastoid cell lines used in this study; perhaps significant in view of a proposed promoter-specific hypoacetylation.

It is difficult to reconcile the differences between the work presented here and by Gilbert and Sharp, (1999) based on the immunoprecipitation technique. Whilst native (NChIP) and cross-linking (XChIP) chromatin immunoprecipitation differ significantly in the preparation of chromatin, I have shown using XChIP that the level of H3 acetylation (and $H3Me_2K4$) of the X-linked gene *Pgk-1* falls in both coding and promoter regions during differentiation. Therefore it seems most likely that the discrepancy reflects a relaxation of the requirement for maintenance of the silent state in hybrid cell lines.

6.2 HISTONE METHYLATION AND X CHROMOSOME INACTIVATION

6.2.1 The inactive X chromosome is differentially methylated at lysines 4 and 9 of H3

The female inactive X chromosome of eutherian mammals serves as an excellent example of heritable, transcriptionally silent chromatin. Using this as an example I have analysed the histone methylation code that distinguishes the human Xi cytogenetically. I was interested in the functional significance of both the site (lysine 4 or 9) and level of methylation (i.e. mono-, di-, or tri-). I have shown that Xi is depleted for H3 di-methylated at lysine 4 and H3 *tri*-methylated at lysine 4. In contrast I have demonstrated that Xi retains H3 di-methylated at lysine 9 ($H3Me_2K9$) at levels at or above the rest of the genome. The data shown in this report is consistent with the established relationship between the site of methylation and transcriptional competence (Kouzarides, 2002). Whilst this does not support the hypothesis of a functional significance to the level of lysine methylation, immunolabelling experiments using antiserum shown by ELISA and western blot to recognise H3 tri-methylated at lysines 4 and 9 ($H3Me_3K4/9$) suggested that the inactive X chromosome is depleted for $H3Me_3K9$. This is in contrast with the data shown here and elsewhere (Boggs *et al.*, 2002; Peters *et al.*, 2002) demonstrating the retention of di-methylated lysine 9. Taken at face value this suggests that the histone code extends to the level of lysine methylation. However, subsequent experiments using an antibody against tri-methylated lysines 9 and 27 of H3 ($H3Me_3K9/27$) suggest that tri-methylated lysine 9 is retained at levels at or above the rest of the genome. This is consistent with published data (Cowell *et al.*, 2002) but directly contradicts the findings discussed above. This raises the question concerning why the antisera support opposing scenarios; depletion ($H3Me_3K4/9$) or retention ($H3Me_3K9/27$) of tri-methylated lysine 9 of H3.

6.2.2 Depletion or retention of tri-methylated lysine 9 of H3 on Xi?

The cross-reactivity of both antisera makes it impossible to construct any firm conclusions. However, one might speculate that the published data from Cowell *et al.,* (2002) is correct and that the depletion on Xi shown using the antiserum against $H3Me_3K4/9$ is a consequence of reduced affinity for tri-methylated lysine 9 on whole chromosomes, leaving the immunolabelling of tri-methylated lysine 4; a modification depleted on Xi. Indeed it has been suggested that ELISA is not always a good determinant of antibody specificity *in vivo* (Suka *et al.*, 2001); albeit in reference to specificity in the technique of cross-linking chromatin immunoprecipitation. However, in light of the data in section 3.2.2 showing a clear depletion of immunostaining on Xi, I do not favour this view as this would suggest absolutely no recognition of tri-methylated lysine 9 on whole chromosomes. Furthermore the results obtained from the immunostaining of metaphase chromosomes prepared from ES cells did not directly mimic those produced using antiserum specific for $H3Me_3K4$. The pale staining chromosome was notable for the variability in its degree of paleness; something not observed using the antiserum specific for $H3Me_3K4$. This in itself suggests that there is recognition of an epitope aside from tri-methylated lysine 4 of H3.

Results obtained using the antiserum against $H3Me_3K9/27$ showed the retention of tri-methylated lysine 9 and/or 27 of H3 on Xi at levels at or above those found in the rest of the genome. It is difficult to distinguish the enrichment for tri-methylation based on the individual lysine due to it being a positive marker. Furthermore we cannot make assumptions of the methylation status of lysine 27 of H3 on Xi. It has recently been shown that methylation at lysine 27 of H3 co-localises with genes repressed by

Polycomb group proteins in *Drosophila* suggesting that methylation at this lysine may be involved transcriptional repression (Cao *et al.*, 2002). In view of this one might infer that Xi is likely to retain significant levels of tri-methylated lysine 27 of H3. This however remains untested due to the unavailability of antiserum. It should be remembered that the antiserum against H3Me_3K4/9 displayed no detectable recognition of lysine 27 despite a similar antigenic motif (A. J. Bannister; data not shown). In view of this I support the idea that Xi is depleted in tri-methylated lysine 9 but specifically retains its di-methylated equivalent supporting a role for the level of lysine methylation in the histone code. Furthermore I suggest that the results obtained using the antiserum against H3Me_3K9/27 can be explained by its recognition of levels of lysine 27 tri-methylation at or above those found in the rest of the genome. One might interpret the data presented by Cowell *et al.,* (2002) showing an enrichment for tri-methylated lysine 9 of H3 on Xi in a similar manner. However, this antiserum remains untested by ELISA or western blot by our Birmingham laboratory due to its unavailability.

6.2.3 Specific enrichment of di-methylated lysine 9 of H3 on the inactive X chromosome?

Whilst the findings here are consistent with data published subsequent to this study showing differential di-methylation at lysines 4 and 9 of H3 on the inactive X chromosome (Boggs *et al.*, 2002; Peters *et al.*, 2002), there are some important differences. Both publications claim to consistently detect Xi based on its elevated levels of lysine 9 di-methylation at metaphase. This is direct contrast to the data shown here documenting an enrichment on Xi in only a fraction (~10%) of metaphase spreads and only when using the antiserum from Upstate. Whilst these brightly labelled chromosomes were subsequently shown to be one of the two X chromosomes using

DNA-FISH it was a concern that the enrichment was detected at such low frequency. The enrichment detected by the Upstate H3Me_2K9 antiserum can be in part explained by the influence of adjacent acetylation at lysine 14. I have shown using peptide inhibition that a synthetic peptide modified at both of these residues displays significantly less inhibition to the binding of metaphase chromosomes than the immunising peptide; di-methylated at lysine 9 of H3. This is consistent with previous data documenting the influence of adjacent histone modifications over the binding of antisera to their cognate antigens (Turner *et al.*, 1989; Clayton *et al.*, 2000). However, this does not explain the relative ubiquity of immunolabelling observed across all of the chromosomes when compared to the published data. It remains possible that the capture settings of the camera associated with the fluorescence microscope were dissimilar to those used in this study such that differences in fluorescence were more readily detectable. Indeed differences in the degrees of fluorescence of individual chromosomes become all the more prominent following artificial changes to the level of the background. This is illustrated in figure 31. By analysing each individual chromosome against its degree of fluorescence it can be shown that a background level of i will report more significant differences than a background level of ii. This would certainly explain the discrepancy between the biochemical data reporting lysine methylation as an extremely common histone modification (Thomas *et al.*, 1975; Strahl *et al.*, 1999) and the selective staining observed by the recent publications (Mermoud *et al.*, 2002; Peters *et al.*, 2002). This is most pronounced in the study by Mermoud *et al.,* (2002) where the immunolabel was shown to be strictly confined to the centric

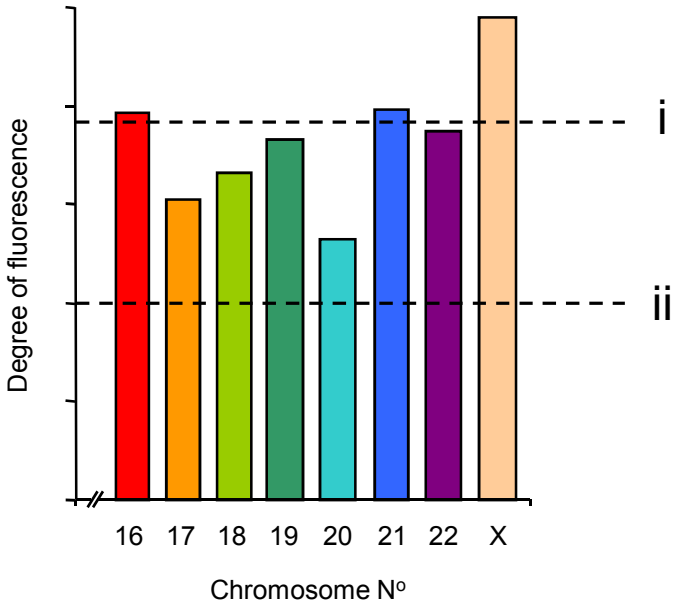

Figure 31. An illustration of how changes to the level of background fluorescence (i and ii) can influence the interpretation of results obtained using immunofluorescence microscopy

heterochromatin and Xi. Once again this is surprising given reports demonstrating significant enrichment of $H3Me_2K9$ across euchromatic regions such as the β-globin locus (Litt *et al.*, 2001). The study by Mermoud *et al.,* (2001) used antiserum raised against a branched hexameric peptide ($H3Me_2K9_{BCH}$). It has subsequently been shown that this antibody has selective recognition of chromatin in a more condensed state; where the histone tails are in a closer configuration thereby mimicking the peptide (Maison *et al.*, 2002). Therefore whilst the antiserum correctly recognises $H3Me_2K9$ when assaying specificity using western blotting, there is preferential recognition of condensed chromatin when applied to whole nuclei. I have shown using ES cells that this is dependent on cross-linking prior to immunolabelling, suggesting that formaldehyde assists the selective staining by bringing the histone tails into a more closed configuration. In view of this one might speculate that the appearance of a brightly stained chromosome during ES cell differentiation as shown by Mermoud *et al.,* (2002) may simply reflect changes in the chromatin compaction of Xi rather than the appearance of the $H3Me_2K9$ antigen. This result also questions the epitope specificity of the antisera under cross-linking conditions; something that cannot be determined by western blot analysis.

The proteins responsible for binding Xi and maintaining transcriptional quiescence are yet to be identified. In light of the recent data showing a specific enrichment for lysine 9 di-methylation on Xi a putative candidate emerged as HP1. Heterochromatin protein 1 is capable of binding H3 di- and tri-methylated lysine 9 of H3 *in vitro* (Bannister *et al.*, 2001; Jacobs and Khorasanizadeh, 2002; Nielsen *et al.*, 2002). However, Heard *et al.,* (2001) found no evidence supporting the association of HP1 with the inactive X chromosome and suggests that an as yet unidentified HP1-like protein, possibly with

specificity towards di-methylated lysine 9 alone, may bind to the facultative heterochromatin of Xi.

In conclusion I have defined the histone methylation status of the inactive X chromosome in female somatic cells. Xi was found to have a specific epigenetic code whereby the retention of H3 lysine 9 di-methylation at levels at or above those found in the rest of the genome was shown to operate in a background of core histone hypoacetylation and a depletion of di- and tri-methylated lysine 4 of H3.

6.2.4 Histone methylation hot spots on the human inactive X chromosome

The inactive X chromosome was found to retain lysine 4 methylation at two localised hot spots on Xi which labelled strongly using antisera against $H3Me_2K4$, $H3Me_3K4$ and $H3Me_3K4/9$. It is likely that one of the regions corresponds to the pseudoautosomal region (PAR) at the distal end of the p arm, a region rich in genes shown to escape X chromosome inactivation in humans (e.g. *MIC2*, *STS*). The other region is located near Xq22-25 and is likely to correspond to the localised staining shown in Boggs *et al.,* (2002) using antiserum against $H3Me_2K4$. Interestingly this region has also been shown to display a specific enrichment for the histone variant macroH2A1.2 (Chadwick and Willard, 2002) at metaphase but does not contain any genes known to escape X inactivation (Carrel *et al.*, 1999). Both of these regions were also labelled using antiserum against acetylated H2B, but not with antisera against acetylated H3 and H4. This is consistent with data presented in Boggs *et al.,* (2002) and suggests that there are domains on the Xi that contain unique patterns of histone modifications. Hot spots have been observed in the past at both regions (PAR and Xq22) using antisera against acetylated H4, but were only reproducibly detected after culturing in the presence of

histone deacetylase inhibitors Trichostatin A and Sodium Butyrate (Jeppesen and Turner, 1993). Indeed Boggs *et al.,* (1996) were unable to detect residual acetylated H3 staining, consistent with the data presented here. However, translocated cell line SP did show localised staining on Xi using antisera against acetylated H3 and H4 suggesting that the human Xi harbours the potential to be acetylated at these regions.

It was noticeable that Xi in metaphase spreads prepared from mouse PMEFs or ES cells never exhibited the residual staining observed in the human lymphoblastoid cells, aside from occasional labelling of the PAR. This was most pronounced in PMEFs where Xi was only detectable using the DAPI (DNA) counterstain. This may have been on account of the murine Xi having fewer genes that escape X chromosome inactivation (Ashworth *et al.*, 1991). In contrast Jeppesen and Turner, (1993) have reported the localised staining of at least four regions on the mouse Xi using antisera against acetylated H4. However, once again this was dependent on culturing the cells in the presence of histone deacetylase inhibitors prior to immunolabelling.

6.2.5 Histone modifications associated with facultative heterochromatin persist in somatic cell hybrids

By performing immuno-FISH I have shown that a Chinese hamster ovary cell line containing a human inactive X chromosome maintains the expected global histone acetylation and methylation patterns on Xi as predicted by mouse and human cells. I have also reported a novel finding in the form of depletion on Xi for H4Me$_2$K20. This finding is difficult to explain given recent data reporting its presence in regions of silent chromatin (Nishioka *et al.*, 2002). Nishioka *et al.,* (2002) found depleted levels on the *Drosophila* male X chromosome. The *Drosophila* male X chromosome is often

described as hyperactive because it displays two fold higher levels of gene transcription to allow for dosage equivalence between the sexes. The *Drosophila* X has been shown to have elevated levels of acetylated lysine 16 of H4 (Turner *et al.*, 1992). In view of the apparent inverse relationship between H4 AcK16 and H4Me$_2$K20 Nishioka *et al.,* (2002) speculate that methylation at lysine 20 serves to preclude neighbouring acetylation on the H4 tail. However, the inverse distribution of the two histone modifications could also be explained by an occlusion of antibody binding by acetyl-lysine at position 16, something not examined by the authors. Even if the H4Me$_2$K20 histone modification is particularly enriched in silent chromatin one cannot exclude the possibility that its exclusion from the inactive X chromosome in female mammals is part of an elaborate epigenetic code defining facultative heterochromatin. Indeed paradoxical combinations of histone modifications have been observed upstream of the *Xist* gene with enrichments of H4 acetylation (O'Neill *et al.*, 1999) and H3 lysine 9 di-methylation (Heard *et al.*, 2001). It was unfortunate that this antiserum consistently failed to give satisfactory results on metaphase spreads prepared from mouse and human cells. This may be in part due to the position of the modification in relation to the nucleosome. Lysine 20 of H4 is close to the globular domain of the nucleosome core particle and I suggest that the poor antibody efficiency may be due to the restricted accessibility of the di-methyl lysine 20 antigen.

The persistence of the histone modifications that characterise Xi was interesting given the failure of *XIST* RNA to associate with Xi in this cell line (Hansen *et al.*, 1998). It was speculated that the somatic cell hybrids lack components needed for *XIST* co-localisation. However, the five translocated lymphoblastoid cell lines used in this study also failed to show correct *XIST* co-localisation (A. J. Sharp, L. Hall, J.

Lawrence, P. Jacobs; unpublished) suggesting that this maybe a property of transformed cell lines. What is clear is that the global histone modifications that distinguish Xi cytogenetically are not dependent on continued *XIST* association. It was also apparent that the localised histone methylation hot spots on the human Xi in the lymphoblastoid cell lines were never present in the hybrid line. Once again this may reflect a relaxation in the requirement for maintaining the epigenetic code of Xi at a more local level. However, as the hamster cells were male it suggests that the molecular machinery responsible for maintaining Xi globally depleted in histone acetylation, di- and tri-methylation at lysine 4 of H3 and a specific retention of lysine 9 di-methylation are present in both sexes.

Using the extended hamster chromosomes from this cell line I have analysed the relationship between DAPI-dense G bands and histone methylation. Whilst di-methylated lysine 9 of H3 co-localised with G bands, consistent with a subsequent publication (Cowell *et al.*, 2002), di-methylated lysine 4 showed an inverse correlation with G bands, being enriched in regions depleted for the DAPI counterstain. In contrast antiserum against tri-methylated lysines 4 and 9 of H3 ($H3Me_3K4/9$) showed an altogether different staining pattern with examples of strongly stained interband and G band regions. This suggests that the distribution of the tri-methylated isoforms of H3 differs from that of their di-methylated equivalents. It was noticeable that the H4 acetylation pattern in relation to G bands was never as conclusive as previously published by Jeppesen and Turner, (1993). However, once again the histone acetylation signal was amplified through the use of inhibitors. From the data presented here it can be concluded that $H3Me_2K9$ and $H3Me_2K4$ are good

correlates of AT rich, G banded regions and GC rich, R banded regions respectively as defined by the DAPI counterstain.

6.2.6 The loss of H3Me$_3$K4 from Xi is an early event in ES cell differentiation and precedes the loss of H3Me$_2$K4 which occurs concurrently with core histone deacetylation – Functional significance to the level of lysine methylation

Using ES cells I have analysed the temporal events leading to the histone methylation code shown in this study to distinguish Xi cytogenetically. Whilst the loss of di-methylated lysine 4 of H3 occurred during a time period of core histone deacetylation (days 3-5), the loss of tri-methylated lysine 4 as determined by two separate antisera (H3Me$_3$K4 and H3Me$_3$K4/9) was shown to be a relatively early event, detectable as early as day one of differentiation.

Firstly and perhaps most importantly this data provides evidence of an active de-methylation mechanism, whereby methyl groups are removed from Xi during ES differentiation. Whilst no histone demethylases (HDMs) have been identified to date, we cannot discount the enzymatic removal of methyl- groups from Xi. Nor can we ignore the importance of adjacent modifications that may influence methylation at lysine 4. For example in *Schizosaccharomyces pombe* the removal of acetylation at lysine 14 of H3 by Clr3 is required for subsequent methylation at lysine 9 by Clr4 (Nakayama *et al.*, 2001). Additionally ubiquitination at lysine 123 of H2B has been shown to mediate methylation at lysine 4 of H3 (Sun and Allis, 2002). In the knowledge that adjacent modifications can influence the deposition of methyl- groups one might suggest that di-methylation at lysine 9 of H3 inhibits methyl-transferase activity towards lysine 4. This would explain the loss of tri-methylation at lysine 4 in

view of the reported timing of di-methylation at lysine 9 (Heard *et al.*, 2001) which largely mimics that of H3Me$_3$K4. It follows that an additional modification several days later in differentiation may prevent the addition of di-methyl groups to lysine 4 thereby giving the impression of a loss of the modification from Xi.

We also cannot discount the possibility that di- and tri-methylation at lysine 4 are simply lost by a gradual "dilution" through each cell division. However, I do not favour this hypothesis given Xi never displayed differing degrees of lysine 4 methylation using antisera against H3Me$_2$K4 and H3Me$_3$K4, something that one would predict given this mechanism. Metaphase spreads could always be categorised based on the presence of a pale staining chromosome. In contrast and in support of this hypothesis metaphase spreads labelled with the antisera against H3Me$_3$K4/9 did contain a chromosome that differed in its degrees of paleness. As discussed earlier I attribute this to the retention of lysine 9 tri-methylation early in the ES cell differentiation making the scoring of metaphase spreads based on the presence of a chromosome depleted for lysine 4 tri-methylation difficult. This in itself suggests that the antiserum is not recognising tri-methylated lysine 4 alone and raises the question regarding <u>when</u> lysine 9 tri-methylation is lost from Xi. However, this requires antiserum specific for H3Me$_3$K9 with no cross-reaction against other lysines or levels of methylation.

In conclusion the data here supports two independent de-methylation mechanisms; one early in differentiation removing the tri-methylated isoform of lysine 4 and one several days later removing the di-methylated equivalent. It remains to be determined whether the loss of mono-methyl lysine 4 occurs subsequently due to the unavailability of antiserum at present.

The work here firmly establishes functional significance to the level of lysine methylation in the epigenetic code hypothesis. Whilst the analysis of Xi in human lymphoblastoid cells did not reveal any conclusive differences between the di- and tri-methylated isoforms given the cross-reaction of antisera, the data obtained here from the immunolabelling of female ES cells suggests that the di- and tri-methylated isoforms of lysine 4 are functionally distinct. The timing of the loss of di-methylation at lysine 4 of H3 occurs during a time period of core histone deacetylation on Xi suggesting that the modifications may be intrinsically linked. It is plausible that the enzymes responsible for removing lysine 4 di-methylation from Xi are targeted to the chromatin by an epigenetic mark in the form of a depletion of core histone acetylation.

In contrast the loss of tri-methylation at lysine 4 of H3 occurs early in the process of X chromosome inactivation during a time period of gene silencing, late replication, *Xist* up-regulation (Keohane *et al.*, 1998) and suggests that it is the depletion of tri-methylated lysine 4 which is the best determinant of transcriptionally silent genes. This is entirely consistent with a recent report (Santos-Rosa *et al.*, 2002) that suggests that it is the presence of tri- rather than di-methylated lysine 4 that defines an active state of gene expression. This adds significant complexity to the histone/epigenetic code hypothesis and dramatically increases the potential information conveyed by the histone N-terminal tails.

Once again there are discrepancies between the data here and previously published data from Heard *et al.,* (2001). The main difference is the timing of the loss of di-methylated lysine 4 of H3. Heard *et al.,* (2001) places this as an early event in X inactivation albeit

concurrent with H3 deacetylation. I attribute this to the different techniques employed given metaphase chromosomes were analysed in contrast to interphase nuclei.

The link between di-methylated lysine 4 of H3 and histone acetylation is intriguing. The data shown in this report suggests the timing of the loss of $H3Me_2K4$ correlates well with the timing of core histone hypoacetylation. Moreover the loss of di-methylated lysine 4 but not tri-methylated lysine 4 can be prevented by culturing cells in the presence of the histone deacetylase inhibitor Trichostatin A (TSA). This inhibitor further distinguishes the mechanisms that remove di- and tri-methylated lysine 4 from Xi by their differential sensitivity to TSA. It also raises questions regarding how the TSA is affecting the degree of global lysine 4 di-methylation and how it prevents the loss of $H3Me_2K4$ from Xi.

Trichostatin A was shown to elevate the global level of $H3Me_2K4$ but not $H3Me_2K9$ as determined by western blotting. The data suggests that the inhibitor interferes with the enzymatic equilibrium responsible for depositing and removing methyl- groups from lysine 4 thereby promoting global histone di-methylation at lysine 4 of H3. However, the inhibitor may be having an indirect effect by promoting elevated levels of histone acetylation. Acetylated histones may a preferred substrate for the SET 1 group of histone methyltransferases, responsible for depositing methylation at lysine 4 of H3.

The effect of TSA on the process of X inactivation has been investigated previously in our Birmingham laboratory (A. Barlow and S. Duthie; unpublished). Using RNA-FISH it was demonstrated that ES cells cultured in the presence of TSA for seven days failed to display elevated levels of the *Xist* transcript. Control cells displayed high level

expression that co-localised with one of the two X chromosomes. This suggests that the inhibitor prevents the loss of histone acetylation and di-methylated lysine 4 of H3 on Xi on account of its inhibition of *Xist* up-regulation. Indeed transgenic *Xist* expression has previously been shown to induce H4 hypoacetylation (Lee and Jaenisch, 1997). Collectively one might suggest that histone hypoacetylation and a depletion of $H3Me_2K4$ may simply be consequences of the silencing mechanisms initiated by *Xist* RNA. In contrast the timing of the loss of tri-methylated lysine 4 of H3 and its insensitivity to TSA suggest that it is intrinsic to the process of X inactivation and not dependent on a chain of events initiated by *Xist* RNA.

6.3 USING CASES OF X;AUTOSOME TRANSLOCATION TO STUDY THE RELATIONSHIP BETWEEN TRANSCRIPTIONAL COMPETENCE, REPLICATION TIMING AND HISTONE MODIFICATIONS

In collaboration with A. J. Sharp we have analysed the spread of X inactivation in five cases of X;autosome translocation. We have studied the degree of spread of transcriptional silencing using allele-specific PCR and the extent of spread of late replication and chromatin depleted in acetylated H3/H4 and di-methylated lysine 4 of H3 using immuno-FISH. This combined analysis has allowed us to examine the relationship between regions of transcriptional quiescence resulting from the spread of X inactivation with the timing of DNA replication and the histone modifications that accompany the facultative heterochromatin of Xi.

6.3.1 Support for the Lyon repeat hypothesis - LINE content of autosomal chromatin is a good correlate for the spread of X inactivation

The study conducted here has shown that the X inactivation signal can spread and silence genes located up to 45Mb from the translocated breakpoint. Therefore the factors responsible for the spread of X inactivation are not unique to the X chromosome. However, spreading was never complete and often occurred in a discontinuous manner, suggesting that autosomal chromatin does not transmit or maintain the inactivation signal as efficiently as the X chromosome. In view of the variability of each case it is interesting to compare the enrichment of the autosomal segments for genomic features that underlie the spread of the X inactivation. This is especially relevant in view of the proposition that Long Interspersed Nuclear Elements (LINEs) might function to facilitate the spread (Lyon, 1998). Lyons repeat hypothesis predicts that the spread of the X inactivation signal into autosomal chromatin is dependent upon its LINE content. Interestingly sequence analysis of the 33 autosomal genes studied by A. J. Sharp revealed significant correlation between the LINE content and the degree of inactivation, supporting the hypothesis that LINEs are DNA elements that mediate the spread of X inactivation. This also explains the variable degrees of spread of the X inactivation signal observed in this study (A. J. Sharp, W. Tapper, P. Strike, D. Robinson, P. Jacobs; unpublished).

It has been reported in the past that the culturing of cells resulted in gene reactivation of the autosomal portion of the translocated chromosome (Schanz and Steinbach, 1989). The authors speculated that the gene reactivation observed in the autosomal portion was on account of ineffective maintenance of the inactivation on the autosome. The data obtained by A. J. Sharp showed concordant results of gene transcription and

late replication studies in both peripheral blood and EBV-transformed lymphoblastoid cells. Additionally in every case there was a good correlation between the pattern of gene silencing and the attenuation of clinical phenotype associated with each trisomy. This suggests that our *in vitro* observations in cultured lymphoblastoids are a good reflection of that *in vivo*.

6.3.2 The spread of X inactivation can occur in the absence of the cytogenetic features associated with facultative heterochromatin

When the transcriptional data is analysed in conjunction with the replication and histone modification analysis we can see that the X inactivation signal can spread in the absence of the cytogenetic features normally associated with the inactive X chromosome; namely late replication and chromatin depleted in acetylated H3/4 and di-methylated lysine 4 of H3. This was most pronounced in the BO0566 case where there was a discontinuous spread of gene silencing, but no spread of late replication or chromatin depleted in histone acetylation or $H3Me_2K4$. Gene silencing has been shown in the past to occur in the absence of late replication (Shao and Takagi, 1991). However, the converse is also true with reactivated genes shown to retain their late replication status (Hors-Cayla *et al.*, 1983). This illustrates the importance of gene expression studies in cases of X;autosome translocation and raises interesting questions regarding what features do accompany the silencing of genes on the translocated chromosome. It remains to be determined whether localised promoter hypoacetylation and depletion of $H3Me_2K4$ do indeed accompany the silencing of autosomal genes on the translocated chromosome; undetectable by immuno-FISH. Another possibility is a localised enrichment of di-methylated lysine 9 of H3 thereby promoting the binding of an HP1-like protein. If however late replication and a

depletion of acetylated H3/4 and H3Me_2K4 do not accompany gene silencing in BO0566, as suggested by the immuno-FISH data, it would confirm the redundancy seen in gene transcriptional control. Indeed transcriptional silencing has been shown to occur in the past in the absence of both histone hypoacetylation and late replication (Wutz and Jaenisch, 2000).

Further analysis of BO0566 using chromatin immunoprecipitation (ChIP) will enable a full assessment of the epigenetics that accompany the spread of gene silencing in this case. However, what is clear is the redundancy displayed by the factors responsible for the maintenance of transcriptional repression.

6.3.3 Histone modifications are a better correlate of transcriptional competence than late replication

It has previously been shown that late replication is a poor cytogenetic correlate of the spread of gene silencing (Sharp *et al.*, 2001). In contrast, immuno-FISH analysis of the same case (AH) showed a good correlation between gene silencing and chromatin depleted in histone acetylation and di-methylated lysine 4 of H3. This demonstrates that these histone modifications are distinct and independent from late replication as observed previously (Keohane *et al.*, 1996).

It was noticeable that in all cases except BO0566, the chromatin depleted for acetylated H3/4 and di-methylated lysine 4 of H3 clearly defined the extent of spread of the X inactivation signal. This is in contrast to late replication which directly corresponded to the spread of gene silencing in only two cases; SR and AL0044.

It was noticeable that the autosomal genes located within cytogenetically late-replicating regions or chromatin domains depleted in acetylated H3/4 and H3 di-methylated at lysine 4 were inactive. We propose that this represents domains in which the spread of X inactivation is maintained in a more stable fashion.

In summary we have characterised the spread of X inactivation through autosomal chromatin in five cases of X;autosome translocation. Our study has permitted the analysis of gene silencing in relation to the epigenetic features that accompany facultative heterochromatin. We have shown that gene silencing can occur in the absence of late replication and chromatin depleted in acetylated H3/4 or di-methylated lysine 4 of H3 raising interesting questions concerning the mechanism by which the X inactivation signal is transmitted and maintained in these cases. Additionally we have shown that whilst these histone modifications do not always correlate with gene silencing, they provide a more reliable indicator of the extent of spread of X inactivation than late replication.

6.4 USING FORMALDEHYDE CROSS-LINKED CHROMATIN IMMUNOPRECIPITATION TO ANALYSE THE CORRELATION BETWEEN CLASS I HDAC DISTRIBUTION AND THE HISTONE MODIFICATIONS

6.4.1 Class I histone deacetylases are globally associated with the chromatin template

I have used cross-linking chromatin immunoprecipitation (XChIP) to study how the distribution of class I histone deacetylases relate to the actual distribution of histone acetylation and di-methylated lysine 4 of H3. The *Xist* gene has been shown previously to be hyperacetylated 5' to promoter P1 in undifferentiated female ES cells (O'Neill *et al.*, 1999). Upon differentiation this region of hyperacetylation is lost. I was interested in the hypothesis that the fall in H4 acetylation was due to targeted histone deacetylase recruitment immediately 5' to the promoter.

I have shown using XChIP that the deacetylases maintain a ubiquitous association with the chromatin template. Indeed significant levels of DNA were recovered from every region analysed including the constitutively expressed *Tuba6* gene. This was particularly surprising given the nature of this gene. The class I Hdacs displayed little correlation with the previously reported distribution of acetylated H4 across *Xist* (O'Neill *et al.*, 1999) and *Pgk-1* (Gilbert and Sharp, 1999). Nor was there an obvious correlation with the acetylated H3 and $H3Me_2K4$ distribution reported in this study. This data presented here raises interesting questions regarding why the class I histone deacetylases are so ubiquitous and how the patterns of histone modifications are established.

The distribution of the histone deacetylases have been most widely studied in yeast. This has also permitted the analysis of the transcription profiles resulting from the deletion of various yeast histone deacetylases (Bernstein *et al.*, 2000). Interestingly deletions of Rpd3, Hda1 and Sir2 each resulted in the down-regulation of a distinctive functional class of genes. This suggests that not only do histone deacetylases have distinct functional roles but they also participate in transcriptional activation. Genome wide analysis of the distribution of Rpd3, the yeast homolog to the class I Hdacs has been studied previously using XChIP (Vogelauer *et al.*, 2000; Kurdistani *et al.*, 2002). Interestingly both studies reported a specific recruitment of Rpd3 to selective promoters by associated proteins such as Ume6 in addition to a genome-wide distribution over large chromosomal domains by an as yet undefined mechanism. This resulted in the authors speculating that the genome wide association of histone deacetylases might serve to create a highly responsive state of histone acetylation. Therefore globally associated Hdacs and Hats might serve to allow a rapid return to the steady state level of histone acetylation following the localised recruitment of a Hat or Hdac complex. Together the evidence suggests that Hdacs are becoming regarded as more than simply transcriptional repressors, and introduces a more dynamic role in gene regulation. Indeed this recent evidence opposes the classical idea that Hdacs are static enzymes occupying the promoter regions of silent genes. Given this evidence it is perhaps not surprising that histone deacetylases were identified in this study in the promoter and coding regions of expressed genes (*Xist*, *Pgk-1* and *Tuba6*). Brehling *et al.,* (2001) have also reported the presence of *Drosophila* Hdac I at active gene promoter and coding regions. A study performed by Ferreira *et al.,* (2000) examining the cell cycle recruitment of Hdac1 to the E2F regulated gene *DHFR* by the Retinoblastoma (Rb) protein provided evidence supporting Hdac1

recruitment during early G1, and a release during the G1-S transition. Whilst there was a clear drop in the association of Hdac1 with *DHFR* during the G1/S transition, the deacetylase is still detectable at significant levels during a time period of *DHFR* expression. Whilst the authors do not address this issue, one could argue that the basal retention of Hdac1 at the *DHFR* promoter could be on account of a background of globally associated Hdac1. Indeed the global association of Hdac1 seems an attractive option given that following the G1-S transition of the cell cycle, E2F associates with histone acetyltransferases to activate transcription. Therefore a global association of Hdac1 might serve to rapidly return the level of histone acetylation to its initial state.

With this in mind I propose that the class I Hdacs in this study maintain a global association with the chromatin template; above which targeted histone acetylation events occur. In light of this proposition one would expect to detect rapid changes in the levels of histone acetylation by interfering with the activity of the Hats or Hdacs. Indeed this is exactly what is observed. Cells cultured for just ten minutes in the presence of the histone deacetylase inhibitor sodium butyrate (50mM) display significantly higher levels of histone acetylation than control cells, as detected by immunoblotting using antisera against acetylated histones. Furthermore this suggests that the rapid accumulation of acetate groups results from the unopposed activity of globally associated Hats.

In view of a proposed global Hdac association one should remember that the technique of XChIP does not discriminate between active and inactive deacetylase complexes. Indeed one could argue that inactive deacetylase complexes maintain a global association with the chromatin template, whilst complexes activated by various

cofactors occupy regions of targeted histone deacetylation. Indeed the deacetylase activity of a complex has been shown to be regulated by its components. For example the activity of the HDAC1/2-RbAp46/48 core complex has been shown to be dependent on the presence of MTA2, recruited through its direct interaction with MBD3 (Zhang *et al.*, 1999). However, yeast Rpd3 has been shown to be specifically enriched at particular loci (Rundlett *et al.*, 1998) favouring the idea of deacetylase recruitment in a background of global Hdac association.

The idea of globally associated Hdacs raises questions regarding how they are delivered and maintained in association with the chromatin template. Class I Hdacs have been shown to associate with proteins capable of binding methylated DNA such as MeCP2 (Nan *et al.*, 1998). However, methyl-binding proteins cannot be responsible for the global Hdac distribution given that DNA is only methylated at selected "islands" throughout the genome. The global deacetylase distribution in yeast occurs in the absence of any known proteins capable of recruiting Rpd3 (Kurdistani *et al.*, 2002). This led Kurdistani *et al.,* (2002) to speculate that Rpd3 was being recruited in a sequence independent manner to histones or histone binding proteins. Similar proposals can be made in mammalian cells. It may even be RbAp48, a protein capable of binding to histone H4 (Verreault *et al.*, 1998) that is delivering the class I Hdacs to the chromatin template. Indeed the study here suggests that class I Hdacs have a similar distribution to RbAp48.

It is interesting to note the global changes in histone acetylation that occur throughout the cell cycle (Waterborg and Matthews, 1984). Histones H3 and H4 are predominantly mono- or di-acetylated in S phase. During G2 H3 and H4 become

hyperacetylated and during mitosis they are deacetylated. Given these changes are occurring on total histones, one might suggest that the global association of class I Hdacs also occurs in a cell cycle dependent manner. Indeed immunofluorescence microscopy of class I Hdacs reveals that they form distinctive "bodies" during interphase but dissociate from chromatin during metaphase (figure 32). This has also been shown in HeLa cells immunolabelled under formaldehyde fixation conditions whereby a specific re-association of the class I Hdacs with the chromosomes occurred during anaphase (J. Lavender, B. M. Turner; unpublished). This suggests that Hdacs do associate in a cell cycle dependent manner, albeit with no direct correlation with the state of histone acetylation. However, these experiments need to be extended by applying XChIP to cells that can be easily synchronised such as 3T3 cells.

6.4.2 Deacetylase association with the facultative heterochromatin of the inactive X chromosome?

What seems clear from this study is that none of the class I Hdacs were significantly enriched at any of the genomic loci tested. This includes the chromatin of the inactive X chromosome suggesting that if there is a deacetylase component to the complex responsible for maintaining the silent state then the class I Hdacs are not involved. This is consistent with immunofluorescence data from a recent study showing the selective association of Polycomb group proteins Eed (embryonic ectoderm development) and Enx1 (enhancer of zeste) with the inactive X chromosome in trophectodermal tissue (Mak *et al.*, 2002). Eed is a protein capable of interacting with Hdacs1 and 2 (van der Vlag and Otte, 1999) and has been shown to be necessary for imprinted X inactivation in mouse extraembryonic tissue (Wang *et al.*, 2001). Whilst Mak *et al.,* (2002) showed a clear association of Eed and Enx1 with Xi at all stages of

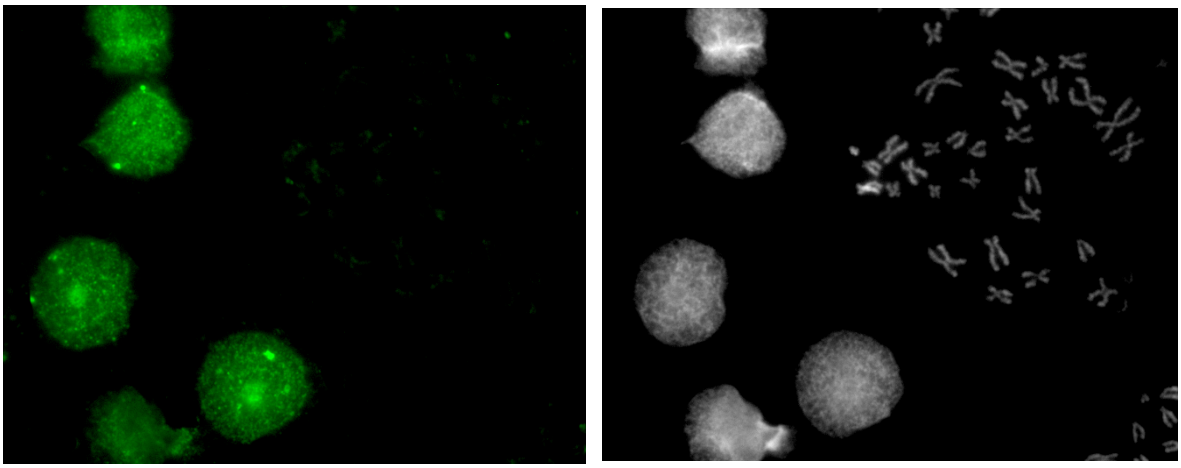

Figure 32. Immunofluorescence microscopy reveals that class I Hdacs, here represented by Hdac1 form distinctive “bodies” during interphase but dissociate from the chromatin template during metaphase (female lymphoblastoid cells: GM12616)

the cell cycle; antisera to Hdacs1, 2 and 3 failed to identify inactive X chromosome specific foci. This is intriguing given the highly specific localisation of both Polycomb group proteins and suggests that class I Hdacs are not specifically retained on the chromatin of Xi. It is a possibility that several Hdacs are involved in the maintenance of a hypoacetylated state including the TSA resistant Sir2 group (class III) of deacetylases. This is of particular relevance given the TSA insensitivity of Xi in female somatic cells shown in this study and previously (O'Neill *et al.*, 1999).

6.4.3 Selective loss of histone acetyltransferases may facilitate the H4 deacetylation 5' to the Xist promoter

Whilst I can suggest a global class I Hdac association in view of my results, this does not explain the local changes in H4 acetylation observed previously (O'Neill *et al.*, 1999), nor does it explain the 4kb region, upstream of the *Xist* P1 promoter shown in this study to be specifically depleted in acetylated H3 and di-methylated lysine 4 of H3. Indeed it still begs the question; how are these patterns of histone modifications established and maintained? Given no specific class I deacetylase enrichment was detectable following differentiation, one could suggest that the developmental H4 deacetylation upstream of *Xist* occurs due to a loss of histone acetyltransferases or through the recruitment of class II or Sir2 (III) Hdacs. The extent of H4 hyperacetylation is intriguing given that the study by O'Neill *et al.,* (1999) scanned 120kb upstream of the *Xist* promoter and found high levels of H4 acetylation in a domain of at least 60kb. This suggests that if there is selective loss of Hats it is occurring in a domain wide manner.

6.4.4 Patterns of H3 acetylation and H3Me$_2$K4 across Xist and Pgk-1

Using XChIP I have examined the pattern of acetylated H3 and di-methylated lysine 4 of H3 across the *Xist* and *Pgk-1* genes. I have identified a region 8kb upstream of the *Xist* P1 promoter that is enriched for both modifications. Following just two days of differentiation the level of acetylated H3 and H3Me$_2$K4 in this region fell significantly and stayed low until day six. Perhaps the most interesting finding was a 4kb region mid way between the *Xist* and *Enox* promoters that was shown to be significantly depleted in acetylated H3 and H3Me$_2$K4. This depletion was retained until at least day six of differentiation, the last time point analysed. I suggest that this localised depletion serves to compartmentalise the chromatin of the *Xist* and *Enox* genes. This would "insulate" *Xist* from any epigenetic silencing mechanisms operating 5' to the gene, allowing its unique expression from the inactive X chromosome. To explore this idea it would be of interest to examine the chromatin downstream of *Xist* in order to determine whether a similar "insulator" element exists thereby compartmentalising the gene 3' and 5'.

The two previous studies that have analysed the distribution of acetylated H4 (O'Neill *et al.*, 1999) and di-methylated lysine 9 of H3 upstream of *Xist* (Heard *et al.*, 2001) identified a large domain of approximately 120kb that displayed high levels of both of the histone modifications. Whilst somewhat paradoxical given the general correlation between gene inactivity, hypoacetylation and di-methylation at lysine 9 of H3, this combination of modifications may serve to recruit non-histone proteins or facilitate the spread of the X-inactivation signal from *Xic* early in differentiation. By the same rationale the localised depletion of acetylated H3 and di-methylated lysine 4 of H3 between the *Xist* and *Enox* promoter regions may have a functional role in the

recruitment of non-histone proteins to *Xist* (and/or the *Xic*). However, it raises the question concerning why this region was not detected in the study made by O'Neill *et al.,* (1999). The study made here analysed five regions local to the *Xist* promoter encompassing 10kb using chromatin with an average size of 500bp. In contrast the study made by O'Neill *et al.,* (1999) analysed seven regions within a 120kb domain using chromatin rich in oligonucleosomes; typically 5-mers. The genomic probes employed by O'Neill *et al.,* (1999) were of an average size of 1kb. A direct comparison of the regions analysed in the respective studies is made in figure 33. O'Neill *et al.,* (1999) reported H4 hyperacetylation in undifferentiated ES cells that extended upstream of the promoter. Following differentiation the level of H4 acetylation fell dramatically to a level equivalent to that detected in the coding region of the gene (W7D). This is consistent with the region X8u in this report in that it was shown to be subject to a fall in acetylated H3 and di-methylated lysine 4 of H3 following differentiation. In contrast the 4kb region depleted for both of these modifications (Hx4 and X4u) throughout differentiation was shown by O'Neill *et al.,* (1999) (HH1.5) to retain high levels of H4 acetylation that were lost following differentiation. Whilst one could explain this discrepancy based on the resolution of the chromatin and the probes employed by O'Neill *et al.,* (1999) coincident acetylated H3 and H4 cannot always be assumed in view of recent examples of H3 but not H4 acetylation (Breiling *et al.*, 2001; Gregory *et al.*, 2001). Indeed opposing changes in H3 and H4 acetylation have been observed in a region approximately 4kb 3' of *Xist* (L. P. O'Neill, B. M. Turner; unpublished).

The distribution of acetylated H3 and di-methylated lysine 4 of H3 across the *Pgk-1* gene agreed well with idea of local histone modifications being intrinsic to

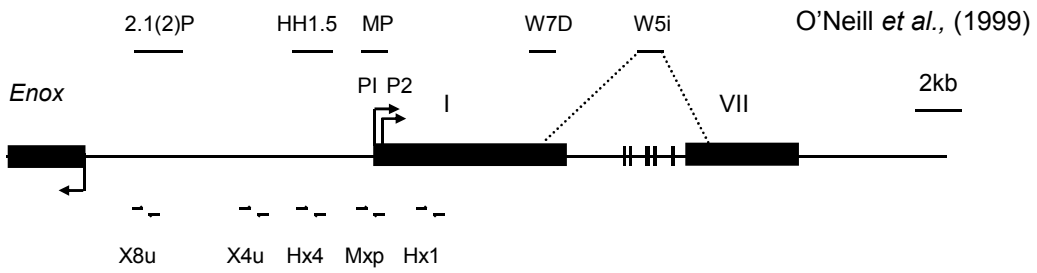

Figure 33. Analysis of the *Xist* regions examined in this study by PCR (arrows) in relation to the DNA probes used by O'Neill *et al.,* (1999) (horizontal lines).

transcriptional activation (Kuo *et al.*, 2000), with the degree of promoter acetylation and di-methylation at lysine 4 of H3 consistently exceeding those found in the coding region of the gene. The data reporting the distribution of acetylated H3 did not support a promoter-specific hypoacetylation of X-linked genes on the inactive X chromosome as previously suggested (Gilbert and Sharp, 1999). Again one might speculate that the somatic cell hybrid lines used in the aforementioned study did not reflect the epigenetics found in female mouse ES cells due to a relaxation of the maintenance of the inactive state.

When the distribution of acetylated H3 and di-methylated lysine 4 of H3 are compared with the ubiquity of the deacetylase distribution one can conclude that the patterns of modification across the *Xist* and *Pgk-1* genes are not driven by specific targeting of Hdacs 1, 2 or 3. This raises interesting question regarding how these modifications are established and maintained. I suggest that there are localised acetylation and deacetylation events that occur above a background of class I Hdac association.

6.5 OVERALL CONCLUSIONS

In conclusion I have used the facultative heterochromatin of the inactive X (Xi) chromosome to study the histone modifications that accompany transcriptionally silent genes. I have applied the techniques of immunocytochemistry and chromatin immunoprecipitation using antisera specific for the histone and site of modification. Female embryonic stem (ES) recapitulate the process of X inactivation *in vitro* and allow us to study the sequential events that are necessary for the formation of an inactive X chromosome. Using ES cells I have shown that all four core histones are

deacetylated concurrently on the inactive X chromosome throughout the coding and promoter regions of X-linked genes.

I have studied the functional significance of histone methylation, exploring the possibility that the level of lysine methylation adds a new complexity to the histone code hypothesis. This has necessitated the generation of new antisera specific for the level of lysine methylation. I have shown that Xi is depleted in di- and tri-methylation at lysine 4 of H3 but retains di-methylated lysine 9 at levels at or above the rest of the genome. When there were discrepancies between the data presented here and the published data I have explored these differences using the available antisera. This study has highlighted the potential problems associated with the use of antisera in molecular biology. I have shown that published data documenting a specific enrichment of di- and tri-methylated lysine 9 of H3 on the inactive X chromosome (Boggs *et al.*, 2002; Cowell *et al.*, 2002) could be interpreted differently in light of the evidence presented here, showing the influence of adjacent modifications on the specificity of antisera.

Using ES cells I have demonstrated the functional significance of levels of lysine methylation. The loss of tri-methylated lysine 4 of H3 was determined to be an early event in the process of X inactivation and preceded the loss of its di-methylated equivalent and the timing of core histone hypoacetylation. Interestingly the histone deacetylase inhibitor Trichostatin A prevented the loss of both core histone acetylation and di-methylated lysine 4 of H3 but not its tri-methylated equivalent, suggesting that they are removed from Xi by different mechanisms.

Through a collaboration we have examined the relationship between actual transcriptional silencing brought about by the spread of gene silencing in cases of X;autosome translocation and the timing of DNA replication and the histone modifications. We have shown that the spread of X inactivation can occur in the absence of late replication and chromatin depleted in acetylated H3/4 or di-methylated lysine 4 of H3. However, we have demonstrated that histone modifications provide a more reliable indicator of the extent of spread of X inactivation than late replication.

By the immunoprecipitation of cross-linked chromatin I have analysed a potential mechanism whereby patterns of histone modification are established. Using the chromatin 5' of the *Xist* gene; a region of defined H4 deacetylation during female ES cell differentiation (O'Neill *et al.*, 1999), I have examined the genomic distribution of the class I histone deacetylases. Surprisingly there were detectable levels of the class I Hdacs across all genomic loci examined throughout differentiation with no apparent correlation with the distribution of acetylated H4 (O'Neill *et al.*, 1999) or acetylated H3 and di-methylated lysine 4. This suggests that the global deacetylase association serves to provide a rapid return the basal level of histone acetylation following specific targeting events.

7 REFERENCES

1 Allis, C. D., Bowen, J. K., Abraham, G. N., Glover, C. V. and Gorovsky, M. A. (1980) Proteolytic processing of histone H3 in chromatin: a physiologically regulated event in Tetrahymena micronuclei. *Cell* **20**(1), 55-64.

2 Ashworth, A., Rastan, S., Lovell-Badge, R. and Kay, G. (1991) X-chromosome inactivation may explain the difference in viability of XO humans and mice. *Nature* **351**(6325), 406-408.

3 Bailey, J. A., Carrel, L., Chakravarti, A. and Eichler, E. E. (2000) Molecular evidence for a relationship between LINE-1 elements and X chromosome inactivation: the Lyon repeat hypothesis. *Proc Natl Acad Sci U S A* **97**(12), 6634-6639.

4 Bannister, A. J., Zegerman, P., Partridge, J. F., Miska, E. A., Thomas, J. O., Allshire, R. C. and Kouzarides, T. (2001) Selective recognition of methylated lysine 9 on histone H3 by the HP1 chromo domain. *Nature* **410**(6824), 120-124.

5 Barr, M. L. and Bertram, E. G. (1949) A morphological distinction between neurones of female and male, and the behaviour of the nucleolar satellite during accelerated nucleoprotein synthesis. *Nature* **163** 676-667.

6 Belyaev, N., Keohane, A. M. and Turner, B. M. (1996) Differential underacetylation of histones H2A, H3 and H4 on the inactive X chromosome in human female cells. *Hum Genet* **97**(5), 573-578.

7 Bernstein, B. E., Humphrey, E. L., Erlich, R. L., Schneider, R., Bouman, P., Liu, J. S., Kouzarides, T. and Schreiber, S. L. (2002) Methylation of histone H3 Lys 4 in coding regions of active genes. *Proc Natl Acad Sci U S A* **99**(13), 8695-8700.

8 Bernstein, B. E., Tong, J. K. and Schreiber, S. L. (2000) Genomewide studies of histone deacetylase function in yeast. *PNAS* **97**(25), 13708-13713.

9 Boggs, B. A., Cheung, P., Heard, E., Spector, D. L., Chinault, A. C. and Allis, C. D. (2002) Differentially methylated forms of histone H3 show unique association patterns with inactive human X chromosomes. *Nat Genet* **30**(1), 73-76.

10 Boggs, B. A., Connors, B., Sobel, R. E., Chinault, A. C. and Allis, C. D. (1996) Reduced levels of histone H3 acetylation on the inactive X chromosome in human females. *Chromosoma* **105**(5), 303-309.

11 Boyle, A. L., Ballard, S. G. and Ward, D. C. (1990) Differential distribution of long and short interspersed element sequences in the mouse genome: chromosome karyotyping by fluorescence in situ hybridization. *Proc Natl Acad Sci U S A* **87**(19), 7757-7761.

12 Braunstein, M., Rose, A. B., Holmes, S. G., Allis, C. D. and Broach, J. R. (1993) Transcriptional silencing in yeast is associated with reduced nucleosome acetylation. *Genes Dev* **7**(4), 592-604.

13 Brehm, A. and Kouzarides, T. (1999) Retinoblastoma protein meets chromatin. *Trends Biochem Sci* **24**(4), 142-145.

14 Breiling, A., Turner, B. M., Bianchi, M. E. and Orlando, V. (2001) General transcription factors bind promoters repressed by Polycomb group proteins. *Nature* **412**(6847), 651-655.

15 Breslauer, K., Frank, R., Blocker, H. and Marky, L. (1986) Predicting DNA duplex stability from the base sequence. *PNAS* **83**(11), 3746-3750.

16 Briggs, S. D., Bryk, M., Strahl, B. D., Cheung, W. L., Davie, J. K., Dent, S. Y., Winston, F. and Allis, C. D. (2001) Histone H3 lysine 4 methylation is mediated by Set1 and required for cell growth and rDNA silencing in Saccharomyces cerevisiae. *Genes Dev* **15**(24), 3286-3295.

17 Brockdorff, N., Ashworth, A., Kay, G. F., Cooper, P., Smith, S., McCabe, V. M., Norris, D. P., Penny, G. D., Patel, D. and Rastan, S. (1991) Conservation of position and exclusive expression of mouse Xist from the inactive X chromosome. *Nature* **351**(6324), 329-331.

18 Brockdorff, N., Ashworth, A., Kay, G. F., McCabe, V. M., Norris, D. P., Cooper, P. J., Swift, S. and Rastan, S. (1992) The product of the mouse Xist gene is a 15 kb inactive X-specific transcript containing no conserved ORF and located in the nucleus. *Cell* **71**(3), 515-526.

19 Brown, C. J., Lafreniere, R. G., Powers, V. E., Sebastio, G., Ballabio, A., Pettigrew, A. L., Ledbetter, D. H., Levy, E., Craig, I. W. and Willard, H. F. (1991) Localization of the X inactivation centre on the human X chromosome in Xq13. *Nature* **349**(6304), 82-84.

20 Brown, C. J. and Willard, H. F. (1994) The human X-inactivation centre is not required for maintenance of X-chromosome inactivation. *Nature* **368**(6467), 154-156.

21 Brownell, J. E., Zhou, J., Ranallio, T., Kobayashi, R., Edmonson, D. G., Roth, S. Y. and Allis, C. D. (1996) Tetrahymena histone acetyltransferase A: a homolog to yeast Gcn5p linking histone acetylation to gene activation. *Cell* **84** 843-851.

22 Butler, L. M., Zhou, X., Xu, W. S., Scher, H. I., Rifkind, R. A., Marks, P. A. and Richon, V. M. (2002) The histone deacetylase inhibitor SAHA arrests cancer cell growth, up-regulates thioredoxin-binding protein-2, and down-regulates thioredoxin. *Proc Natl Acad Sci U S A* **99**(18), 11700-11705.

23 Byvoet, P. (1972) In vivo turnover and distribution of radio-N-methyl in arginine-rich histones from rat tissues. *Arch Biochem Biophys* **152**(2), 887-888.

24 Byvoet, P., Shepherd, G. R., Hardin, J. M. and Noland, B. J. (1972) The distribution and turnover of labeled methyl groups in histone fractions of cultured mammalian cells. *Arch Biochem Biophys* **148**(2), 558-567.

25 Candido, E. P., Reeves, R. and Davie, J. R. (1978) Sodium butyrate inhibits histone deacetylation in cultured cells. *Cell* **14**(1), 105-113.

26 Canun, S., Mutchinick, O., Shaffer, L. G. and Fernandez, C. (1998) Combined trisomy 9 and Ullrich-Turner syndrome in a girl with a 46,X,der(9)t(X;9)(q12;q32) karyotype. *Am J Med Genet* **80**(3), 199-203.

27 Cao, R., Wang, L., Wang, H., Xia, L., Erdjument-Bromage, H., Tempst, P., Jones, R. S. and Zhang, Y. (2002) Role of Histone H3 Lysine 27 Methylation in Polycomb-Group Silencing. *Science*.

28 Carrel, L., Cottle, A. A., Goglin, K. C. and Willard, H. F. (1999) A first-generation X-inactivation profile of the human X chromosome. *Proc Natl Acad Sci U S A* **96**(25), 14440-14444.

29 Carrel, L. and Willard, H. F. (1999) Heterogeneous gene expression from the inactive X chromosome: an X-linked gene that escapes X inactivation in some human cell lines but is inactivated in others. *Proc Natl Acad Sci U S A* **96**(13), 7364-7369.

30 Chadwick, B. P. and Willard, H. F. (2002) Cell cycle-dependent localization of macroH2A in chromatin of the inactive X chromosome. *J Cell Biol* **157**(7), 1113-1123.

31 Clayton, A. L., Rose, S., Barratt, M. J. and Mahadevan, L. C. (2000) Phosphoacetylation of histone H3 on c-fos- and c-jun-associated nucleosomes upon gene activation. *Embo J* **19**(14), 3714-3726.

32 Clemson, C. M., Chow, J. C., Brown, C. J. and Lawrence, J. B. (1998) Stabilization and localization of Xist RNA are controlled by separate mechanisms and are not sufficient for X inactivation. *J Cell Biol* **142**(1), 13-23.

33 Clemson, C. M., McNeil, J. A., Willard, H. F. and Lawrence, J. B. (1996) XIST RNA paints the inactive X chromosome at interphase: evidence for a novel RNA involved in nuclear/chromosome structure. *J Cell Biol* **132**(3), 259-275.

34 Conaway, R. C. and Conaway, J. W. (1993) General initiation factors for RNA polymerase II. *Annu Rev Biochem* **62** 161-190.

35 Costanzi, C. and Pehrson, J. R. (1998) Histone macroH2A1 is concentrated in the inactive X chromosome of female mammals. *Nature* **393**(6685), 599-601.

36 Costanzi, C., Stein, P., Worrad, D. M., Schultz, R. M. and Pehrson, J. R. (2000) Histone macroH2A1 is concentrated in the inactive X chromosome of female preimplantation mouse embryos. *Development* **127**(11), 2283-2289.

37 Couturier, J., Dutrillaux, B., Garber, P., Raoul, O., Croquette, M. F., Fourlinnie, J. C. and Maillard, E. (1979) Evidence for a correlation between late replication and autosomal gene inactivation in a familial translocation t(X;21). *Hum Genet* **49**(3), 319-326.

38 Cowell, I. G., Aucott, R., Mahadevaiah, S. K., Burgoyne, P. S., Huskisson, N., Bongiorni, S., Prantera, G., Fanti, L., Pimpinelli, S., Wu, R., Gilbert, D. M., Shi, W., Fundele, R., Morrison, H., Jeppesen, P. and Singh, P. B. (2002) Heterochromatin, HP1 and methylation at lysine 9 of histone H3 in animals. *Chromosoma* **111**(1), 22-36.

39 Csankovszki, G., Nagy, A. and Jaenisch, R. (2001) Synergism of Xist RNA, DNA methylation, and histone hypoacetylation in maintaining X chromosome inactivation. *J Cell Biol* **153**(4), 773-784.

40 Csordas, A. (1990) On the biological role of histone acetylation. *Biochem J* **265**(1), 23-38.

41 Dedon, P. C., Soults, J. A., Allis, C. D. and Gorovsky, M. A. (1991) Formaldehyde cross-linking and immunoprecipitation demonstrate developmental changes in H1 association with transcriptionally active genes. *Mol Cell Biol* **11**(3), 1729-1733.

42 Delange, R. J., Fambrough, D. M., Smith, E. L. and Bonner, J. (1969) Calf and pea histone IV. *J Biol Chem* **244** 5669-5679.

43 Dhalluin, C., Carlson, J. E., Zeng, L., Cheung, H., Aggarwal, A. K. and Zhou, M.-M. (1999) Structure and ligand of a histone acetyltransferase bromodomain. *Nature* **399** 491-496.

44 Downes, M., Ordentlich, P., Kao, H. Y., Alvarez, J. G. and Evans, R. M. (2000) Identification of a nuclear domain with deacetylase activity. *Proc Natl Acad Sci U S A* **97**(19), 10330-10335.

45 Drewell, R. A., Goddard, C. J., Thomas, J. O. and Surani, M. A. (2002) Methylation-dependent silencing at the H19 imprinting control region by MeCP2. *Nucleic Acids Res* **30**(5), 1139-1144.

46 Duerre, J. A. and Chakrabarty, S. (1975) Methylated basic amino acid composition of histones from the various organs from the rat. *J Biol Chem* **250**(21), 8457-8461.

47 Edmonson, D. G., Smith, M. M. and Roth, S. Y. (1996) Repression domain of the yeast global repressor Tup1 interacts directly with histones H3 and H4. *Genes Dev* **10** 1247-1259.

48 Eils, R., Dietzel, S., Bertin, E., Schrock, E., Speicher, M. R., Ried, T., Robert-Nicoud, M., Cremer, C. and Cremer, T. (1996) Three-dimensional reconstruction of painted human interphase chromosomes: active and inactive X chromosome territories have similar volumes but differ in shape and surface structure. *J Cell Biol* **135**(6 Pt 1), 1427-1440.

49 Ekwall, K., Olsson, T., Turner, B. M., Cranston, G. and Allshire, R. C. (1997) Transient inhibition of histone deacetylation alters the structural and functional imprint at fission yeast centromeres. *Cell* **91**(7), 1021-1032.

50 Ferreira, R., Naguibneva, I., Mathieu, M., Ait-Si-Ali, S., Robin, P., Pritchard, L. L. and Harel-Bellan, A. (2001) Cell cycle-dependent recruitment of HDAC-1 correlates with deacetylation of histone H4 on an Rb-E2F target promoter. *EMBO Rep* **2**(9), 794-799.

51 Garcia-Heras, J., Martin, J. A., Witchel, S. F. and Scacheri, P. (1997) De novo der(X)t(X;10)(q26;q21) with features of distal trisomy 10q: case report of paternal origin identified by late replication with BrdU and the human androgen receptor assay (HAR). *J Med Genet* **34**(3), 242-245.

52 Gartler, S. M. and Riggs, A. D. (1983) Mammalian X-chromosome inactivation. *Annu Rev Genet* **17** 155-190.

53 Gilbert, S. L., Pehrson, J. R. and Sharp, P. A. (2000) XIST RNA associates with specific regions of the inactive X chromatin. *J Biol Chem* **275**(47), 36491-36494.

54 Gilbert, S. L. and Sharp, P. A. (1999) Promoter-specific hypoacetylation of X-inactivated genes. *Proc Natl Acad Sci U S A* **96**(24), 13825-13830.

55 Goto, T. and Monk, M. (1998) Regulation of X-chromosome inactivation in development in mice and humans. *Microbiol Mol Biol Rev* **62**(2), 362-378.

56 Grant, M., Zuccotti, M. and Monk, M. (1992) Methylation of CpG sites of two X-linked genes coincides with X-inactivation in the female mouse embryo but not in the germ line. *Nat Genet* **2**(2), 161-166.

57 Graves, J. A. (1982) 5-azacytidine-induced re-expression of alleles on the inactive X chromosome in a hybrid mouse cell line. *Exp Cell Res* **141**(1), 99-105.

58 Gregory, R. I., Randall, T. E., Johnson, C. A., Khosla, S., Hatada, I., O'Neill, L. P., Turner, B. M. and Feil, R. (2001) DNA methylation is linked to deacetylation of histone H3, but not H4, on the imprinted genes Snrpn and U2af1-rs1. *Mol Cell Biol* **21**(16), 5426-5436.

59 Grozinger, C. M., Hassig, C. A. and Schreiber, S. L. (1999) Three proteins define a class of human histone deacetylases related to yeast Hda1p. *Proc Natl Acad Sci U S A* **96**(9), 4868-4873.

60 Grozinger, C. M. and Schreiber, S. L. (2000) Regulation of histone deacetylase 4 and 5 and transcriptional activity by 14-3-3-dependent cellular localization. *Proc Natl Acad Sci U S A* **97**(14), 7835-7840.

61 Hansen, R. S., Canfield, T. K., Fjeld, A. D. and Gartler, S. M. (1996) Role of late replication timing in the silencing of X-linked genes. *Hum Mol Genet* **5**(9), 1345-1353.

62 Hansen, R. S., Canfield, T. K., Stanek, A. M., Keitges, E. A. and Gartler, S. M. (1998) Reactivation of XIST in normal fibroblasts and a somatic cell hybrid: abnormal localization of XIST RNA in hybrid cells. *Proc Natl Acad Sci U S A* **95**(9), 5133-5138.

63 Hansen, R. S., Stoger, R., Wijmenga, C., Stanek, A. M., Canfield, T. K., Luo, P., Matarazzo, M. R., D'Esposito, M., Feil, R., Gimelli, G., Weemaes, C. M., Laird, C. D. and Gartler, S. M. (2000) Escape from gene silencing in ICF syndrome: evidence for advanced replication time as a major determinant. *Hum Mol Genet* **9**(18), 2575-2587.

64 Hassig, C. A., Tong, J. K., Fleischer, T. C., Owa, T., Grable, P. G., Ayer, D. E. and Schreiber, S. L. (1998) A role for histone deacetylase activity in HDAC1-mediated transcriptional repression. *Proc Natl Acad Sci U S A* **95**(7), 3519-3524.

65 Heard, E., Clerc, P. and Avner, P. (1997) X-chromosome inactivation in mammals. *Annu Rev Genet* **31** 571-610.

66 Heard, E., Rougeulle, C., Arnaud, D., Avner, P., Allis, C. D. and Spector, D. L. (2001) Methylation of histone H3 at Lys-9 is an early mark on the X chromosome during X inactivation. *Cell* **107**(6), 727-738.

67 Hebbes, T. R., Thorne, A. W. and Crane-Robinson, C. (1988) A direct link between core histone acetylation and transcriptionally active chromatin. *Embo J* **7**(5), 1395-1402.

68 Hecht, A. and Grunstein, M. (1999) Mapping DNA interaction sites of chromosomal proteins using immunoprecipitation and polymerase chain reaction. *Methods Enzymol* **304** 399-414.

69 Hecht, A., Laroche, T., Strahl-Bolsinger, S., Gasser, S. M. and Grunstein, M. (1995) Histone H3 and H4 N-termini interact with SIR3 and SIR4 proteins: a molecular model for the formation of heterochromatin in yeast. *Cell* **80**(4), 583-592.

70 Hendrich, B. D., Brown, C. J. and Willard, H. F. (1993) Evolutionary conservation of possible functional domains of the human and murine XIST genes. *Hum Mol Genet* **2**(6), 663-672.

71 Hong, Y. K., Ontiveros, S. D., Chen, C. and Strauss, W. M. (1999) A new structure for the murine Xist gene and its relationship to chromosome choice/counting during X-chromosome inactivation. *Proc Natl Acad Sci U S A* **96**(12), 6829-6834.

72 Hors-Cayla, M. C., Heuertz, S. and Frezal, J. (1983) Coreactivation of four inactive X genes in a hamster x human hybrid and persistence of late replication of reactivated X chromosome. *Somatic Cell Genet* **9**(6), 645-657.

73 Huntriss, J., Lorenzi, R., Purewal, A. and Monk, M. (1997) A methylation-dependent DNA-binding activity recognising the methylated promoter region of the mouse Xist gene. *Biochem Biophys Res Commun* **235**(3), 730-738.

74 Imai, S., Armstrong, C. M., Kaeberlein, M. and Guarente, L. (2000) Transcriptional silencing and longevity protein Sir2 is an NAD-dependent histone deacetylase. *Nature* **403**(6771), 795-800.

75 Jacobs, S. A. and Khorasanizadeh, S. (2002) Structure of HP1 chromodomain bound to a lysine 9-methylated histone H3 tail. *Science* **295**(5562), 2080-2083.

76 Jenuwein, T. and Allis, C. D. (2001) Translating the histone code. *Science* **293**(5532), 1074-1080.

77 Jeppesen, P. and Turner, B. M. (1993) The inactive X chromosome in female mammals is distinguished by a lack of histone H4 acetylation, a cytogenetic marker for gene expression. *Cell* **74**(2), 281-289.

78 Johnson, C. A. (2000) Chromatin modification and disease. *J Med Genet* **37**(12), 905-915.

79 Johnson, C. A., O'Neill, L. P., Mitchell, A. and Turner, B. M. (1998) Distinctive patterns of histone H4 acetylation are associated with defined sequence elements within both heterochromatic and euchromatic regions of the human genome. *Nucleic Acids Res* **26**(4), 994-1001.

80 Johnson, C. A., White, D. A., Lavender, J. S., O'Neill, L. P. and Turner, B. M. (2002) Human class I histone deacetylase complexes show enhanced catalytic activity in the presence of ATP and co-immunoprecipitate with the ATP-dependent chaperone protein Hsp70. *J Biol Chem* **277**(11), 9590-9597.

81 Johnston, C., Newall, A., Brockdorff, N. and Nesterova, T. (2002) Enox, a Novel Gene That Maps 10 kb Upstream of Xist and Partially Escapes X Inactivation. *Genomics* **80**(2), 236-244.

82 Johnstone, R. W. (2002) Histone-deacetylase inhibitors: novel drugs for the treatment of cancer. *Nat Rev Drug Discov* **1**(4), 287-299.

83 Jones, C., Booth, C., Rita, D., Jazmines, L., Brandt, B., Newlan, A. and Horsthemke, B. (1997) Bilateral retinoblastoma in a male patient with an X; 13 translocation: evidence for silencing of the RB1 gene by the spreading of X inactivation. *Am J Hum Genet* **60**(6), 1558-1562.

84 Kadosh, D. and Struhl, K. (1997) Repression by Ume6 involves recruitment of a complex containing Sin3 corepressor and Rpd3 histone deacetylase to target promoters. *Cell* **89**(3), 365-371.

85 Kanda, N. (1973) A new differential technique for staining the heteropycnotic X-chromosome in female mice. *Exp Cell Res* **80**(2), 463-467.

86 Kao, H. Y., Lee, C. H., Komarov, A., Han, C. C. and Evans, R. M. (2002) Isolation and characterization of mammalian HDAC10, a novel histone deacetylase. *J Biol Chem* **277**(1), 187-193.

87 Kaslow, D. C. and Migeon, B. R. (1987) DNA methylation stabilizes X chromosome inactivation in eutherians but not in marsupials: evidence for multistep maintenance of mammalian X dosage compensation. *Proc Natl Acad Sci U S A* **84**(17), 6210-6214.

88 Keitges, E. A. and Palmer, C. G. (1986) Analysis of spreading of inactivation in eight X autosome translocations utilizing the high resolution RBG technique. *Hum Genet* **72**(3), 231-236.

89 Keller, G. M. (1995) In vitro differentiation of embryonic stem cells. *Curr Opin Cell Biol* **7**(6), 862-869.

90 Keohane, A. M., Barlow, A. L., Waters, J., Bourn, D. and Turner, B. M. (1999) H4 acetylation, XIST RNA and replication timing are coincident and define x;autosome boundaries in two abnormal X chromosomes. *Hum Mol Genet* **8**(2), 377-383.

91 Keohane, A. M., Lavender, J. S., O'Neill, L. P. and Turner, B. M. (1998) Histone acetylation and X inactivation. *Dev Genet* **22**(1), 65-73.

92 Keohane, A. M., O'Neill L, P., Belyaev, N. D., Lavender, J. S. and Turner, B. M. (1996) X-Inactivation and histone H4 acetylation in embryonic stem cells. *Dev Biol* **180**(2), 618-630.

93 Khan, A. U. and Hampsey, M. (2002) Connecting the DOTs: covalent histone modifications and the formation of silent chromatin. *Trends Genet* **18**(8), 387-389.

94 Khochbin, S., Verdel, A., Lemercier, C. and Seigneurin-Berny, D. (2001) Functional significance of histone deacetylase diversity. *Curr Opin Genet Dev* **11**(2), 162-166.

95 Knoepfler, P. S. and Eisenman, R. N. (1999) Sin meets NuRD and other tails of repression. *Cell* **99**(5), 447-450.

96 Korenberg, J. R. and Rykowski, M. C. (1988) Human genome organization: Alu, lines, and the molecular structure of metaphase chromosome bands. *Cell* **53**(3), 391-400.

97 Kornberg, R. D. and Lorch, Y. (1992) Chromatin structure and transcription. *Ann Rev Cell Biol* **8** 563-587.

98 Kornberg, R. D. and Lorch, Y. (1999) Twenty-five years of the nucleosome, fundamental particle of the eukaryote chromosome. *Cell* **98**(3), 285-294.

99 Kosugi, H., Towatari, M., Hatano, S., Kitamura, K., Kiyoi, H., Kinoshita, T., Tanimoto, M., Murate, T., Kawashima, K., Saito, H. and Naoe, T. (1999) Histone deacetylase inhibitors are the potent inducer/enhancer of differentiation in acute myeloid leukemia: a new approach to anti-leukemia therapy. *Leukemia* **13**(9), 1316-1324.

100 Kouzarides, T. (2002) Histone methylation in transcriptional control. *Curr Opin Genet Dev* **12**(2), 198-209.

101 Kulharya, A. S., Roop, H., Kukolich, M. K., Nachtman, R. G., Belmont, J. W. and Garcia-Heras, J. (1995) Mild phenotypic effects of a de novo deletion Xpter-->Xp22.3 and duplication 3pter-->3p23. *Am J Med Genet* **56**(1), 16-21.

102 Kuo, M. H., vom Baur, E., Struhl, K. and Allis, C. D. (2000) Gcn4 activator targets Gcn5 histone acetyltransferase to specific promoters independently of transcription. *Mol Cell* **6**(6), 1309-1320.

103 Kurdistani, S. K., Robyr, D., Tavazoie, S. and Grunstein, M. (2002) Genome-wide binding map of the histone deacetylase Rpd3 in yeast. *Nat Genet* **31**(3), 248-254.

104 Lachner, M., O'Carroll, D., Rea, S., Mechtler, K. and Jenuwein, T. (2001) Methylation of histone H3 lysine 9 creates a binding site for HP1 proteins. *Nature* **410**(6824), 116-120.

105 Lee, J., Chen, Y., Tolstykh, T. and Stock, J. (1996) A specific protein carboxyl methylesterase that demethylates phosphoprotein phosphatase 2A in bovine brain. *Proc Natl Acad Sci U S A* **93**(12), 6043-6047.

106 Lee, J. T., Davidow, L. S. and Warshawsky, D. (1999) Tsix, a gene antisense to Xist at the X-inactivation centre. *Nat Genet* **21**(4), 400-404.

107 Lee, J. T. and Jaenisch, R. (1997) Long-range cis effects of ectopic X-inactivation centres on a mouse autosome. *Nature* **386**(6622), 275-279.

108 Lee, J. T. and Lu, N. (1999) Targeted mutagenesis of Tsix leads to nonrandom X inactivation. *Cell* **99**(1), 47-57.

109 Lemercier, C., Brocard, M. P., Puvion-Dutilleul, F., Kao, H. Y., Albagli, O. and Khochbin, S. (2002) Class II histone deacetylases are directly recruited by BCL6 transcriptional repressor. *J Biol Chem* **277**(24), 22045-22052.

110 Lewin, B. (1997) Genes VI. Oxford, Oxford University Press.

111 Li, J., Wang, J., Nawaz, Z., Liu, J. M., Qin, J. and Wong, J. (2000) Both corepressor proteins SMRT and N-CoR exist in large protein complexes containing HDAC3. *Embo J* **19**(16), 4342-4350.

112 Litt, M. D., Simpson, M., Gaszner, M., Allis, C. D. and Felsenfeld, G. (2001) Correlation between histone lysine methylation and developmental changes at the chicken beta-globin locus. *Science* **293**(5539), 2453-2455.

113 Luger, K., Mader, A. W., Richmond, R. K., Sargent, D. F. and Richmond, T. J. (1997) Crystal structure of the nucleosome core particle at 2.8 A resolution. *Nature* **389**(6648), 251-260.

114 Luo, J., Nikolaev, A. Y., Imai, S., Chen, D., Su, F., Shiloh, A., Guarente, L. and Gu, W. (2001) Negative control of p53 by Sir2alpha promotes cell survival under stress. *Cell* **107**(2), 137-148.

115 Lyon, M. F. (1998) X-chromosome inactivation: a repeat hypothesis. *Cytogenet Cell Genet* **80**(1-4), 133-137.

116 Magnaghi-Jaulin, L., Groisman, R., Naguibneva, I., Robin, P., Lorain, S., Le Villain, J. P., Troalen, F., Trouche, D. and Harel-Bellan, A. (1998) Retinoblastoma protein represses transcription by recruiting a histone deacetylase. *Nature* **391**(6667), 601-605.

117 Maison, C., Bailly, D., Peters, A. H., Quivy, J. P., Roche, D., Taddei, A., Lachner, M., Jenuwein, T. and Almouzni, G. (2002) Higher-order structure in pericentric heterochromatin involves a distinct pattern of histone modification and an RNA component. *Nat Genet* **30**(3), 329-334.

118 Mak, W., Baxter, J., Silva, J., Newall, A. E., Otte, A. P. and Brockdorff, N. (2002) Mitotically stable association of polycomb group proteins eed and enx1 with the inactive x chromosome in trophoblast stem cells. *Curr Biol* **12**(12), 1016-1020.

119 Marahrens, Y., Panning, B., Dausman, J., Strauss, W. and Jaenisch, R. (1997) Xist-deficient mice are defective in dosage compensation but not spermatogenesis. *Genes Dev* **11**(2), 156-166.

120 Martin, G. R. and Evans, M. J. (1975) Differentiation of clonal lines of teratocarcinoma cells: formation of embryoid bodies in vitro. *Proc Natl Acad Sci U S A* **72**(4), 1441-1445.

121 McCabe, V., Formstone, E. J., O'Neill, L. P., Turner, B. M. and Brockdorff, N. (1999) Chromatin structure analysis of the mouse Xist locus. *Proc Natl Acad Sci U S A* **96**(13), 7155-7160.

122 Meller, V. H. and Kuroda, M. I. (2002) Sex and the single chromosome. *Adv Genet* **46** 1-24.

123 Mermoud, J. E., Costanzi, C., Pehrson, J. R. and Brockdorff, N. (1999) Histone macroH2A1.2 relocates to the inactive X chromosome after initiation and propagation of X-inactivation. *J Cell Biol* **147**(7), 1399-1408.

124 Mermoud, J. E., Popova, B., Peters, A. H., Jenuwein, T. and Brockdorff, N. (2002) Histone H3 lysine 9 methylation occurs rapidly at the onset of random X chromosome inactivation. *Curr Biol* **12**(3), 247-251.

125 Miller, A. P. and Willard, H. F. (1998) Chromosomal basis of X chromosome inactivation: identification of a multigene domain in Xp11.21-p11.22 that escapes X inactivation. *Proc Natl Acad Sci U S A* **95**(15), 8709-8714.

126 Miska, E. A., Karlsson, C., Langley, E., Nielsen, S. J., Pines, J. and Kouzarides, T. (1999) HDAC4 deacetylase associates with and represses the MEF2 transcription factor. *Embo J* **18**(18), 5099-5107.

127 Mohandas, T., Sparkes, R. S., Hellkuhl, B., Grzeschik, K. H. and Shapiro, L. J. (1980) Expression of an X-linked gene from an inactive human X chromosome in mouse-human hybrid cells: further evidence for the noninactivation of the steroid sulfatase locus in man. *Proc Natl Acad Sci U S A* **77**(11), 6759-6763.

128 Mohandas, T., Sparkes, R. S. and Shapiro, L. J. (1981) Reactivation of an inactive human X chromosome: evidence for X inactivation by DNA methylation. *Science* **211**(4480), 393-396.

129 Mohandas, T., Sparkes, R. S. and Shapiro, L. J. (1982) Genetic evidence for the inactivation of a human autosomal locus attached to an inactive X chromosome. *Am J Hum Genet* **34**(5), 811-817.

130 Monk, M. and Kathuria, H. (1977) Dosage compensation for an X-linked gene in pre-implantation embryos. *Nature* **270** 599-600.

131 Moretti, P., Freeman, K., Coodly, L. and Shore, D. (1994) Evidence that a complex of SIR proteins interacts with the silencer and telomere binding protein RAP1. *Genes and Development* **8** 2257-2269.

132 Nakayama, J., Rice, J. C., Strahl, B. D., Allis, C. D. and Grewal, S. I. (2001) Role of histone H3 lysine 9 methylation in epigenetic control of heterochromatin assembly. *Science* **292**(5514), 110-113.

133 Nan, X., Ng, H. H., Johnson, C. A., Laherty, C. D., Turner, B. M., Eisenman, R. N. and Bird, A. (1998) Transcriptional repression by the methyl-CpG-binding protein MeCP2 involves a histone deacetylase complex. *Nature* **393**(6683), 386-389.

134 Nasir, J., Maconochie, M. K. and Brown, S. D. (1991) Co-amplification of L1 line elements with localised low copy repeats in Giemsa dark bands: implications for genome organisation. *Nucleic Acids Res* **19**(12), 3255-3260.

135 Ng, H. H. and Bird, A. (2000) Histone deacetylases: silencers for hire. *Trends in Biochemical Sciences* **25**(3), 121-126.

136 Nichols, J., Evans, E. P. and Smith, A. G. (1990) Establishment of germ-line-competent embryonic stem (ES) cells using differentiation inhibiting activity. *Development* **110**(4), 1341-1348.

137 Nielsen, P. R., Nietlispach, D., Mott, H. R., Callaghan, J., Bannister, A., Kouzarides, T., Murzin, A. G., Murzina, N. V. and Laue, E. D. (2002) Structure of the HP1 chromodomain bound to histone H3 methylated at lysine 9. *Nature* **416**(6876), 103-107.

138 Nielsen, S. J., Schneider, R., Bauer, U. M., Bannister, A. J., Morrison, A., O'Carroll, D., Firestein, R., Cleary, M., Jenuwein, T., Herrera, R. E. and Kouzarides, T. (2001) Rb targets histone H3 methylation and HP1 to promoters. *Nature* **412**(6846), 561-565.

139 Nishioka, K., Rice, J. C., Sarma, K., Erdjument-Bromage, H., Werner, J., Wang, Y., Chuikov, S., Valenzuela, P., Tempst, P., Steward, R., Lis, J. T., Allis, C. D. and Reinberg, D. (2002) PR-Set7 is a nucleosome-specific methyltransferase that modifies lysine 20 of histone H4 and is associated with silent chromatin. *Mol Cell* **9**(6), 1201-1213.

140 Noma, K., Allis, C. D. and Grewal, S. I. (2001) Transitions in distinct histone H3 methylation patterns at the heterochromatin domain boundaries. *Science* **293**(5532), 1150-1155.

141 Norris, D. P., Brockdorff, N. and Rastan, S. (1991) Methylation status of CpG-rich islands on active and inactive mouse X chromosomes. *Mamm Genome* **1**(2), 78-83.

142 Norris, D. P., Patel, D., Kay, G. F., Penny, G. D., Brockdorff, N., Sheardown, S. A. and Rastan, S. (1994) Evidence that random and imprinted Xist expression is controlled by preemptive methylation. *Cell* **77**(1), 41-51.

143 Norton, V. G., Imai, B. S., Yau, P. and Bradbury, E. M. (1989) Histone acetylation reduces nucleosomal core particle linking number change. *Cell* **57** 449-457.

144 O'Neill, L. P., Keohane, A. M., Lavender, J. S., McCabe, V., Heard, E., Avner, P., Brockdorff, N. and Turner, B. M. (1999) A developmental switch in H4 acetylation upstream of Xist plays a role in X chromosome inactivation. *Embo J* **18**(10), 2897-2907.

145 O'Neill, L. P. and Turner, B. M. (1995) Histone H4 acetylation distinguishes coding regions of the human genome from heterochromatin in a differentiation-dependent but transcription-independent manner. *Embo J* **14**(16), 3946-3957.

146 Orlando, V. (2000) Mapping chromosomal proteins in vivo by formaldehyde-crosslinked-chromatin immunoprecipitation. *Trends Biochem Sci* **25**(3), 99-104.

147 Orlando, V., Strutt, H. and Paro, R. (1997) Analysis of chromatin structure by in vivo formaldehyde cross-linking. *Methods* **11**(2), 205-214.

148 Palmieri, S. L., Peter, W., Hess, H. and Scholer, H. R. (1994) Oct-4 transcription factor is differentially expressed in the mouse embryo during establishment of the first two extraembryonic cell lineages involved in implantation. *Dev Biol* **166**(1), 259-267.

149 Panning, B., Dausman, J. and Jaenisch, R. (1997) X chromosome inactivation is mediated by Xist RNA stabilization. *Cell* **90**(5), 907-916.

150 Penny, G. D., Kay, G. F., Sheardown, S. A., Rastan, S. and Brockdorff, N. (1996) Requirement for Xist in X chromosome inactivation. *Nature* **379**(6561), 131-137.

151 Perche, P. Y., Vourc'h, C., Konecny, L., Souchier, C., Robert-Nicoud, M., Dimitrov, S. and Khochbin, S. (2000) Higher concentrations of histone macroH2A in the Barr body are correlated with higher nucleosome density. *Curr Biol* **10**(23), 1531-1534.

152 Perry, J., Palmer, S., Gabriel, A. and Ashworth, A. (2001) A short pseudoautosomal region in laboratory mice. *Genome Res* **11**(11), 1826-1832.

153 Peters, A. H., Mermoud, J. E., O'Carroll, D., Pagani, M., Schweizer, D., Brockdorff, N. and Jenuwein, T. (2002) Histone H3 lysine 9 methylation is an epigenetic imprint of facultative heterochromatin. *Nat Genet* **30**(1), 77-80.

154 Pillet, N., Bonny, C. and Schorderet, D. F. (1995) Characterization of the promoter region of the mouse Xist gene. *Proc Natl Acad Sci U S A* **92**(26), 12515-12519.

155 Platero, J. S., Hartnett, T. and Eissenberg, J. C. (1995) Functional analysis of the chromo domain of HP1. *Embo J* **14**(16), 3977-3986.

156 Rack, K. A., Chelly, J., Gibbons, R. J., Rider, S., Benjamin, D., Lafreniere, R. G., Oscier, D., Hendriks, R. W., Craig, I. W., Willard, H. F. and et al. (1994) Absence of the XIST gene from late-replicating isodicentric X chromosomes in leukaemia. *Hum Mol Genet* **3**(7), 1053-1059.

157 Rastan, S. (1983) Non-random X-chromosome inactivation in mouse X-autosome translocation embryos--location of the inactivation centre. *J Embryol Exp Morphol* **78** 1-22.

158 Rastan, S. and Robertson, E. J. (1985) X-chromosome deletions in embryo-derived (EK) cell lines associated with lack of X-chromosome inactivation. *J Embryol Exp Morphol* **90** 379-388.

159 Rea, S., Eisenhaber, F., O'Carroll, D., Strahl, B. D., Sun, Z. W., Schmid, M., Opravil, S., Mechtler, K., Ponting, C. P., Allis, C. D. and Jenuwein, T. (2000) Regulation of chromatin structure by site-specific histone H3 methyltransferases. *Nature* **406**(6796), 593-599.

160 Rice, J. C. and Allis, C. D. (2001) Histone methylation versus histone acetylation: new insights into epigenetic regulation. *Curr Opin Cell Biol* **13**(3), 263-273.

161 Richon, V. M., Emiliani, S., Verdin, E., Webb, Y., Breslow, R., Rifkind, R. A. and Marks, P. A. (1998) A class of hybrid polar inducers of transformed cell differentiation inhibits histone deacetylases. *Proc Natl Acad Sci U S A* **95**(6), 3003-3007.

162 Robertson, E. J. (1987) Teratocarcinomas and embryonic stem cells : a practical approach, Oxford.

163 Roguev, A., Schaft, D., Shevchenko, A., Pijnappel, W. W., Wilm, M., Aasland, R. and Stewart, A. F. (2001) The Saccharomyces cerevisiae Set1 complex includes an Ash2 homologue and methylates histone 3 lysine 4. *Embo J* **20**(24), 7137-7148.

164 Rundlett, S. E., Carmen, A. A., Suka, N., Turner, B. M. and Grunstein, M. (1998) Transcriptional repression by UME6 involves deacetylation of lysine 5 of histone H4 by RPD3. *Nature* **392**(6678), 831-835.

165 Russell, L. B. (1963) Mammalian X-chromosome action: inactivation limited in spread and region of origin. *Science* **140** 976-978.

166 Sambrook, J., Fritsch, E. and Maniatis, T. (1989) Molecular cloning: a laboratory manual. NY, Cold Spring Harbor Press.

167 Santos-Rosa, H., Schneider, R., Bannister, A. J., Sherriff, J., Bernstein, B. E., Emre, N. C., Schreiber, S. L., Mellor, J. and Kouzarides, T. (2002) Active genes are tri-methylated at K4 of histone H3. *Nature* **419**(6905), 407-411.

168 Sayre, M. H., Tschochner, H. and Kornberg, R. D. (1992) Reconstitution of transcription with five purified initiation factors and RNA polymerase II from Saccharomyces cerevisiae. *J Biol Chem* **267**(32), 23376-23382.

169 Schanz, S. and Steinbach, P. (1989) Investigation of the "variable spreading" of X inactivation into a translocated autosome. *Hum Genet* **82**(3), 244-248.

170 Schneider, R., Bannister, A. J. and Kouzarides, T. (2002) Unsafe SETs: histone lysine methyltransferases and cancer. *Trends Biochem Sci* **27**(8), 396-402.

171 Sealy, L. and Chalkley, R. (1978) The effect of sodium butyrate on histone modification. *Cell* **14**(1), 115-121.

172 Shao, C. S. and Takagi, N. (1991) Karyotypes and X chromosome inactivation in segregants of a murine X-autosome translocation, T(X;4)37H. *Jpn J Genet* **66**(4), 433-447.

173 Sharp, A., Robinson, D. O. and Jacobs, P. (2001) Absence of correlation between late-replication and spreading of X inactivation in an X;autosome translocation. *Hum Genet* **109**(3), 295-302.

174 Sheardown, S. A., Duthie, S. M., Johnston, C. M., Newall, A. E., Formstone, E. J., Arkell, R. M., Nesterova, T. B., Alghisi, G. C., Rastan, S. and Brockdorff, N.

(1997) Stabilization of Xist RNA mediates initiation of X chromosome inactivation. *Cell* **91**(1), 99-107.

175 Shepherd, G. R., Hardin, J. M. and Noland, B. J. (1971) Methylation of lysine residues of histone fractions in synchronized mammalian cells. *Arch Biochem Biophys* **143**(1), 1-5.

176 Smith, A. G. (1991) Culture and differentiation of embryonic stem cells. *J Tiss Cult Meth* **13** 89-94.

177 Smith, E. R., Pannuti, A., Gu, W., Steurnagel, A., Cook, R. G., Allis, C. D. and Lucchesi, J. C. (2000) The drosophila MSL complex acetylates histone H4 at lysine 16, a chromatin modification linked to dosage compensation. *Mol Cell Biol* **20**(1), 312-318.

178 Strahl, B. D. and Allis, C. D. (2000) The language of covalent histone modifications. *Nature* **403**(6765), 41-45.

179 Strahl, B. D., Ohba, R., Cook, R. G. and Allis, C. D. (1999) Methylation of histone H3 at lysine 4 is highly conserved and correlates with transcriptionally active nuclei in Tetrahymena. *PNAS* **96**(26), 14967-14972.

180 Strahl-Bolsinger, S., Hecht, A., Luo, K. and Grunstein, M. (1997) SIR2 and SIR4 interactions differ in core and extended telomeric heterochromatin in yeast. *Genes Dev* **11**(1), 83-93.

181 Suka, N., Suka, Y., Carmen, A. A., Wu, J. and Grunstein, M. (2001) Highly specific antibodies determine histone acetylation site usage in yeast heterochromatin and euchromatin. *Mol Cell* **8**(2), 473-479.

182 Sun, Z. W. and Allis, C. D. (2002) Ubiquitination of histone H2B regulates H3 methylation and gene silencing in yeast. *Nature* **418**(6893), 104-108.

183 Takagi, N. and Sasaki, M. (1975) Preferential inactivation of the paternally derived X chromosome in the extraembryonic membranes of the mouse. *Nature* **256** 640-642.

184 Takagi, N., Sugawara, O. and Sasaki, M. (1982) Regional and temporal changes in the pattern of X chromosome replication during the early postimplantation of the female mouse. *Chromosoma* **85** 275-286.

185 Taunton, J., Hassig, C. A. and Schreiber, S. L. (1996) A mammalian histone deacetylase related to yeast transcriptional regulator Rpd3. *Science* **272** 409-411.

186 Thomas, G., Lange, H. W. and Hempel, K. (1975) Kinetics of histone methylation in vivo and its relation to the cell cycle in Ehrlich ascites tumor cells. *Eur J Biochem* **51**(2), 609-615.

187 Turner, B. M. (1993) Decoding the nucleosome. *Cell* **75**(1), 5-8.

188 Turner, B. M. (1998) Histone acetylation as an epigenetic determinant of long term transcriptional competence. *Cell Mol Life Sci* **54** 21-31.

189 Turner, B. M. (2000) Histone acetylation and an epigenetic code. *Bioessays* **22**(9), 836-845.

190 Turner, B. M., Birley, A. J. and Lavender, J. (1992) Histone H4 isoforms acetylated at specific lysine residues define individual chromosomes and chromatin domains in Drosophila polytene nuclei. *Cell* **69**(2), 375-384.

191 Turner, B. M. and Fellows, G. (1989) Specific antibodies reveal ordered and cell-cycle-related use of histone-H4 acetylation sites in mammalian cells. *Eur J Biochem* **179**(1), 131-139.

192 Turner, B. M., O'Neill, L. P. and Allan, I. M. (1989) Histone H4 acetylation in human cells. Frequency of acetylation at different sites defined by immunolabeling with site-specific antibodies. *FEBS Lett* **253**(1-2), 141-145.

193 van der Vlag, J. and Otte, A. P. (1999) Transcriptional repression mediated by the human polycomb-group protein EED involves histone deacetylation. *Nat Genet* **23**(4), 474-478.

194 Verdel, A. and Khochbin, S. (1999) Identification of a new family of higher eukaryotic histone deacetylases. Coordinate expression of differentiation-dependent chromatin modifiers. *J Biol Chem* **274**(4), 2440-2445.

195 Verreault, A., Kaufman, P. D., Kobayashi, R. and Stillman, B. (1998) Nucleosomal DNA regulates the core-histone-binding subunit of the human Hat1 acetyltransferase. *Curr Biol* **8**(2), 96-108.

196 Vogelauer, M., Wu, J., Suka, N. and Grunstein, M. (2000) Global histone acetylation and deacetylation in yeast. *Nature* **408**(6811), 495-498.

197 Wakefield, M. J., Keohane, A. M., Turner, B. M. and Graves, J. A. (1997) Histone underacetylation is an ancient component of mammalian X chromosome inactivation. *Proc Natl Acad Sci U S A* **94**(18), 9665-9668.

198 Wang, J., Mager, J., Chen, Y., Schneider, E., Cross, J. C., Nagy, A. and Magnuson, T. (2001) Imprinted X inactivation maintained by a mouse Polycomb group gene. *Nat Genet* **28**(4), 371-375.

199 Waterborg, J. H. and Matthews, H. R. (1984) Patterns of histone acetylation in Physarum polycephalum. H2A and H2B acetylation is functionally distinct from H3 and H4 acetylation. *Eur J Biochem* **142**(2), 329-335.

200 Watson, A. D., Edmondson, D. G., Bone, J. R., Mukai, Y., Yu, Y., Du, W., Stillman, D. J. and Roth, S. Y. (2000) Ssn6-Tup1 interacts with class I histone deacetylases required for repression. *Genes Dev* **14**(21), 2737-2744.

201 White, D. A., Belyaev, N. D. and Turner, B. M. (1999) Preparation of site-specific antibodies to acetylated histones. *Methods* **19**(3), 417-424.

202 White, W. M., Willard, H. F., Van Dyke, D. L. and Wolff, D. J. (1998) The spreading of X inactivation into autosomal material of an x;autosome translocation: evidence for a difference between autosomal and X-chromosomal DNA. *Am J Hum Genet* **63**(1), 20-28.

203 Williams, R. L., Hilton, D. J., Pease, S., Willson, T. A., Stewart, C. L., Gearing, D. P., Wagner, E. F., Metcalf, D., Nicola, N. A. and Gough, N. M. (1988) Myeloid leukaemia inhibitory factor maintains the developmental potential of embryonic stem cells. *Nature* **336**(6200), 684-687.

204 Winston, F. and Allis, C. D. (1999) The bromodomain: a chromatin targeting module? *Nat Struct Biol* **6** 601-604.

205 Wolffe, A. (1998) Chromatin : structure and function. San Diego, California, Academic Press.

206 Wolffe, A. P. and Hayes, J. J. (1999) Chromatin disruption and modification. *Nucleic Acids Res* **27** 711-720.

207 Wu, J. and Grunstein, M. (2000) 25 years after the nucleosome model: chromatin modifications. *Trends Biochem Sci* **25**(12), 619-623.

208 Wutz, A. and Jaenisch, R. (2000) A shift from reversible to irreversible X inactivation is triggered during ES cell differentiation. *Mol Cell* **5**(4), 695-705.

209 Xin, Z., Allis, C. D. and Wagstaff, J. (2001) Parent-specific complementary patterns of histone H3 lysine 9 and H3 lysine 4 methylation at the Prader-Willi syndrome imprinting center. *Am J Hum Genet* **69**(6), 1389-1394.

210 Yang, X. J., Ogryzko, V. V., Nishikawa, J. H., Howard, B. and Nakatani, Y. (1996) A p300/CBP associated factor that competes with adenoviral E1A oncoprotein. *Nature* **382** 319-324.

211 Yoshida, M., Kijima, M., Akita, M. and Beppu, T. (1990) Potent and specific inhibition of mammalian histone deacetylase both in vivo and in vitro by trichostatin A. *J Biol Chem* **265**(28), 17174-17179.

212 Zhang, K., Tang, H., Huang, L., Blankenship, J. W., Jones, P. R., Xiang, F., Yau, P. M. and Burlingame, A. L. (2002) Identification of Acetylation and Methylation Sites of Histone H3 from Chicken Erythrocytes by High-Accuracy Matrix-Assisted Laser Desorption Ionization-Time-of-Flight, Matrix-Assisted Laser Desorption Ionization-Postsource Decay, and Nanoelectrospray Ionization Tandem Mass Spectrometry. *Anal Biochem* **306**(2), 259-269.

213 Zhang, W., Bone, J. R., Edmondson, D. G., Turner, B. M. and Roth, S. Y. (1998a) Essential and redundant functions of histone acetylation revealed by mutation of target lysines and loss of the Gcn5p acetyltransferase. *Embo J* **17**(11), 3155-3167.

214 Zhang, Y., LeRoy, G., Seelig, H. P., Lane, W. S. and Reinberg, D. (1998b) The dermatomyositis-specific autoantigen Mi2 is a component of a complex containing histone deacetylase and nucleosome remodeling activities. *Cell* **95**(2), 279-289.

215 Zhang, Y., Ng, H. H., Erdjument-Bromage, H., Tempst, P., Bird, A. and Reinberg, D. (1999) Analysis of the NuRD subunits reveals a histone deacetylase core complex and a connection with DNA methylation. *Genes Dev* **13**(15), 1924-1935.

216 Zhou, X., Marks, P. A., Rifkind, R. A. and Richon, V. M. (2001) Cloning and characterization of a histone deacetylase, HDAC9. *Proc Natl Acad Sci U S A* **98**(19), 10572-10577.

PUBLICATIONS

1 Spotswood, H. T. and Turner, B. M. (2002) An increasingly complex code. *J Clin Invest* **110**(5), 577-82.

2 Travers, H., Spotswood, H. T., Moss, P. A. H. and Turner, B. M. (2002) Human CD34+ hematopoietic progenitor cells hyperacetylate core histones in response to sodium butyrate, but not trichostatin A. *Exp Cell Res* **280**(2), 149-58

3 Sharp, A. J., Spotswood, H. T., Robinson D. O., Turner B. M. and Jacobs P. A. (2002) Molecular and cytogenetic analysis of the spreading of X inactivation in X;autosome translocations. *Hum Mol Genet* **11**(25), 3145-56